9-12-2016

microRNA-433 Inhibits Glucocorticoid and TGF-β Signaling: Impacts on Osteoblast Circadian Rhythm, Commitment, and Differentiation

Spenser Scott Smith
University of Connecticut, spsmith@uchc.edu

microRNA-433 Inhibits Glucocorticoid and TGF-β Signaling: Impacts on Osteoblast Circadian Rhythm, Commitment, and Differentiation

Spenser S. Smith, Ph.D.
University of Connecticut, 2016

Lineage commitment and differentiation of skeletal cells requires coordinated regulation of multiple signaling systems by microRNAs (miRNAs). Transforming growth factor β (TGFβ) is important for osteoblastogenesis, chondrogenesis and adipogenesis. Here, we show that miR-433 limits TGFβ signaling and is a negative regulator of osteoblastogenesis and chondrogenesis. miR-433 has also been found to target the glucocorticoid receptor, and rhythmic secretion of glucocorticoids is critical for synchronizing circadian clocks. We hypothesized that miR-433 regulates the circadian clocks by regulating glucocorticoid signaling.

In vivo, miR-433 displays robust rhythmicity in mouse calvaria. Its expression pattern was anti-phasic in relation to Bmal1, peaking after light removal. To determine if miR-433 regulates circadian rhythm *in vitro*, its activity was inhibited using a miR-433 competitive inhibitor (miR-433 decoy) in stably transduced C3H/10T1/2 cells. miR-433 inhibition modestly affected Bmal1 rhythm and it dramatically altered the phase of Per2. Inhibiting miR-433 activity amplified the glucocorticoid responsive genes Dusp1 and Per2, and induced nuclear localization of the glucocorticoid receptor. *In vivo* inhibition of miR-433 activity using a Col1a1 driven miR-433 decoy transgenic model altered the phase and amplitude of the circadian clocks. Overall, we found that miR-433 displays a circadian

rhythm in calvaria, alters the phase of circadian clocks, and regulates sensitivity to glucocorticoids.

BMSCs cultured in osteogenic medium caused a progressive decline in miR-433. In contrast, miR-433 was dramatically increased in BMSCs and iPSCs cultured in micromass to induce chondrogenesis. miR-433 levels remained constant during adipogenesis. miR-433 decoy cells were differentiated with BMP2 and miR-433 inhibition induced alkaline phosphatase, Runx2, and osteocalcin mRNAs. In micromass cultures treated with BMP2 and TGFβ, miR-433 inhibition promoted expression of chondrogenic mRNAs, Sox9 and Col2a1. In cells treated with an adipogenic cocktail, miR-433 inhibition failed to alter adipogenic gene markers or Oil-red O staining.

Bioinformatic analyses suggested that miR-433 might target critical components of the TGFβ pathway. miR-433 inhibition amplified TGFβ signaling, evidenced by increased activity of a TGFβ-responsive SBE4 luciferase reporter and enhanced TGFβ-induced pSMAD2. To determine underlying mechanisms, we used Luciferase-3'UTR reporter assays, and experimentally validated SMAD2 and TGFBR1 as novel miR-433 targets. Overall, miR-433 attenuates TGFß signaling, and restrains osteoblastic and chondrogenic differentiation.

microRNA-433 Inhibits Glucocorticoid and TGF-β Signaling: Impacts on Osteoblast Circadian Rhythm, Commitment, and Differentiation

Spenser S. Smith

B.A., The College of Idaho, 2008

A Dissertation

Submitted in Partial Fulfillment of the

Requirements for the Degree of

Doctor of Philosophy

at the

University of Connecticut

2016

2016

APPROVAL PAGE

Doctor of Philosophy Dissertation

microRNA-433 Inhibits Glucocorticoid and TGF-β Signaling: Impacts on Osteoblast Circadian Rhythm, Commitment, and Differentiation

Presented by

Spenser S. Smith, B.A.

Major Advisor

_____

Anne Delany

Associate Advisor

_____

Barbara Kream

Associate Advisor

_____

Peter Maye

Associate Advisor

_____

Rosa Guzzo

Associate Advisor

_____

Mina Mina

University of Connecticut
2016

ACKNOWLEDGEMENTS

I would like to express my special appreciation to my terrific advisor, Dr. Anne Delany. Over the years, Anne has spent a tremendous amount of time mentoring me and building me as I scientist. She's help to improve my communication and writing skills, my critical thinking skills, and has taught me not only how to address scientific questions but which questions are the right ones to ask. Anne has always been there for me whenever I have a question. She is quite the character in the lab, and I have not had a boring moment since I've been here. Anne is the type of mentor that I aspire to me, and she has set quite a high bar.

I also want to thank two of my very close friends, Neha Dole and Tiziana Franceschetti. They were crucial in teaching me technical skills and there were countless times where they mentored me. They also made significant contributions to the circadian project and aiding in late night harvests. More importantly, they are two of my closest friends. I would especially like to thank Neha for her contributions to the TGF-β project, and also for getting me in the door for my next adventure in California.

I would also like to thank my little brother and lab mate Hank Hrdlicka, who has always been there for me when I needed help with my project, and for his sunny optimism in the lab. Hank made significant contributions to the circadian paper through his microscopy work. I wish him the best success.

I would like to thank Cathy, who trained me in Anne's lab when I first joined, and enhanced my meticulousness and cleanliness as a scientist. I want to also thank some of the undergraduate students who contributed to this project over the years, Laura, Michelle, and Darby.

I want to thank my committee members, especially Dr. Guzzo for all of her contributions to this research, for teaching me how to differentiate cells towards chondrocytes, and for always being there for me when I had problems. I also want to thank Dr. Maye, who also was one of the labs I rotated in, for all of his mentorship and intellectual contributions to this project. I want to thank Dr. Kream for her help in aiding me with the glucocorticoid project, but also for making sure that I was always on track with my milestones. I want to especially thank Dr. Mina, who has not only been a mentor for me but also has been funding me over the years through the training grant, as well as Dr. Goldberg.

I would also like to thank Kyeong, who has been a great deal of support along the way. She would help mediate differences between me and Anne, or to provide some crucial supplies for y experiments, or to bring in my favorite cakes to comfort me. I would also like to thank many members of the Skeletal Biology and Regeneration department, Dr. Kalajzic, Dr. Dealy, Dr. Hurley, Dr. Gronowicz, and many others who have been there

to support me and ask me tough questions about my project. Of course, I want to acknowledge the funding that supported this research.

I also would like to acknowledge my wonderful family. My wife Jackie first recruited me into research during my undergraduate degree, and therefore shaped my life towards this path. Jackie has been a source of encouragement and support along the way. She is a constant source of inspiration for me through her dedication to her own work, and she encourages me to keep striving to be the best I can. I also want to thank my parents for being an inspiration and a source of support to me through the years, and are here today to support me as well. I also want to thank my grandparents for always instilling from early on the importance of education and encouraging me to become the best that I can be.

TABLE OF CONTENTS

LIST OF TABLES

LIST OF FIGURES

CHAPTER 1

Introduction:

Bone Formation, Circadian Rhythm, and Lineage Commitment of Mesenchymal Stem Cells

Bone Formation

The skeleton forms through two distinct processes, endochondral and intramembranous ossification. The skull, clavicle, and sternum form through intramembranous ossification, a process by which mesenchymal precursors directly differentiate into osteoblasts. The appendicular skeleton forms through endochondral ossification, a developmental process whereby a cartilage template is gradually replaced by bone. Bone, itself, is a highly dynamic tissue that is continuously remodeled, in a tightly regulated cycle of coupled osteoclast-mediated bone resorption followed by osteoblast-mediated bone formation. This is the only process whereby adults can renew bone tissue, and it is also critical for mineral homeostasis. Prevalent skeletal diseases, such as osteoporosis, are caused by an imbalance in bone remodeling. Osteoporosis is a major metabolic bone disease affecting 10 million adults in the United States and results in an estimated annual health care cost of $20 billion (1-3). It is characterized by reduced bone mineral density and deterioration of the bone microarchitecture as a result of disrupted remodeling, therefore increasing risk of fracture.

Osteoblasts

Osteoblasts are the cells within the skeleton that are responsible for bone formation. Osteoblasts differentiate from a multi-potential mesenchymal progenitor cell in

response to pro-osteogenic signaling molecules, including transforming growth factor β (TGF- β), bone morphogenetic proteins (BMPs), and Wnts (Figure 1.1). During early bone formation, osteoprogenitors are recruited to the bone formation surface and proliferate. Further maturation initiates synthesis and secretion of extracellular matrix proteins, the most abundant protein being type I collagen. Early osteoblasts express many factors, including alkaline phosphatase (AP), an enzyme that plays a role in matrix mineralization. Osteoblasts also synthesize non-collagenous bone matrix proteins, including bone sialoprotein, osteopontin, osteonectin, and osteocalcin (Figure 1.1). These proteins play an important role in maintaining bone mineral homeostasis and bone metabolism (4).

During the early stages of osteogenesis, many osteogenic transcription factors are induced, including the key transcription factor Runt related transcription factor 2 (Runx2), as well as Osterix (Figure 1.1). Runx2-deficient mice display defects in skeletal development, and lack ossification due to arrested osteoblast differentiation (5,6). Osterix is downstream of Runx2, and Osterix-null mice also lack bone formation despite formation of a cartilagenous skeleton (7). During later osteogenesis, bone sialoprotein and osteocalcin are induced, and the extracellular matrix matures and becomes mineralized. Following terminal differentiation, several fates await osteoblasts. They can become bone lining cells or become osteocytes or can undergo apoptosis. Bone lining cells are flat cells lining bone surfaces, and are believed to signal osteoclasts and osteoblasts to initiate bone remodeling, and are therefore important in maintaining the overall structural integrity of bone (reviewed by (8)). Osteocytes are dendritic cells that become embedded within the mineralized matrix of bone. Osteocytes primarily function as the bone

mechanosensors and can release signaling molecules to induce bone remodeling or initiate repair for damaged bone (9). Although the role of osteocytes is still not completely understood, they are thought to regulate bone mass, regulate phosphate metabolism, and even resorb bone.

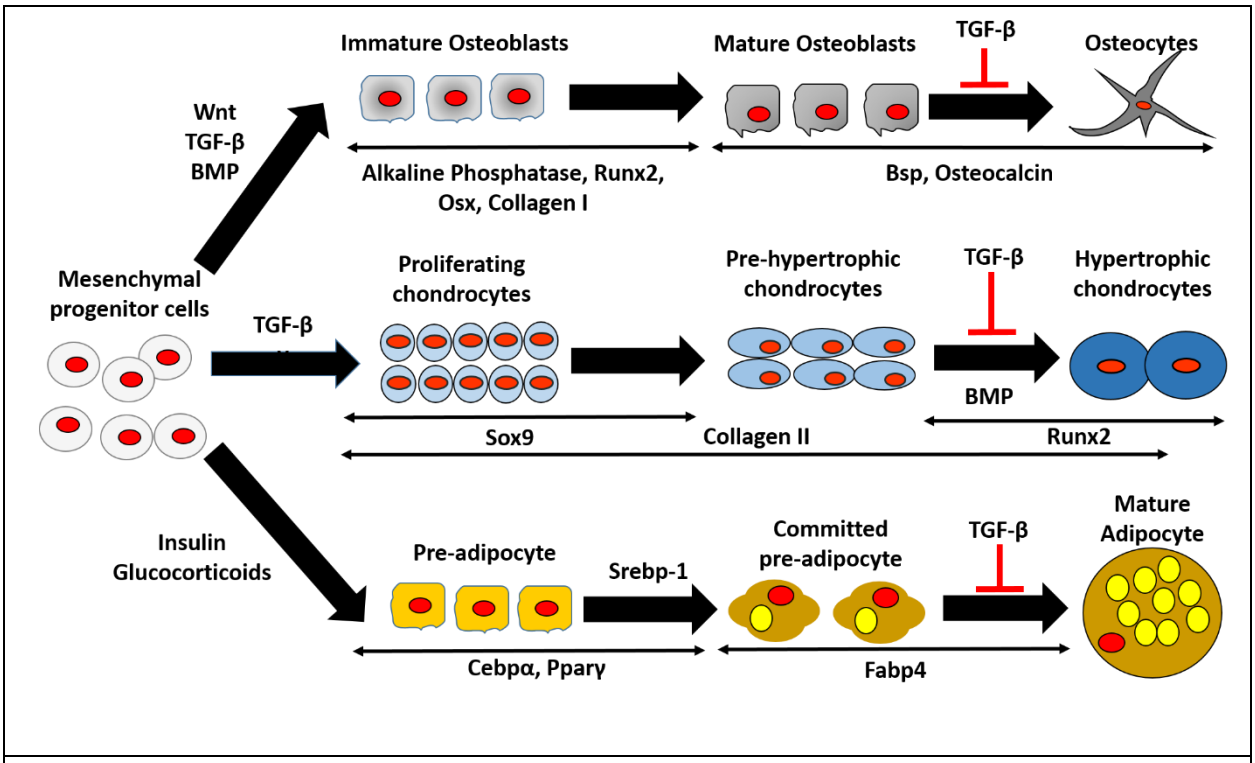

Figure 1.1. Lineage commitment of mesenchymal stem cells. Diagram illustrating the lineage commitment of mesenchymal stem cells towards osteoblasts, chondrocytes, and adipocytes, including key differentiation factors and lineage marker genes.

Adipocytes

Osteoblasts differentiate from a common multi-lineage precursor cell which can be directed by differential signaling molecules towards alternate lineages, including adipocytes or chondrocytes. Signals important for specifying lineage choice play an important role in the regulation of bone mass, as signals promoting the differentiation of progenitors down the alternate lineages tend to be negative regulators of

osteoblastogenesis. For example, Wnt6, Wnt10a, Wnt10b are well established promoters of osteogenic differentiation and restrain adipogenesis (10). For adipogenic differentiation, CCAAT enhancer binding protein α (Cebpα) and peroxisome proliferator activated receptor gamma (Pparγ) are critical adipogenic transcription factors and are potent repressors of osteoblastic commitment (Figure 1.1) (reviewed by (11)). Cebpα and Pparγ initiate transcriptional activation of several adipogenic genes and permanently arrest growth of these cells to allow for the development of a fully differentiated phenotype (reviewed by (11)). Adipocytes play a vital role in energy homeostasis and are the largest reservoir of triglycerides in the body. Insulin and glucocorticoids are major signaling molecules that promote the expansion of adipocytes (reviewed by (11)). Mature adipocytes are characterized by the expression of fatty acid binding protein 4 (Fabp4), and form large lipid droplets within the cell (reviewed by (11)).

Chondrocytes

Chondrocytes are the cells responsible for cartilage formation. Cartilage is critical for bone development in the process of endochondral ossification, but also plays important roles in repair and as mechanoabsorbers for joints. Repair of fractured bone mirrors bone formation, so chondrocytes also play a critical role in the repair process.

Cartilage formation begins with the condensation of mesenchymal stem cells, which then become closely packed together, and mature towards chondrocytes. Osteochondral progenitors proliferate and begin expressing Sox9, the master transcriptional factor that promotes the commitment of mesenchymal progenitors to the

chondrogenic lineage (Figure 1.1). Sox9 promotes the proliferation and survival of mesenchymal cells, as well as stimulating the expression of cartilage matrix proteins, including type II collagen. Sox9 deficient mice have shortened limbs and the lack of Sox9 disables the ability of mesenchymal cells to condense, therefore altering subsequent cartilage and bone formation (12). However, Sox9 can also inhibit chondrocyte hypertrophy and prevent vascularization of the cartilage template (13).

As differentiation progresses, the rate of proliferation decreases and cells become flattened and pre-hypertrophic. Chondrocytes will synthesize proteoglycans and type II collagen, which remains sustained throughout chondrogenesis. Terminal differentiation of chondrocytes results in hypertrophy, where chondrocytes calcify their matrix and vascular invasion occurs. Hypertrophic chondrocytes dramatically increase their size and volume. Hypertrophic chondrocytes also express the transcription factor Runx2, which promotes the synthesis of the hypertrophic cartilage matrix protein type X collagen. Runx2 also promotes the expression of vascular endothelial growth factor (Vegf), which is critical for blood vessel invasion and the replacement of the mineralized cartilage matrix with bone (14).

TGF-β Signaling in Bone Marrow Stromal Cell Lineage Commitment

The transforming growth factor ß (TGF-ß) superfamily is involved in a diverse array of cellular processes, including mesenchymal stem cell differentiation. The TGF-ß family contains three isoforms, ß1, ß2, and ß3, with ß1 being the most abundant. Across many tissues, TGF-ß plays a major role in promoting cell proliferation, as well as cell survival,

migration, and production of extracellular matrix (15-20). TGF-β signaling is initiated upon ligand binding to a cell surface receptor complex containing one type I and one type II TGF-β receptor. Ligand induced phosphorylation of type I receptor by the type II receptor activates receptor kinases, resulting in downstream phosphorylation of SMAD2 and/or SMAD3. These SMADs then dissociate from the receptor complex and associate with SMAD4, allowing for translocation into the nucleus and interaction with SMAD binding elements (SBEs) and other DNA binding proteins, to activate or repress gene transcription (reviewed by (21)).

TGF-ß plays an important role in every stage of bone formation, and its function is context dependent (Figure 1.1). During early stages of differentiation, TGF-ß promotes chemotactic attraction of osteoblasts and osteoblast proliferation (22). Osteoblasts also secrete and deposit TGF-ß in the bone, which then gets released when osteoclasts resorb bone, to recruit osteoblasts to enable new bone formation (reviewed by (21)). However, TGF-ß inhibits terminal differentiation by suppressing alkaline phosphatase and osteocalcin, as well as mineralization ((15), reviewed by (23)). TGF-ß also opposes BMP-2 actions during later stages of differentiation, causing SMAD3 to physically interact with Runx2 to repress its activity (24).

TGF-β is a crucial mediator of chondrogenesis, promoting the commitment and recruitment of osteochondral progenitor cells (Figure 1.1) (reviewed by (25)). TGF-β promotes condensation and proliferation of osteochondral progenitor cells by stimulating

MAPK and Wnt signaling pathways (26-28). TGF-β induces expression of Sox9 and is a potent stimulator of proteoglycan and type II collagen synthesis (29,30). TGF-β stimulates the synthesis of type II collagen synthesis by initiating downstream signaling and complex formation of SMAD3 and SMAD4, which associates with a Sox9 protein complex to activate a type II collagen enhancer region (31). However, TGF-β can restrain chondrocyte hypertrophy by reducing extracellular matrix mineralization (reviewed by (25)). The role of TGF-β in the pathogenesis in osteoarthritis has also gained much attention in recent years, where inhibition of TGF-β has been found to attenuate the degeneration of articular cartilage (32).

Although the role of TGF-β in lineage commitment is complex and context dependent, it is an important mediator of both osteogenic and chondrogenic differentiation. By understanding the mechanisms regulating TGF-β signaling, such as post-transcriptional and post-translational regulation, we can better develop therapeutics to treat diseases such as osteoporosis or osteoarthritis.

Circadian Rhythm

The circadian rhythm is an internal timing mechanism important for orchestrating physiological homeostasis by coordinating behavioral and physiological patterns, as well as other functions. The circadian rhythm synchronizes key biological processes such as tissue repair and growth, maintenance of the immune response, and optimization of metabolism, maintaining overall health. The circadian rhythm is driven by a complex

interaction between the hypothalamic suprachiasmatic nucleus (SCN), also known as the central clock, and the peripheral circadian clocks. The SCN is the central oscillator that responds to environmental periodic cues such as light, eating patterns, and temperature. In response to these cues, the SCN entrains peripheral circadian clocks through stimulation of neural or hormonal signals (e.g. glucocorticoids) to enact their effects on target tissues (33). The entrainment of tissues throughout the body is crucial to optimize physiological processes to the light/dark cycle.

In the central and peripheral tissues, the circadian rhythm is maintained locally by clock genes which interact through transcriptional/translational feedback loops. The main positive regulators are aryl hydrocarbon receptor nuclear translocator-like (Bmal1) and circadian locomotor output cycles kaput (Clock), which are negatively regulated by the period genes (Per1, Per2, Per3), the cryptochrome genes (Cry1, Cry2), and the regulator orphan nuclear receptor gene Rev-Erbα (Figure 1.2). Bmal1 and Clock form a heterodimer, and bind to E-box elements of target genes to rhythmically induce gene transcription, including the expression of Per and Cry. Per, Cry, and Rev-Erbα proteins can then translocate back into the nucleus where they repress Bmal1 transcription (Figure 1.2). The positive feedback loop involves the rhythmic regulation of Bmal1 transcription, whose mRNA levels peak 12 hours out of phase relative to Per and Cry. As a result, Bmal1 mRNA levels fall, whereas Per and Cry mRNA levels rise (Figure 1.2). This interaction between the clock proteins determines the oscillatory expression of target genes and contributes to the rhythmicity of physiological systems.

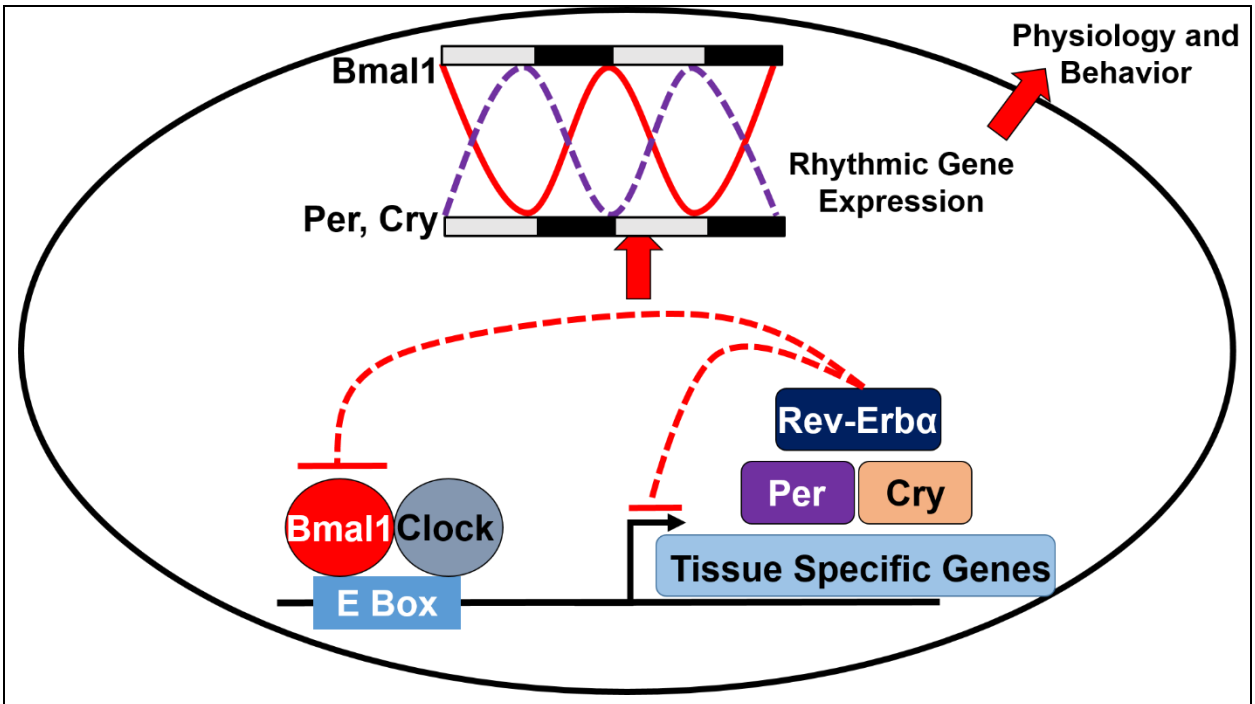

Figure 1.2. Circadian clock transcriptional regulation. Diagram of circadian clock transcription feedback loops. Bmal1 and Clock form a heterodimer and bind to E Box elements in the DNA to drive transcription, including Per, Cry, and Rev-Erbα. In turn, Per, Cry, and Rev-Erbα can inhibit their own transcription as well as the transcription of Bmal1. This feedback loop ensures anti-phasic expression pattern of Bmal1 (red line) and the negative regulators Cry and Per (purple line), promoting rhythmic gene expression to affect physiology and behavior.

Importance of Circadian Rhythm in Maintaining Skeletal Homeostasis

A substantial fraction of genes throughout the body display a rhythmic pattern, with nearly 43% protein coding genes within 12 organs displaying rhythmic transcriptional expression (34). Within the skeleton, the circadian rhythm is critical to maintain normal homeostasis, especially in chondrocytes, osteoclasts, and osteoblasts. Several key osteogenic genes have a clear diurnal expression, such as Runx2, osteocalcin, and Insulin-like Growth Factor 1 (Igf1) (35,36). Current evidence suggests that the circadian

rhythm coordinates bone remodeling to occur at night. Markers of bone formation and resorption peak at night, with lower levels during the day. Serum osteocalcin, levels of which are associated with bone mineral density, as well as type I collagen, have the highest levels in pre-menopausal women at night (37,38). Moreover, murine calvarial organ cultures display circadian mineral deposition with bursts of mineralization occurring at night (39).

To determine if clock genes directly regulate bone mass, one study targeted the negative clock regulators using $Per1^{-/-}$;$Per2^{-/-}$ and $Cry1^{-/-}$;$Cry2^{-/-}$ mice and examined their bone phenotype. The $Per1^{-/-}$;$Per2^{-/-}$ and $Cry1^{-/-}$;Cry2 mice display a high bone mass phenotype in both vertebrae and long bones, and the phenotype continued to intensify as the mice aged (40). These mice had increased bone formation rate (BFR), mineral apposition rate (MAR), and osteoblast proliferation (40,41). $Bmal1^{-/-}$ mice display a similar phenotype, with higher BFR, MAR, and increased osteoblast number (40). Although the circadian clocks play an important role in maintaining skeletal health, the molecular mechanisms whereby circadian clocks regulate the skeleton is still poorly understood.

Disturbance of circadian rhythm can occur when environmental cues are shifted, as is the case for jet lag, night shift work, or insufficient sleep. This can result in changes of circadian clock amplitude, period length, or frequency of expression, which leads to alterations in chromatin modification, gene regulation, cellular metabolism, and immune responses (42). In fact, a single night of sleep loss can result in epigenetic and transcriptional alterations in clock genes within metabolic tissues (43). Alterations of the

circadian clocks can impact the stability, amplitude, or period length of activity, therefore affecting circadian clock targets and impacting cell homeostasis (44). The peripheral clocks resynchronize at a slower pace compared to the central clock, leading to desynchronization of tissues and their physiological processes (45). Chronic desynchrony is associated with the development and progression of cardiovascular disease, cancer, mental illnesses, and severe metabolic disorders (45,46).

In addition, disruption of circadian rhythm can negatively impact the skeleton, leading to increased risk of developing osteoporosis or fractures (47). Patients with obstructive sleep apnea, one of the most common sleep disorders, are 2.7 times more likely to develop osteoporosis (48-50). Self-reporting insomnia patients in Norway also showed an increased risk of developing osteoporosis (51). The functional outcome of low bone mass can be observed in the Nurses' Health Study which found an increased risk of wrist and hip fracture in postmenopausal women working night shifts (52). At the molecular level, patients with a low bone mineral density and adult growth hormone deficiency are unable to produce circadian expression of parathyroid hormone (PTH), a known bone anabolic agent (53). A similar phenotype is observed in sleep deprived rats. In these animals, plasma levels of IGF1, a critical regulator of osteoblast proliferation and differentiation, were decreased by 30% (54). Sleep-deprived rats displayed reduced osteoid, decreased osteoblast number, and reduced bone mineral density (54). Overall, it is clear that disruptions to circadian rhythm can negatively impact bone health.

The importance of circadian rhythm on cartilage has also been well established. Chondrocyte proliferation within the growth plate has a diurnal pattern, with the largest growth occurring during the early morning (55). To examine if chondrocytes have a similar circadian clock pattern as other tissues, one group used a Per2:luc clock reporter mouse model and found that Per2 activity is highly rhythmic in articular cartilage, sternal cartilage, and in the femoral bone. Additionally, glucocorticoid treatment and temperature modifications were able to entrain the circadian clocks within cartilage tissue (56). Cartilage-restricted deletion of Bmal1$^{-/-}$ in mice (Col2-cre) results in shorter bone length and reduced body size compared to wildtype controls (57). One possible mechanism is altered diurnal expression of Indian Hedgehog (Ihh) protein in Bmal1$^{-/-}$ mice, an important regulator of chondrocyte differentiation (57). However, the phenotype of Bmal1$^{-/-}$ mice may also be due to altered circadian expression of multiple chondrocyte genes. In fact, microarray data from cartilage finds 615 genes (3.9% total transcripts in cartilage tissue) display circadian rhythmicity, including many genes involved in differentiation, extracellular matrix production, and apoptosis (56).

Disruptions in circadian rhythms have also been linked to the development of osteoarthritis. Osteoarthritis is one of the most common joint disorders, characterized by a degeneration of the articular cartilage and damage to the joint extracellular matrix, where catabolic activity outpaces anabolic activity. The development of osteoarthritis has been linked to several risk factors, including age, mechanical injury, and chronic inflammation. One possible mechanism linking aging and the development of osteoarthritis is a disruption in circadian rhythms in cartilage tissue. Aged tissue showed

diminished amplitude of the circadian clocks (56). Additionally, Bmal1 deficient mice have damaged articular cartilage, with reduced levels of phosphorylated SMAD 2/3, as well as decreased expression of nuclear factor of activated T cells 2 (NFATC2), Sox9, aggrecan, and Col2a1 (58). Bmal1 is also important in maintaining energy homeostasis in articular cartilage. Bmal1 inhibits the expression of Sirt1, an NAD+ dependent deacetylase protein, which is repressed in osteoarthritis patients displaying induced Bmal1 levels (59). The rhythmic expression of anabolic and catabolic chondrocyte genes could play a role in maintaining the growth and repair of cartilage in sync with physical activity.

The importance of circadian rhythm in osteoclasts is still being investigated. Bone resorption by osteoclasts displays a diurnal pattern with high levels occurring at night (60). Osteoclast-restricted knockdown of Bmal1 (Cathepsin K-cre) reduced bone resorption and increased bone formation (61). Additionally, Bmal1 controls the rhythmic expression of several osteoclastic genes, including nuclear factor of activated T cells (NFATC1), dendrocyte expressed seven transmembrane protein (DCSTAMP), and acid phosphatase 5 (Acp5) (61). Steroid receptor coactivator (SRC) can initiate transcription of Bmal1/Clock in osteoclasts to activate the Nfatc1 promoter, thus generating its rhythmic expression (61). As with other peripheral tissues, glucocorticoids have also been found to be a major regulator of osteoclast entrainment and rhythmic expression of tartrate-resistance acid phosphatase (Trap), Nfatc1, and cathepsin K (62). However, much is still unknown about circadian clocks in osteoclasts.

Glucocorticoid Signaling

The glucocorticoid receptor is encoded by the Nr3c1 gene, and can be alternatively spliced into multiple isoforms, of which GRα and GRβ are the most prominent. GRα is classically known as a transcriptional activator or repressor, and is found in the cytoplasm when not bound to ligand. GRβ is located in the nucleus and is thought to have a dominant-negative effect on GRα. In addition, it can act on a set of targets genes not regulated by GRα. GRα complexes with heat shock protein 90 (HSP90) and 70 (HSP70), non-receptor tyrosine kinases, and immunophilins within the cytoplasm (reviewed by (63)). Glucocorticoids pass through the plasma membrane where the bind to the glucocorticoid receptor, causing homodimerization and release from the inhibitory complex, opening its to conformation to expose the nuclear localization signal (reviewed by (63)).

Heat shock proteins chaperone and translocate the ligand-bound glucocorticoid receptor to the nucleus. The glucocorticoid receptor then recruits coactivators and chromatin-remodeling complexes to interact with palindromic sequences termed Glucocorticoid Responsive Elements (GREs), found in promoters or within target genes, to activate transcription. Direct glucocorticoid receptor target genes include dual specificity phosphatase 1 (Dusp1), glucocorticoid induced leucine zipper (Gilz), and serum/glucocorticoid regulated kinase 1 (Sgk1) (reviewed by (64)). The glucocorticoid receptor can also indirectly regulate gene expression by recruiting other transcription factors (reviewed by (65)). In addition, the glucocorticoid receptor can target negative

GREs, recruiting corepressors nuclear corepressor 1 (NCoR1) and nuclear corepressor 2 (NCoR2) to engage histone deacetylases, to repress transcription (reviewed by (63).

The activity of the glucocorticoid receptor can be modified post-translationally by phosphorylation, acetylation, and SUMOylation. Phosphorylation of the glucocorticoid receptor by kinases including MAPK, cyclin-dependent kinase, and glycogen-synthase kinase-3 (GSK-3) occur post-ligand binding and have been reported to activate or repress activity (66,67). Acetylation of the glucocorticoid receptor impairs its activity, and its levels and acetylation are regulated in a circadian manner. Glucocorticoid receptor levels peak at night and dip in the morning, whereas acetylation of the glucocorticoid receptor peaks in the morning and is lowest at night, which increases cell sensitivity to glucocorticoids at night (68). Additionally, hyperacetylation of HSP90 can inhibit its activity and prevent nuclear localization of the glucocorticoid receptor (68). Moreover, SUMOylation of the glucocorticoid receptor have been shown to regulate its subcellular localization, organization of chromatin structure, and its overall stability (69).

Glucocorticoids, among other hormones, are important entrainment signals that synchronize circadian rhythms in the kidney, liver, heart, and other tissues (70). The SCN acts as the master synchronizer in part by stimulating the release of glucocorticoids through the hypothalamic-pituitary-adrenal (HPA) axis (71,72). In humans, serum levels of glucocorticoids cycle, with their peak in the early morning, just before waking, and their lowest levels in the evening (73). The circadian clocks can be directly regulated by glucocorticoid signaling, as the glucocorticoid receptor transcriptionally activates

expression of Per1 through a GRE in its promoter, and Per2 through a GRE in the first intron (74-76). Indeed, oscillating levels of circulating glucocorticoids correspond to Per1 mRNA levels in peripheral tissues (77).

High levels of glucocorticoids can disrupt the circadian rhythm, and several disorders have been linked to altered glucocorticoids levels (reviewed by (78)). Patients with Cushing's syndrome display high levels of endogenous glucocorticoids, have an altered daily rhythm and frequently experience sleep disorders such as sleep apnea or sleep fragmentation (reviewed by (78)). Patients with this disorder frequently have diabetes mellitus, hypertension and osteoporosis, as well as other secondary disorders and diseases (reviewed by (78)).

The role of glucocorticoid signaling in bone is complex. Normal, endogenous glucocorticoids are critical for skeletal health (reviewed by (79)). Glucocorticoids can enhance the expression of osteoblast differentiation markers such as alkaline phosphatase, osteocalcin, and bone sialoprotein *in vitro* (reviewed by (80)). In contrast, excessive exposure of the skeleton to glucocorticoids leads to the development of osteoporosis, which is frequently seen in patients treated long term with glucocorticoids for autoimmune disorders, inflammatory disease or malignancy. Glucocorticoid excess causes bone loss due to decreased osteoblast activity, reduced osteoblast number, increased osteocyte apoptosis, and disruption of extracellular matrix production (reviewed by (81)). Osteocalcin, particularly the undercarboxylated form, is thought to be involved in glucose metabolism, modifying insulin secretion and sensitivity (82,83). Most

recently, it was shown that glucocorticoid-mediated suppression of osteocalcin synthesis in bone mediated at least some of the adverse effects of glucocorticoids on energy metabolism, such as increased adiposity, insulin resistance and glucose intolerance (84).

MicroRNAs (miRNAs, miRs)

microRNAs (miRNAs) play a crucial role in osteoblasts by regulating multiple genes involved in osteoblast differentiation and function. miRNAs are short (19-25 nucleotides) non-coding RNAs that bind specific target mRNA sequences, resulting in either mRNA degradation or translational suppression. Primary miRNAs (pri-miRNAs) are transcribed by RNA polymerase II or III and are processed by the Drosha-DiGeorge syndrome region gene 8 (DGCR8) complex to form precursor miRNAs (pre-miRNAs) (Figure 1.3; (85)). The Dicer complex cleaves the pre-miRNA allowing its incorporation into the RNA-induced silencing complex (RISC). Helicase mediates the unwinding of the miRNA complex and removal of the unselected strand. The RISC complex will then guide the mature strand towards the seed binding region of a target mRNA, frequently located in the 3' Untranslated Region (UTR), ultimately suppressing translation or causing mRNA degradation. miRNA activity can be complex, with a single miRNA regulating several mRNAs, or multiple miRNAs regulating a single mRNA.

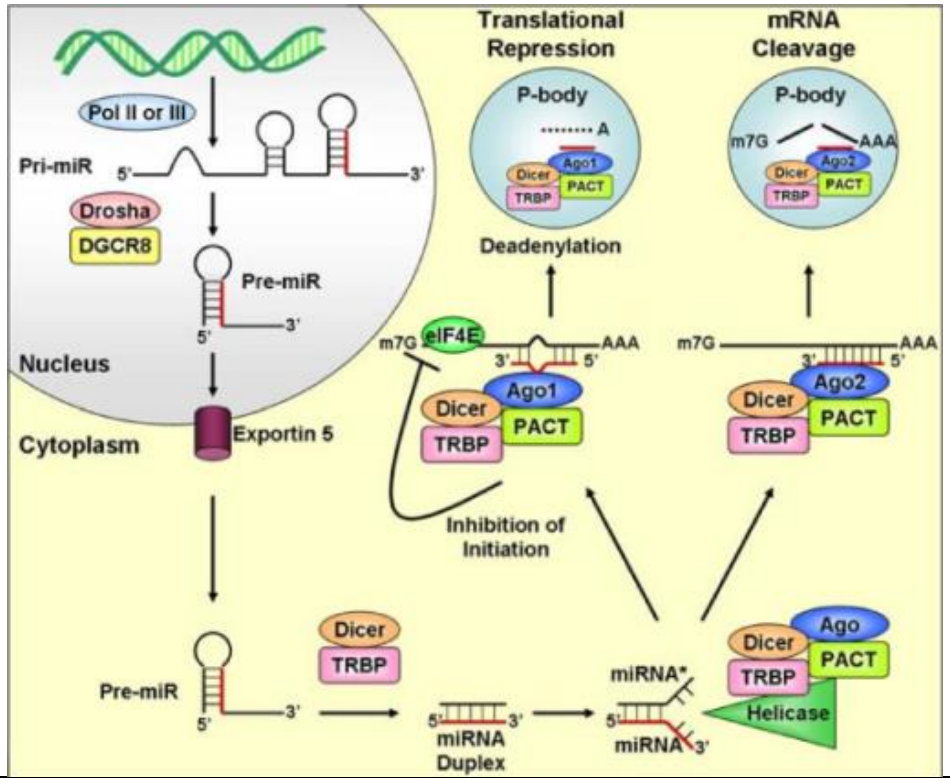

Figure 1.3: miRNA biosynthesis. pri-miRNA are transcribed from DNA and cleaved by the Drosha/DGCR8 complex to form the precursor miRNA. The pre-miRNA is exported from the nucleus by Exportin. The Dicer complex cleaves the pre-miRNA into a 21 nucleotide duplex which is incorporated into the miRNA RISC complex where helicase unwinds the double stranded miRNA to form a mature strand and a complementary passenger stand. RISC allows binding of the miRNA to target mRNA to result in either mRNA degradation or a suppression of translation (85).

The general importance of miRNAs in osteoblast biology was first demonstrated in mice in which Dicer was deleted in mature osteoblasts. These mice displayed increased cortical and trabecular bone volume, as well as perinatal bone formation (86). However, it is critical to keep in mind that individual miRNAs may have a positive or negative effect on osteoblast differentiation and function. For example, miRNAs targeting the bone morphogenic protein (BMP) pathway, can decrease osteogenesis. Overexpression of miR-133 and miR-135 antagonizes BMP induction of alkaline phosphatase, osteocalcin, and Runx2 (87,88). In our lab, miR-29 was found to induce osteoblast maturation and

target negative regulators of the Wnt signaling pathway, providing a potential underlying mechanism (89-91).

MicroRNA Regulation of Circadian Rhythm

Increasing evidence suggests that post-transcriptional regulators are an essential component of circadian clock control and make significant contributions to mRNA rhythms. The expression of more than 1000 non-coding RNAs have been found to be rhythmic (34). Among these, miRNAs were shown to display circadian rhythmicity in tissues including the liver, retina and SCN (92,93). One microRNA has even been found to display diurnal variation in human breast milk (94).

On a macro scale, the rhythmicity of miRNAs can be determined by the levels of Dicer, since it is important for processing the mature miRNA. Indeed, Dicer displays a robust and differential rhythmicity in a variety of tissues. In the SCN and bone marrow mononuclear cells (BMNC), Dicer expression peaks at ZT5, while in retina its expression peaks at ZT 21, and in liver at ZT 9 (95). However, in mice aged to 24 months or in mice with diabetes, the peak expression of Dicer was shifted in the liver and SCN, and was decreased in the retina and in BMNC (95). In BMNC, the shift in Dicer expression changed the anti-phasic expression pattern of miR-146a and miR-125a (95). In Dicer deficient mouse embryonic fibroblasts (MEFs), the period for rhythmic expression of circadian clock genes was shortened by 2 hours, which was attributed to miR-24, miR-29a, and miR-30a targeting of the 3'UTR of the Per2 and Per3 mRNAs (96). Another study examining Dicer deficient mice also revealed changes in the liver, with an increase in the

period of circadian clock gene expression, with the most dramatic effect observed on all Per mRNA isoforms (97). However, the overall changes on liver physiological function were not as substantial as those seen in MEFs, indicating tissue-specific effects of miRNAs on circadian rhythm or inherent differences in *in vivo* or *in vitro* systems.

miRNAs can help maintain circadian rhythm; conversely, miRNA expression can be regulated by circadian outputs (98-101). miRNAs can reduce targets' oscillation amplitude and alter frequency by interfering with temporal gene expression (102). miRNAs can directly regulate circadian clocks in multiple tissues, and much of the work on miRNA targeting of clock genes has been done in the SCN (98,100,103-108). For example, miR-191 inhibits Bmal1 in the SCN, while miR-181 targets Clock (99). Moreover, miR-142 also targets the 3'UTR of Bmal1 in the SCN, and its overexpression represses the rhythmic expression of Bmal1 (108). Additionally, miR-185 targets the 3'UTR of Cry1 and helps maintain its rhythmic expression in the SCN (107). In fibroblasts, the miR-192/miR-194 cluster was shown to target the 3'UTR of each of the Period genes, and overexpression of this cluster caused secondary effects by shortening the period of Bmal1 expression (108). Lastly, miR-107 targets Clock in enterocytes, which are the cells that line the intestinal tract; inhibition of miR-107 leads to deregulation of the circadian clocks, altering the phase and amplitude of their expression (109).

Circadian Clocks Regulate miRNA Rhythmicity

Conversely, the circadian clocks can regulate the rhythmic expression of miRNAs. Theoretical computational analysis predicted that miR-219 and miR-132, 2 miRNAs

expressed in the brain, could potentially modulate the rhythmicity of the circadian clocks (110). Indeed, experimental analysis of these miRNAs show they play an important role in regulating the circadian rhythm in the SCN. Bmal1/Clock can induce expression of miR-219 by direct binding to its promotor (111). *In vivo* antisense knockdown of miR-219 and miR-132 in the SCN results in a lengthened circadian period and a defective light-induced clock resetting (111). However, miR-132 was shown to work independently of Bmal1 and Clock regulation, and is instead regulated by the negative transcriptional regulators Cry1 and Cry2 (111).

miRNA Regulation of Liver Rhythmicity

The impact of miRNA regulation of circadian rhythm is most apparent in the liver. The liver's circadian rhythm is determined primarily by feeding patterns, and therefore its function is highly cyclical. Liver metabolism is under circadian control, with glucose, bile acids, lipids, and cholesterol displaying diurnal patterns (112). RNA sequencing studies of liver from mice kept under a 12 hour light/dark cycle revealed that the liver has 1,160 oscillating protein coding transcripts, composing approximately 10% of the total genes (92,99). Interestingly, 373 of the transcripts had highest expression in the evening, while 301 transcripts were high in the morning, corresponding to murine feeding patterns (92). RNA sequencing also revealed that the liver had 54 miRNAs that were expressed in a circadian manner, including miR-33, let-7, miR-103, and miR-122, many of which have been shown to impact liver function (92).

The miR-122 locus is highly expressed and is regulated by the circadian clocks (113-115). The pri and pre-miRNA forms of miR-122 display rhythmic expression in murine liver, with peak expression early in the morning (115). However, despite this pattern, mature miR-122 expression does not change throughout the day, suggesting differences in stability between the mature and pri and pre-miRNA forms (115). The miR-122 promoter contains 2 regions under the control of Rev-erbα, with Rev-erbα deficient mice showing an inability to produce cycling miR-122 (115). Conditional knockdown of liver miR-122 results in substantial alterations in several rhythmic mRNAs, with changes in amplitude, magnitude, and phase, especially in cholesterol and lipid metabolism genes (115). For example, peroxisome proliferator-activated receptor β/δ (Pparβ/δ) and the Pparα coactivator Smarcd1/Baf60a (Swi/Snf-related, matrix-associated, actin dependent regulator of chromatin, subfamily d, member 1/Brg1-associated factor 60a) were directly targeted by miR-122 in the 3'UTR (115).

Moreover, miR-122 targets Nocturnin, a key deadenylase highly rhythmic in liver. Mice deficient in Nocturnin have altered lipid metabolism (116). Anti-sense oligonucleotide knockdown of miR-122 activity in the liver increased Nocturnin amplitude and heightened its expression at night, suggesting that miR-122 mediates its rhythmic expression (117). In turn, Nocturnin influences the rhythmic expression of other genes, such as Igf1, which could potentially regulate the clock output pathway to impact tissue function. Overall, miR-122 appears to be a potent modulator of circadian output pathways that can alter liver homeostasis. The circadian expression of miRNAs in the liver impacts the regulation of their targets, thereby affecting liver physiology and metabolism.

MicroRNA Regulation of Circadian Rhythm in the SCN

The suprachiasmatic nucleus is the master synchronizer of the circadian clocks, and as such, is a highly rhythmic tissue that is under miRNA regulation. miR-132 displays robust rhythmicity within the SCN, with its expression increasing after exposure to light (111). The expression of miR-132 is regulated by the MAPK and CREB pathways (111). *In vivo* knockdown of miR-132 activity increases SCN sensitivity to light, revealing miR-132 as a negative regulator of light entrainment (111). Overexpression of miR-132 alters mouse behavior by diminishing wheel-running activities and shifting their phase in response to light (98). miR-132 regulates the circadian clocks response to light by targeting chromatin and translational regulators. miR-132 directly targets Mecp2, a CpG repeat binding protein, a chromatin regulator, p300, and Jarid1a, a translational regulator, in *vitro* and *in vivo* (98). miR-132 also inhibits the translational regulators Btg2 and Paip2a (98). Overexpression of Mecp2 increased promoter activity of Per1 and Per2, indicating a potential mechanism whereby miR-132 could regulate entrainment (98). In turn, mice deficient for the translational regulator Paip2a have reduced expression of the Period genes (98). Most interestingly, Paip2a and Btg2 can feedback on Period transcripts to accelerate their decay (98). Taken together, these results suggest a highly interconnected transcriptional and post-transcriptional loop involving the circadian clocks, miR-132, and miR-132 target genes. As a result, miR-132 can alter entrainment of the SCN, thereby potentially affecting downstream synchronization of peripheral tissues throughout the body. In addition, miR-132 actions can modify chromatin remodeling and translation within the SCN.

miRNA Regulation of Circadian Rhythm in the Immune System

Like many other physiological functions, innate immunity is under circadian control. The immune response fluctuates during different times of the day, altering immune cell number, cell movement, and cytokine production to match peak activity within the organism. This allows the immune system to coordinate the inflammatory response to times when pathogen exposure is higher, improving immune efficiency and recovery (118). The expression of miR-155, a pro-inflammatory microRNA, and miR-146, an immune repressor, appear to help mediate the rhythmic immune response. miR-155 expression increases at night, correlating with the active phase in mice (119). In response to lipopolysaccharides (LPS), the transcription factor ETS2 induces miR-155 expression (119,120). Additionally, miR-155 is suppressed by interleukin-10 (IL-10), and IL-10 is under circadian control as its expression is induced by Bmal1 (119,120). miR-155 suppresses Bmal1 in myeloid cells and inhibits Bmal1-mediated repression of nuclear factor κB (NF-κB) and TNFα (119). Inhibition or overexpression of miR-155 also alters the phase of Bmal1 expression and ablates the cytokine response to LPS (119). Overall, the innate immune system, in response LPS exposure, can induce miR-155 expression to downregulate Bmal1, thereby activating an inflammatory response by myeloid cells.

Additionally, chronic inflammation can disrupt circadian rhythm, which has been linked to the pathogenesis of diabetic retinopathy and the alteration of miR-146 expression (121). In diabetic rats, Bmal1 amplitude is markedly increased while Per1 expression is repressed, when compared to non-diabetic rats (121). Whereas non-

diabetic rats exhibited oscillatory expression of miR-146 in retinas, rhythmicity was ablated in diabetic rats (121). miR-146 directly targets IL-1 receptor-associated kinase 1 (Irak1), a pro-inflammatory cytokine, and the expression pattern of these 2 genes is anti-phasic. In diabetic rats, Irak1 rhythmic expression was also ablated (121). In humans, Irak1 expression was upregulated in diabetic patients, increasing downstream intracellular adhesion molecule 1 (Icam-1) activity, which alters monocyte adhesion and leukocyte migration (121). Overall, microRNAs can modulate the immune response by regulating rhythmic expression of target genes.

miRNA Regulation of Circadian Rhythm During Development

Although understudied, there is evidence that miRNAs can regulate developmental processes. One study used deep sequencing to examine the miRNA profile in chickens before and after gonad development; 144 miRNAs were found to be induced or decreased within the hypothalamus, the region that hosts the SCN (122). 15 of the most differentially expressed miRNAs during gonad development were predicted to target 7 circadian clock genes, including Per2, Bmal1, Bmal2, Clock, and Cry1/2 (122). Circadian clock genes show significant upregulation following gonad development. It is important to note that the impact of the circadian clocks during development is still vastly unknown, and therefore potential interpretations of the impact of miRNAs are still limited.

Clinical Implications

miRNA regulation of circadian rhythms has potential clinical implications. For example, there are no reliable non-invasive tests for diagnosing women with

endometriosis, and as a result, many women presenting with pelvic pain undergo a laparoscopy. In healthy patients, circulating plasma levels miR-200a and miR-141 increase in the evening (123). However, patients with endometriosis were unable to generate circadian expression of miR-200a and miR-141, with suppressed expression during the evening (123). These findings support the concept that serum levels of these miRNAs may potentially be used as biomarkers for diagnosing endometriosis, although further research is needed.

Recently, miR-182 has been implicated in a circadian rhythm disorder in neonatal patients with hypoxic-ischemic brain damage (HIBD) (124). In patients with HIBD, there is a significant upregulation of circadian clock protein levels but no change in mRNA expression within the pineal gland. Administration of miR-182 agonists or mimic in the pineal gland inhibited Clock protein expression, whereas oxygen deprivation of pinealocytes downregulated miR-182 expression, increasing Clock protein levels (124). This study suggested that miR-182 may be a potential therapeutic target to restore circadian rhythms in patients with HIBD (124).

Within the brain, miR-96 could potentially be targeted to protect the nervous system from damage caused by oxidative stress. miR-96 displays a diurnal rhythm and inhibits glutathione production, a well-established anti-oxidant which protects against oxidative stress (125). miR-96 targets the 3’UTR of cysteine transporter excitatory amino acid carrier 1 (EEAAC1), an important transporter of the amino acid cysteine, which is considered a major determinant for glutathione synthesis in neurons (125). Glutathione

and reactive oxygen species display anti-phasic expression patterns in the mesencephalon and SCN, which could be modulated by miR-96 activity (125). Since there is not current therapeutic method of inducing glutathione production, a miR-96 antagomir could potentially be a future option.

Although the function and impact of many miRNAs on circadian clock output pathways have been examined in many cell types *in vitro*, their impact *in vivo* is still vastly understudied. Therefore, the overall importance of miRNAs on circadian rhythm in animals not well understood. In our research, we aim to elucidate the role of a specific miRNA in regulating the circadian clocks *in vitro* and *in vivo,* in osteoblasts and other skeletal cells.

CHAPTER 2

Research Aims and Hypotheses

miRNA regulation of circadian rhythm in the skeleton has not been reported. However, microRNA-433 (miR-433) was shown to target the glucocorticoid receptor 3' UTR within the adrenal gland (126). Rhythmic secretion of glucocorticoids is critical for synchronizing local clocks in peripheral tissues, in part by activating transcription of Per genes (127). Moreover, as circulating glucocorticoid levels fluctuate diurnally, so does the sensitivity of tissues to glucocorticoids (128). We hypothesize that miR-433 helps maintain circadian rhythm in osteoblasts by regulating glucocorticoid signaling, potentially altering skeletal homeostasis.

Additionally, preliminary data suggest that miR-433 could alter lineage commitment in the skeleton. Previously, our lab found that miR-433 could differentially target a single nucleotide polymorphism (SNP) in osteonectin (SPARC). This SNP was associated with bone mass in men with idiopathic osteoporosis and caused changes in bone mass in a knock-in mouse model (129-134). In human cells, inhibition of miR-433 activity enhanced expression of the osteoblast marker genes alkaline phosphatase and osteocalcin (134). Additionally, a mutation in the miR-433 binding site in histone deacetylase 6 (HDAC6) is associated with a form of X-linked chondrodysplasia (135). However, the function of miR-433 in chondrogenesis has not been established. Bioinformatic analyses suggested that miR-433 might target critical components of the TGF-β signaling pathway. Since TGF-β signaling is important for differentiation of

osteoblasts and chondrocytes, we hypothesized that miR-433 would inhibit differentiation of these cells.

Aim 1: Determine if miR-433 displays rhythmic expression *in vivo* and *in vitro* and whether it regulates circadian clocks

miRNAs can regulate osteoblast circadian rhythm through several mechanisms: direct inhibition of the circadian clocks, regulation of entrainment, or through targeting rhythmic osteoblastic genes. Previous studies have shown that miRNAs can display circadian expression patterns in a tissue specific manner, therefore potentially impacting the rhythmic expression of their mRNA targets. To elucidate the role of miR-433 on circadian rhythm, we will determine if it is under circadian regulation in the skeleton. To understand if miR-433 is involved in regulating circadian rhythm, we will develop an *in vitro* model of synchronized osteoblast progenitor cells, and correlate miR-433 expression with what is observed *in vivo*.

A: Examine calvarial miR-433 expression in mice maintained in a 12 hour light/dark cycle

To examine whether miR-433 displays circadian rhythmicity in the skeleton, we will examine miR-433 expression in the calvaria. Previous studies have shown calvaria to be an excellent model for circadian research within the skeleton (39,136). We will examine miR-433 expression in calvaria from C57Bl/6 mice kept under a 12 hour light/dark cycle.

Samples will be characterized based on their Zeitgeber times (ZT), with ZT0 indicating the beginning of light exposure and ZT12 as light removal. RNA will be extracted and analyzed by qRT-PCR. Bmal1 and Per2 mRNA expression will be used as markers of circadian rhythm. Previous reports show that Bmal1 and Per have anti-phasic expression, where Bmal1 expression is high and Per expression is low at the beginning of a circadian day. miR-433 expression will be examined and compared to clock gene expression, as well as other potentially rhythmic miRNAs, miR-29 and miR-30. Gene expression will be analyzed for amplitude, frequency, and period length using previously published methods (137). We anticipate that miR-433 will be regulated in a circadian manner.

B: Develop an *in vitro* model to study circadian rhythm and examine miR-433 rhythmic expression in osteoblast precursor cells.

To study the potential mechanism of miR-433 regulation on circadian rhythm, we will develop an *in vitro* model utilizing C3H/10T1/2 cells, a mesenchymal-like cell line previously shown to differentiate along the osteoblastic, chondrogenic, and adipogenic lineages (138,139). C3H/10T1/2 cells will be synchronized by a short pulse with the synthetic glucocorticoid dexamethasone, a well-established method for synchronizing cells and for studying circadian rhythm *in vitro* (140-143). We anticipate miR-433 expression will display rhythmic expression. However, it is also possible that miR-433 expression is regulated by systemic factors not present in vitro.

C: Knockdown miR-433 activity in synchronized C3H10T1/2 cells and determine the impact on the expression of circadian clock genes.

The impact of miR-433 on the circadian clocks will be determined by measuring Bmal1 and Per2 mRNA expression in synchronized C3H/10T1/2 cells stably transduced with an inducible miR-433 decoy and a non-targeting decoy. We will use a previously described inducible knockdown (pSLIK) system that allows for tight regulation of transgene expression through control of the tet responsive promoter (TRE) (144). Cells will be transduced and pools of stably transfected cells selected using hygromycin. To achieve knockdown of miR-433 activity, we will use a miR-433 tough decoy (TuD) in which the green fluorescent protein (GFP) reporter gene carries 2 miR-433 binding sites in its 3'UTR (145). When transcribed, the miR-433 tough decoy will act as a competitive inhibitor for endogenous miR-433, therefore relieving suppression of its targets. As a control, C3H/10T1/2 cells will be transduced with a non-targeting *C. elegans* tough decoy construct.

C3H/10T1/2 miR-433 and non-targeting decoy cells will be synchronized using dexamethasone and treated with or without the tetracycline Doxycycline (Dox). Cells will be harvested every 6 hours for a 48 hour period. Bmal1 and Per2 mRNA expression will be quantified by qRT-PCR. Rhythmicity will be examined for changes in amplitude, period length, frequency, and phase of expression. We predict that miR-433 inhibition will disrupt the rhythmic expression of both Bmal1 and Per2. We hypothesize that miR-433 may promote Bmal1 expression and activity through suppressing expression of its negative regulator, Per2. Therefore, miR-433 knockdown could result in induced amplitude,

frequency, and period length of Per2 expression, with the opposite effect for Bmal1 expression.

Aim 2: Determine miR-433 regulation of glucocorticoid signaling and its impact on circadian rhythm.

miR-433 was recently shown to target the glucocorticoid receptor (Nr3c1) 3'UTR, and rhythmic secretion of glucocorticoids is critical for synchronizing local clocks in peripheral tissues, in part by activating transcription of Per genes (126,127). Moreover, as circulating glucocorticoid levels fluctuate diurnally, so does the sensitivity of tissues to glucocorticoids (128). We hypothesize that miR-433 maintains circadian rhythm in osteoblasts by regulating glucocorticoid signaling.

A: Determine if miR-433 inhibition increases Nr3c1 protein expression and affects sensitivity to glucocorticoids.

To examine if miR-433 affects glucocorticoid sensitivity in cells of the osteoblastic lineage, stably transduced C3H/10T1/2 cells expressing a miR-433 decoy will be treated with several doses of dexamethasone. Glucocorticoid treatment directly activates Dusp1 and Per2 transcription within minutes to hours of treatment, making them excellent markers for glucocorticoid signaling (127,146). Since miR-433 targets the glucocorticoid receptor, we expect miR-433 inhibition to increase Nr3c1 protein, which may augment expression of Dusp1 and Per2 after treatment with glucocorticoids. We will also examine temporal changes of Dusp1 and Per2 after dexamethasone treatment in the presence of

miR-433 inhibition. A non-targeting C3H/10T1/2 stably transduced cell line will be used as a control. Ultimately, altering glucocorticoid signaling could interfere with synchronization of the cells, thereby influencing the circadian rhythm and osteoblast function.

Aim 3: Determine miR-433 regulation of mesenchymal stem cell lineage commitment towards osteoblasts, adipocytes, or chondrocytes.

Lineage commitment and differentiation of skeletal cells requires coordinated regulation of multiple signaling systems by miRNAs. *In silico* analysis suggested that miR-433 may target important components of the TGF-β pathway, which is important for osteoblastogenesis, chondrogenesis and adipogenesis. We will use transduced C3H/10T1/2 miR-433 and non-targeting decoy cells to examine the role of miR-433 in regulating TGF-β signaling, as well as lineage commitment.

A: Determine whether miR-433 targets TGF-β pathway components and inhibits signaling.

To examine if miR-433 inhibits TGF-β signaling, we will use the C3H/10T1/2 cell line transfected with a construct carrying a luciferase reporter gene driven by a TGF-β responsive promoter (SBE4), along with a non-targeting and miR-433 inhibitor. Cells will be treated with vehicle or TGF-β1 and luciferase activity will be measured. We will confirm our results with C3H/10T1/2 non-targeting and miR-433 decoy cells, using the same reporter construct. Additionally, we will examine the activity of miR-433 on the 3'UTR of components of the TGF-β pathway predicted to be miR-433 targets (TGFBR1, TGFBR2,

SMAD2, and SMAD4) using a series of luciferase-3'UTR reporter assays. Protein levels of SMAD2 and SMAD2 phosphorylation will also be measured in response to vehicle or TGF-β treatment in miR-433 decoy cells, to examine potential regulation by miR-433. We anticipate miR-433 to inhibit TGF-β signaling by targeting multiple members in the pathway.

B: Inhibit miR-433 activity and determine effect on lineage commitment and expression of differentiation marker genes.

To determine whether miR-433 regulates mesenchymal lineage commitment, miR-433 expression will be examined in bone marrow stromal cells differentiated toward the osteoblastic, adipogenic, or chondrogenic pathways. BMSCs will be differentiated with an osteogenic cocktail containing ascorbic acid and β-glycerophosphate, and early and late markers of osteogenesis, miR-433 expression, and staining for alkaline phosphatase and Alizarin Red will be examined. C3H/10T1/2 non-targeting and miR-433 decoy cells will be differentiated towards osteoblasts using a similar cocktail, with the addition of BMP-2, and expression of osteogenic genes will be used as markers for osteogenesis. BMSCs will be differentiated towards adipocytes using rosiglitazone and insulin and early, intermediate, and late markers of adipogenesis, miR-433 levels and Oil Red O staining will be examined. C3H/10T1/2 cells non-targeting and miR-433 decoy cells will be differentiated using the same adipogenic cocktail, and expression of adipocyte genes and Oil Red O staining will be used to evaluate the effect of miR-433 on adipogenesis. To determine the impact of miR-433 on chondrogenesis, BMSCs will be grown in micromass culture, differentiated with TGF-β1 and a chondrogenic cocktail. Expression of miR-433

expression, chondrocyte marker genes and Alcian blue staining will be examined. C3H/10T1/2 non-targeting and miR-433 decoy cells grown in micromass will be differentiated with TGF-β1 and BMP-2 to measure the effect on chondrocyte markers. We predict miR-433 will inhibit osteoblastic and chondrogenic differentiation. In contrast, we predict that miR-433 might increase adipogenesis, since negative regulators of osteogenesis are often positive regulators of adipogenesis.

C. Preliminary phenotype of miR-433 decoy mice

To determine whether the function of miR-433 in osteoblast differentiation *in vivo*, we will develop a transgenic mouse model in which the miR-433 decoy, contained within the 3' UTR of the red fluorescent reporter gene tdTomato, is expressed under the control of a 3.6 kb fragment of the rat Col1a1 promoter. Circadian clock and osteoblast mRNA expression will be measured in calvaria in mice kept under a 12 hour light/dark cycle, and transgenic mice will be compared to wildtype littermates. Additionally, transgenic and wildtype controls will be examined by microCT analysis, to determine the potential impact of miR-433 on cortical and trabecular bone parameters. We predict miR-433 will be an important regulator of the circadian clocks in the calvaria, and that transgenic mice will have enhanced bone formation.

CHAPTER 3

microRNA-433 Dampens Glucocorticoid Receptor Signaling, Impacting Circadian Rhythm and Osteoblastic Gene Expression

Spenser S. Smith[1], Neha S. Dole[1,2], Tiziana Franceschetti[1,3], Henry C. Hrdlicka[1], Anne M. Delany[1,*]

[1] Center for Molecular Medicine, UConn Health, Farmington, CT, 06030, USA

Present Address:
[2]Department of Orthopedic Surgery, University of California San Francisco School of Medicine, San Francisco, CA, 94143 USA
[3]Institute of Medical Sciences, University of Aberdeen, Aberdeen, AB25 2ZD UK

ABSTRACT

Serum glucocorticoids play a critical role in synchronizing circadian rhythm in peripheral tissues, and multiple mechanisms regulate tissue sensitivity to glucocorticoids. In the skeleton, circadian rhythm helps coordinate bone formation and resorption. Circadian rhythm is regulated through transcriptional and post-transcriptional feedback loops that include microRNAs. How microRNAs regulate circadian rhythm in bone is unexplored. We show that in mouse calvaria, miR-433 displays robust circadian rhythm, peaking just after dark. In C3H/10T1/2 cells synchronized with a pulse of dexamethasone, inhibition of miR-433 using a tough decoy altered the period and amplitude of Per2 gene expression, suggesting that miR-433 regulates rhythm. Although miR-433 does not directly target the Per2 3'UTR, it does target 2 rhythmically expressed genes in calvaria, Igf1 and Hif1α. miR-433 can target the glucocorticoid receptor; however glucocorticoid receptor protein abundance was unaffected in miR-433 decoy cells. Rather, miR-433 inhibition dramatically enhanced glucocorticoid signaling due to increased nuclear

receptor translocation, activating glucocorticoid receptor transcriptional targets. Lastly, in calvaria of transgenic mice expressing a miR-433 decoy in osteoblastic cells (Col3.6 promoter), the amplitude of Per2 and Bmal1 mRNA oscillation was increased. miR-433 was previously shown to target Runx2, and mRNA for Runx2 and its downstream target, osteocalcin were also increased in miR-433 decoy mouse calvaria. We hypothesize that miR-433 helps maintain circadian rhythm in osteoblasts by regulating sensitivity to glucocorticoid receptor signaling.

INTRODUCTION

The circadian rhythm is an internal timing mechanism important for orchestrating physiological homeostasis, through synchronizing behavioral and physiological patterns. This coordinates biological processes critical for overall health, such as tissue repair and growth, maintenance of the immune response, and optimization of metabolism. The circadian rhythm is driven by a complex interaction between the hypothalamic suprachiasmatic nucleus (SCN), also known as the central clock, and the peripheral circadian clocks. As the central oscillator, the SCN responds to environmental periodic cues such as light, eating patterns, and temperature. In response to these cues, the SCN entrains peripheral circadian clocks through stimulation of neural or hormonal signals (e.g. glucocorticoids) to enact their effects on target tissues (147).

In the central oscillator and peripheral tissues, the rhythm is maintained locally by clock genes that interact through transcriptional and post-transcriptional feedback loops. The main positive regulators are aryl hydrocarbon receptor nuclear translocator-like (Arntl

or Bmal1) and circadian locomotor output cycles kaput (Clock), which are negatively regulated by the period genes (Per1, Per2, Per3) and the cryptochrome genes (Cry1, Cry2), among others (reviewed by (148)). Bmal1 and Clock form a heterodimer and bind to E-box elements of target genes, including the Per and Cry genes, to rhythmically induce transcription. Per/Cry can negatively feedback to inhibit their own transcription as well as the transcription of Bmal1/Clock, ensuring the anti-phasic expression of clock proteins. This interaction between the clock proteins determines the oscillatory expression of target genes and contributes to the rhythmicity of physiological systems (149).

Bone is a continuously remodelling tissue, and disturbances in circadian rhythm have a negative impact on skeletal health (36,37,150,151). Bone remodelling is the coupled cycle of osteoclast-mediated bone resorption followed by osteoblast-mediated bone formation. This process is critical for renewal of bone in adults and for mineral homeostasis. Imbalance in the bone remodelling process can lead to prevalent diseases, such as osteoporosis.

In osteoblasts, 26% of genes display a diurnal expression pattern, including the master osteoblast transcription factor Runt-related transcriptional factor (Runx2), bone morphogenetic protein 2 (BMP2), Osteocalcin (Oc, Bglap), Insulin-like Growth Factor 1 (Igf1), and Hypoxia-inducible factor 1α (Hif1α) (150,151). Evidence suggests that, in humans, circadian rhythm coordinates bone remodelling so that it occurs primarily at night. For example, bone formation markers such as serum osteocalcin, as well as serum markers of type I collagen synthesis, the major protein component of bone matrix, are highest in pre-menopausal women at night (37,38). Moreover, serum levels of

glucocorticoids, which are known to play an important role in synchronizing peripheral clocks, are critical for the diurnal variation in serum osteocalcin (152).

microRNAs (miRNAs) are key mediators of post-transcriptional regulation. These short (19-25 nucleotide) non-coding RNAs bind specific target mRNAs, resulting in mRNA degradation and/or translational suppression. Many miRNAs fine tune the timing and tempo of gene expression programs, and these post-transcriptional regulators are an important component of circadian clock control. Indeed, miRNAs display circadian rhythmicity in many tissues, including the liver, retina and SCN (92,93). miRNAs can directly regulate circadian clocks; for example, miR-191 directly targets the 3' untranslated region (UTR) of Bmal1 in the liver (99). Alternatively, miRNAs can indirectly control circadian rhythm by targeting downstream regulators, as is the case for miR-122 targeting of Nocturnin, a key circadian deadenylase. (117). Conversely, clock genes can directly regulate miRNA expression; for example, Bmal1/Clock induces expression of miR-219, and *in vivo* miR-219 knockdown results in a lengthened circadian period (111).

miRNA regulation of circadian rhythm in the skeleton has not been reported. However, within the adrenal gland, miR-433 was recently shown to target the glucocorticoid receptor (Nr3c1, GR) 3' UTR (126). Rhythmic secretion of glucocorticoids is critical for synchronizing local clocks in peripheral tissues, in part by activating transcription of Per genes (76). Moreover, as circulating glucocorticoid levels fluctuate diurnally, so does the sensitivity of tissues to glucocorticoids (128). Herein, we demonstrate that miR-433 regulates glucocorticoid signaling and impacts the expression of the circadian clocks and osteoblastic genes *in vitro* and *in vivo*.

RESULTS

miR-433 expression is rhythmic in calvaria

To determine whether miR-433 might play a role in osteoblast circadian rhythm, we first determined if it is under circadian regulation in the skeleton. RNA was isolated from calvaria of male mice kept under a 12 hour light/dark cycle, represented as Zeitgeber time (ZT). ZT0 is the beginning of light exposure, whereas ZT12 is the beginning of light removal. Examining two markers of circadian rhythm Bmal1 and Per2 over two 24 hour cycles, these 2 circadian genes displayed the expected anti-phasic pattern of expression throughout each 24 hour cycle. For example, Bmal1 mRNA expression was highest at ZT1 while Per2 mRNA was low; the nadir for Bmal1 mRNA was just prior to light removal, while Per2 mRNA had its peak expression just after dark (Figure 3.1A).

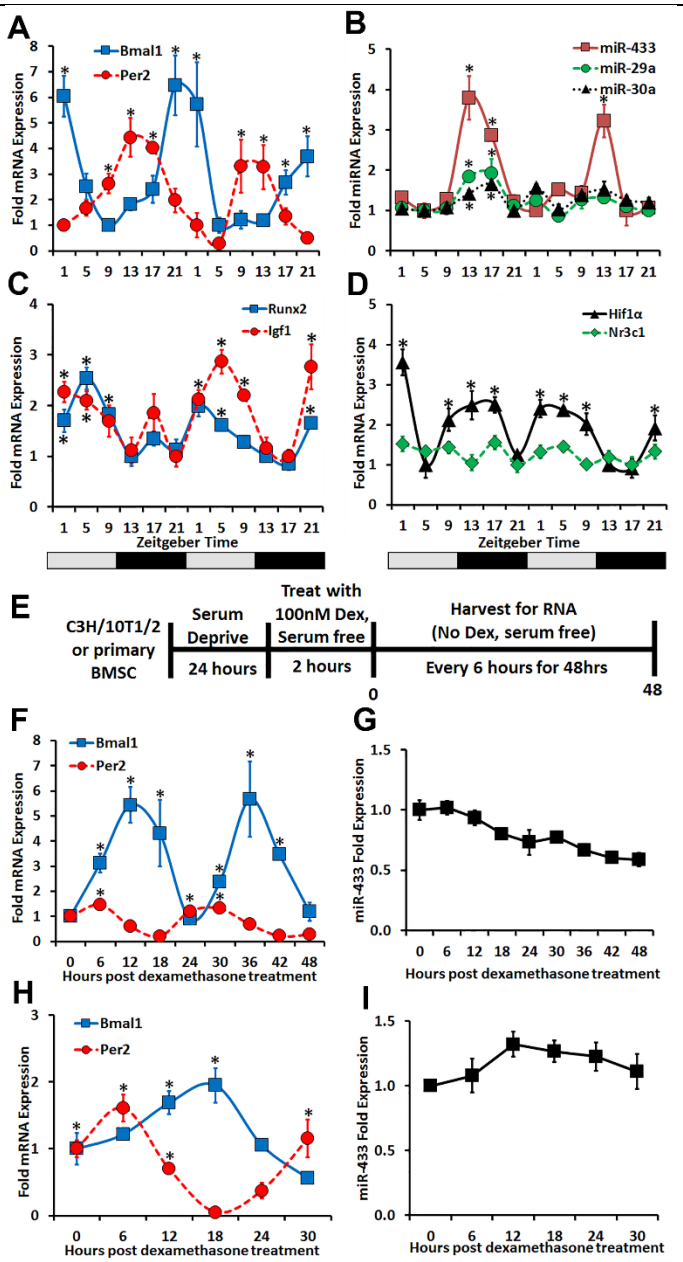

Figure 3.1. Rhythmic expression of circadian clock mRNAs, miRNAs and osteogenic genes in mouse calvaria and validation of an *in vitro* model to study circadian rhythm.

C57BL/6J mice were kept under a 12 hour light/dark cycle; calvaria were harvested every 4 hours. Two 24 hour cycles are shown. RNA levels were quantified by qRT-PCR. Zeitgeber time (ZT): ZT0 indicates the beginning of light exposure and ZT12 the beginning of light removal. (A) Markers of circadian rhythm, Bmal1 (blue) and Per2 (red). (B) miR-433 (red), miR-29a (green) and miR-30a (black). (C) Osteogenic genes Runx2 (blue), Igf1 (red), and (D) Hif1α (black), and Nr3c1 (glucocorticoid receptor) (green). Fold change in each gene is expressed relative to the nadir (n=5). (E) Experimental design for synchronizing C3H/10T1/2 cells and primary BMSCs.

Expression of Bmal1 (blue) and Per2 (red) mRNA, and miR-433 in synchronized (F, G) C3H/10T1/2 cells (n=6) and (H, I) BMSCs (n=3). Data are expressed as fold change in gene expression, relative to time 0. * = significantly different from the nadir, $p < 0.05$.

We analyzed the expression of three microRNAs, miR-433, miR-29a, and miR-30a, because they were either shown to display rhythmic expression in other tissues or predicted via bioinformatics analysis to potentially target the glucocorticoid receptor or circadian clock genes (92). miR-433 displayed robust rhythmicity in mouse calvaria (Figure 3.1B). The miR-433 expression pattern was anti-phasic in relation to Bmal1 mRNA, peaking 4 fold after light removal, and decreasing as night progressed. miR-29a and miR-30a expression peaked at ZT17, but the amplitude of their rhythm was more modest in comparison to miR-433 (Figure 3.1B).

We also examined the mRNA expression of osteogenic genes previously reported to display circadian rhythmicity *in vivo* (36,150). Both Runx2 and Igf1 mRNAs appeared to peak early in the day, while Hif1α mRNA displayed a broad peak during each 24 hour cycle (Figure 3.1C, D). In contrast, glucocorticoid receptor (Nr3c1) mRNA did not display rhythmic expression in calvaria (Figure 3.1D).

Development of an *in vitro* model to study circadian rhythm

To better understand the role of miR-433 in circadian rhythm, we used a well-established protocol in which the multi-potent mouse C3H/10T1/2 cell line and primary mouse bone marrow stromal cells (BMSCs) were synchronized with a pulse of the synthetic glucocorticoid dexamethasone (140,141). Briefly, C3H/10T1/2 cells and BMSCs

were serum deprived for 24 hours, then treated with a 2 hour pulse of 100 nM dexamethasone. The dexamethasone was removed (time 0), replaced with serum free medium, and RNA was collected for up to 48 hours (Figure 3.1E). The C3H/10T1/2 cells remained synchronized for 48 hours, whereas the BMSCs only remained synchronized for ~30 hours. Bmal1 and Per2 mRNA expression displayed rhythmic and anti-phasic expression patterns in both C3H/10T1/2 cells and BMSCs, confirming synchronization of the cultures (Figure 3.1F, H). However, miR-433 did not display rhythmicity in either cell type, suggesting that a systemic factor establishes miR-433 rhythm *in vivo* (Figure 3.1G, I).

miR-433 targets the 3'UTR of Hif1α and Igf1, but not Per2

To determine whether miR-433 may directly target the circadian clocks, we employed a bioinformatic approach using several online databases (miRanda, TargetScan, RNAhybrid) to examine complementarity of the miR-433 seed binding region to the 3' UTR of clock mRNAs (153-155). Of the circadian clock genes, only Per2 contained a potential miR-433 binding site at position 1829 (Figure 3.2A). Runx2, Hif1α and Igf1 are rhythmically expressed genes in bone. Whereas Runx2 was previously confirmed as a miR-433 target (101), Hif1α and Igf1 had yet to be examined. The Hif1α 3' UTR contained 2 potential miR-433 binding sites at positions 352 and 879; the Igf1 3' UTR contained 2 potential sites at 4237 and 6113 (Figure 3.2A). To determine whether Per2, Igf1, and Hif1α were miR-433 targets, target gene 3' UTRs were cloned downstream of a constitutively expressed luciferase gene in the reporter plasmid pMIR-

REPORT. The luciferase constructs containing the target 3' UTRs were transiently cotransfected into

A

Target mRNA	Site Position	Seed Binding Region 3' Untranslated Region	miR-SVR Score
Per2	1829	3' uguggcuccUCGG-GUAGUACUa 5'miR-433 ||:| ||||||| 5' ugccucuaaAGUCAGAUCAUGAa 3' mRNA	-0.264
Hif1α	352	3' uguggcuccucGGGUAGUACUa 5'miR-433 ::|||||||| 5' ggcaguaaccuUUCAUCAUGAu 3' mRNA	-0.8488
Hif1α	879	3' uguggcuccucgggUAGUACua 5'miR-433 |||||| 5' acaagaaaaaaaaaAUCAUGca 3' mRNA	-0.4316
Igf1	4237	3' uguggCUCCUCG--GGUAGUACUa 5'miR-433 ||| ||: |: |||||| 5' ucaaaGAGCAGUAGCUCUCAUGAa 3' mRNA	-0.008
Igf1	6113	3' uguggcuccuCGGGUAGUACUa 5' miR-433 |: :||||||| 5' aucugugucuGUGUAUCAUGAa 3' mRNA	-0.2121

B

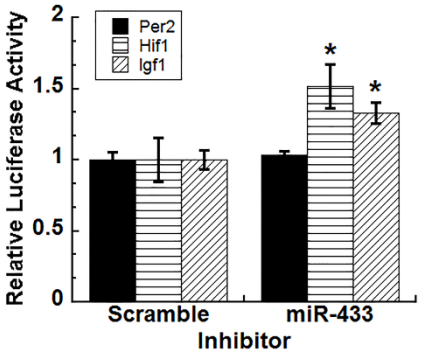

Figure 3.2. Examination of miR-433 targets.
(A) Potential interaction of miR-433 with Hif1α, Igf1, and Per2 3' UTRs, as predicted by miRanda (153). (B) Activity of the Per2, Hif1α and Igf1 luciferase-3' UTR reporter constructs transiently transfected into C3H/10T1/2 cells, along with a miR-433 or non-targeting inhibitor. * = significantly different from non-targeting control, $p < 0.05$. n=12.

C3H/10T1/2 cells with a non-targeting or miR-433 inhibitor, and luciferase activity was quantified. miR-433 inhibition significantly increased the luciferase activity of Hif1α and Igf1 constructs compared to the non-targeting control, but it did not affect Per2 3' UTR activity (Figure 3.2B). These data suggest that miR-433 directly targets Igf1 and Hif1α, but not Per2.

miR-433 tough decoy suppresses miR-433 activity

To better study the impact of miR-433 on circadian rhythm, we developed a stably transduced C3H/10T1/2 cell line in which the activity of miR-433 could be knocked down in an inducible manner. We used a previously described lentiviral knockdown (pSLIK) system that allows for tight regulation of transgene expression via a Doxycycline (Dox) inducible promoter (144). To achieve knockdown of miR-433 activity, we created a miR-433 tough

decoy, in which a green fluorescent protein (GFP) reporter carries 2 miR-433 binding sites in its 3' UTR (Table 3.1) (156). The miR-433 tough decoy contains a secondary structure that enhances resistance to degradation. When transcribed, the miR-433 tough decoy acts as a competitive inhibitor for endogenous miR-433, therefore relieving suppression of its targets (Figure 3.4A). As a control, a C3H/10T1/2 cell line was also established expressing a Dox-inducible non-targeting tough decoy construct.

A.

GACGGCGCTAGGATCATCAACACACCGAGGAGCCTAACCATCATGATCAAGTATTCTGG
TCACAGAATACAACACACCGAGGAGCCTAACCATCATGATCAAGATGATCCTAGCGCCG
TCCGA

B.

GATATCGACGGCGCTAGGATCATCAACTCTACTCTTTCTAGAGCTGAGGTTGTGACAAGT
ATTCTGGTCACAGAATACAACTCTACTCTTTCTAGAGCTGAGGTTGTGACAAGATGATCC
TAGCGCCGTCATCGAT

Table 3.1. Sequence of miR-433 decoy and non-targeting decoys used *in vitro*.
(A) miR-433 tough decoy used in vitro, with miR-433 binding sites underlined (GenScript custom synthesis)
(B) Non-targeting tough decoy used in vitro. It contains C. elegans miR-67 binding sites, which are underlined (GenScript custom synthesis)

To confirm doxycycline-inducible expression of the transgene, we quantified GFP mRNA in the non-targeting and miR-433 decoy cells treated for 24 hours with increasing doses of Dox. Dox induced GFP mRNA in both non-targeting and miR-433 decoy cells in a dose dependent manner (Figure 3.3B). To confirm the decoy inhibited miR-433 actions, we examined luciferase activity of the target 3'UTR constructs that were previously studied using the transiently transfected miR-433 inhibitor. In these experiments, the miR-433 decoy phenocopied the effects observed with transiently transfected miR-433 inhibitor, with similar increases in luciferase activity with Igf1 and Hif1α 3' UTR reporter

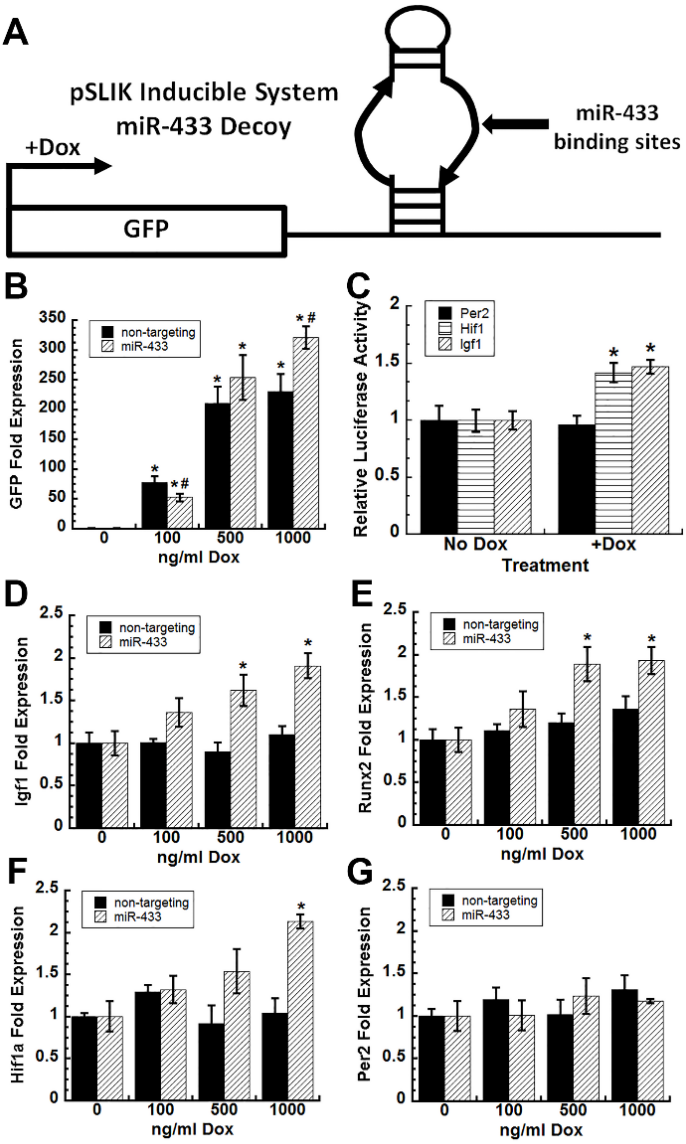

Figure 3.3. miR-433 decoy relieves repression of miR-433 target genes *in vitro*
(A) C3H/10T1/2 cells were stably transduced with a Doxycycline (Dox)-inducible construct carrying either a non-targeting or miR-433 decoy in the 3' UTR of the reporter gene GFP. Location of the miRNA binding site is denoted by the bold arrows. (B) Dose dependent Dox-mediated induction of non-targeting and miR-433 decoy in C3H/10T1/2 cells. (C) Activity of Per2, Hif1α, and Igf1 luciferase-3' UTR reporter constructs transiently transfected into miR-433 decoy cells cultured in the presence or absence of Dox (n=12). Dose dependent Dox-mediated induction of (D) Igf1, (E) Runx2 and (F) Hif1α mRNA in miR-433 decoy cells, compared with non-targeting decoy cells (n=4). (G) Per2 mRNA was not induced by Dox treatment in either miR-433 or non-targeting decoy cells (n=4). * = significantly different from no Dox control, $p < 0.05$, # = significantly different from non-targeting control, $p < 0.05$.

constructs, but no change with Per2 (Figure 3.3C). In miR-433 decoy cells, we also examined mRNA levels for a previously defined miR-433 target Runx2 (101), as well as Igf1 and Hif1α. Runx2, Igf1 and Hif1α mRNA levels were significantly increased in the presence of 1000 ng/ml Dox in the miR-433 decoy cells, but not in the non-targeting decoy cells (Figure 3.3D-F). In contrast, Per2 mRNA was unaffected at any dose tested (Figure 3.3G). Analysis of miR-433 decoy cells at additional time points after Dox treatment also failed to demonstrate significant differences in Per2 mRNA (data not shown), confirming that Per2 is not a miR-433 target. Overall, these data demonstrate that the miR-433 decoy inhibits miR-433 activity.

Disruption of miR-433 activity impacts the rhythmicity of circadian clock

Although miR-433 did not display a cell-autonomous rhythm *in vitro*, it is possible that this miRNA could still play a role in maintenance or regulation of rhythm. To examine this *in vitro*, non-targeting and miR-433 decoy cells were synchronized with a short pulse of dexamethasone, in the presence or absence of Dox. In the synchronized non-targeting decoy cells, both Bmal1 and Per2 mRNA displayed 2 peaks within the 48 hour interval. Treatment of the non-targeting decoy cells with Dox did not affect the rhythmicity of either Bmal1 or Per2 mRNA (Figure 3.4A, D). However, in cells expressing the miR-433 decoy, the first peak in Bmal1 mRNA was shifted from 6 hours to 12 hours (Figure 3.4B), and the amplitude of the peaks was decreased, an effect particularly evident when the Bmal1 mRNA levels were expressed as fold change compared with time zero (Figure 3.4C). For Per2 mRNA, the effect of miR-433 inhibition was more striking. In miR-433 decoy cells treated with Dox, Per2 mRNA levels were significantly higher at time zero, and the phase

of the Per2 rhythm was shifted (Figure 3.4E). Like Bmal1, the amplitude of Per2 mRNA peaks was decreased in the presence of the miR-433 decoy (Figure 3.4E, F).

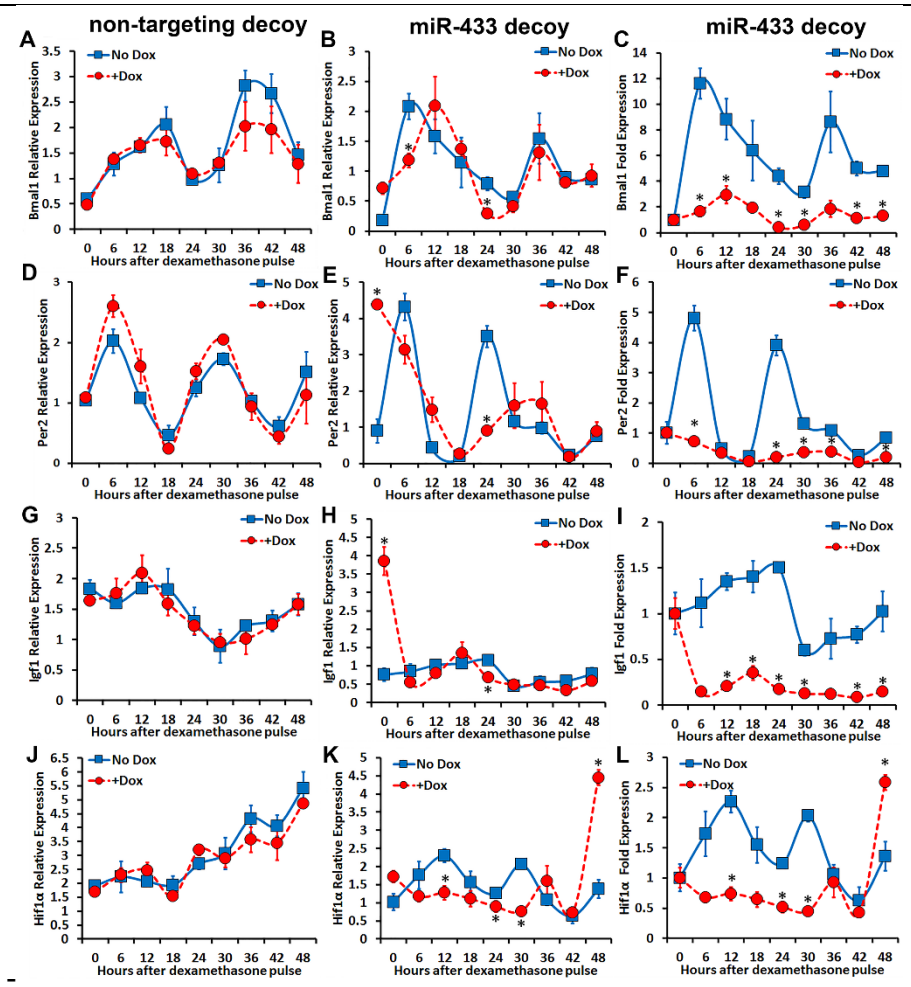

Figure 3.4. Expression of the miR-433 decoy affects circadian clock mRNA rhythmic expression.
Non-targeting and miR-433 decoy cells were cultured in the absence or presence of 1000 ng/ml doxycycline, and then synchronized using a 2 hour pulse of 100 nM dexamethasone. mRNA was isolated immediately after removal of dexamethasone (time 0) and at intervals up to 48 hours thereafter. Data are represented as relative expression (left and center columns) or fold change (right column) in non-targeting or miR-433 decoy cells. (A-C) Bmal1, (D-F) Per2, Igf1 (G-I), Hif1α (J-L). * = significantly different from corresponding time point with no Dox treatment, $p < 0.05$. n=3.

We also examined expression of osteogenic genes Igf1 and Hif1α in the synchronized cultures. Igf1 mRNA was modestly rhythmic in non-targeting decoy cells,

exhibiting a single broad peak, and its expression was unaffected by the addition of Dox (Fig. 3.4G). Similarly, in miR-433 decoy cells cultured without Dox, Igf1 mRNA also had a broad peak at 18-24 hours, and was strongly decreased at 30 hours. In contrast, when the miR-433 decoy cells were treated with Dox, Igf1 mRNA levels were significantly higher at time zero, and displayed a dramatic decrease between 0 and 6 hours (Fig. 3.4H). The effect of the miR-433 inhibition on Igf1 mRNA rhythm was most appreciated when the data were expressed as fold change compared with time zero (Fig. 3.4I). In non-targeting cells, Hif1α mRNA did not display a clear rhythmic expression pattern, but rather increased in expression over time (Fig. 3.4J). However, in miR-433 decoy cells in the absence of Dox, Hif1α had 2 peaks of expression at 12 and 30 hours (Fig. 3.4K). In cells expressing the miR-433 decoy, Hif1α mRNA was increased at time 0, and the onset of Hif1α mRNA rhythm was delayed to 36 hours (Fig. 3.4K, L). Overall, miR-433 levels appear necessary for maintenance of rhythmic expression of the circadian clock genes, Igf1 and Hif1α mRNA in synchronized cells *in vitro*.

miR-433 regulates glucocorticoid sensitivity

Glucocorticoids play a prominent role in synchronizing the peripheral clock genes, in part by activating transcription of Per genes (76). Moreover, as circulating glucocorticoids levels fluctuate diurnally, so does the sensitivity of tissues to glucocorticoids. Since miR-433 was previously shown by others to target the glucocorticoid receptor 3’ UTR (126), and because our cell cultures were synchronized using dexamethasone, we hypothesized that miR-433 could help maintain circadian rhythm in cells of the osteoblastic lineage through regulation of glucocorticoid signaling.

Dusp1 and Per2 are both direct transcriptional targets of the glucocorticoid receptor, and we used their mRNA levels as markers of glucocorticoid signaling (76,146). In C3H/10T1/2 cells, dexamethasone induced Dusp1 mRNA at 1-3 hours, whereas the increase in Per2 was more transient, peaking at 2 hours (Figure 3.5A, B). To determine whether miR-433 regulated the sensitivity of cells to glucocorticoids, we examined Dusp1 and Per2 mRNA in miR-433 decoy cells treated for 2 hours with vehicle or dexamethasone, in the absence or presence of Dox. In the absence of miR-433 decoy, dexamethasone caused a modest increase in Per2 mRNA, independent of the dose used (Figure 3.5C). In contrast, expression of the miR-433 decoy augmented the induction of Per2 mRNA, and caused a dose-responsive increase. In the absence of miR-433 decoy, 10 or 100 nM dexamethasone increased Dusp1 mRNA ~6 fold (Figure 3.5D). Expression of the miR-433 decoy further enhanced Dusp1 mRNA at both 10 nM and 100 nM dexamethasone (Figure 3.5D). Since inhibition of miR-433 activity allowed the cells to become responsive to higher levels of glucocorticoids, it is possible that miR-433 functions to limit exposure of cells to excessive glucocorticoid signaling.

To determine how miR-433 might regulate sensitivity to glucocorticoid signaling, we first examined the impact of the miR-433 decoy on glucocorticoid receptor mRNA (Nr3c1) and protein levels. To mimic the conditions of the circadian synchronization

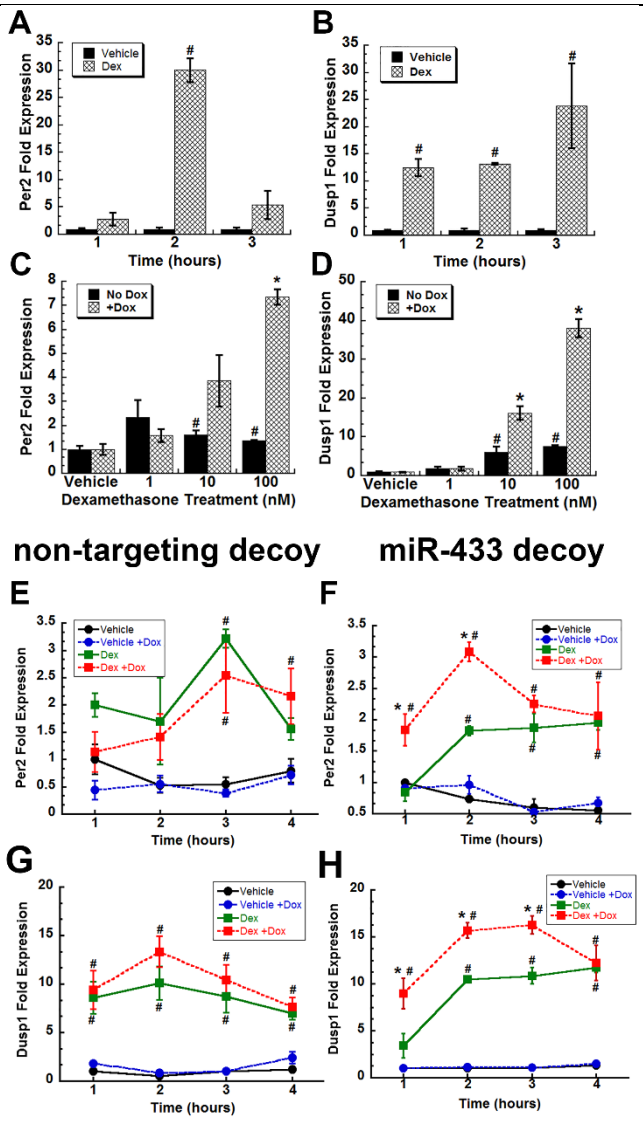

Figure 3.5. miR-433 dampens sensitivity to glucocorticoid signaling.

(A) Per2 and (B) Dusp1 mRNA in serum-deprived C3H/10T1/2 cells treated with vehicle or 100 nM dexamethasone for up to 3 hours. (C) Per2 and (D) Dusp1 mRNA levels in miR-433 decoy cells that were serum-deprived in the presence or absence of Dox, and then treated with increasing doses of dexamethasone for 2 hours. Per2 mRNA levels in (E) non-targeting decoy or (F) miR-433 decoy cells that were serum-deprived in the presence or absence of Dox, and then treated with vehicle or 100 nM dexamethasone for up to 4 hours (n=8). Dusp1 mRNA levels in (G) non-targeting decoy or (H) miR-433 decoy cells that were serum-deprived in the presence or absence of Dox, and then treated with vehicle or 100 nM dexamethasone for up to 4 hours (n=8). * = significantly different from corresponding no Dox control, $p < 0.05$; # = significantly different from corresponding vehicle treated control, $p < 0.05$.

experiments, we performed these studies in cells cultured for 24 hours in the presence or absence of Dox, then treated with 100 nM dexamethasone for 2 hours. In non-targeting

decoy cells, culture in the presence or absence of Dox did not affect mRNA or protein levels of Nr3c1 (Figure 3.6A, D). In contrast, miR-433 decoy cells treated with Dox displayed a 3 fold induction of Nr3c1 mRNA (Figure 3.6A). However, significant differences in total glucocorticoid receptor (GR) protein levels were not observed at any time point measured (Figure 3.6D). It is possible that inhibition of miR-433 alters GR mRNA translation efficiency, perhaps by indirectly modifying the complement of miRNAs or RNA binding proteins interacting with the transcript. GR protein stability could also be affected, since GR is subject to ubiquitin-mediated degradation. Overall, these data suggest that an increase in total glucocorticoid receptor levels was not responsible for the increased sensitivity to dexamethasone.

Alternative forms of the mouse glucocorticoid receptor, GRα or GRβ, are generated by alternative splicing (157). It was previously reported that GRα acts as a transcriptional activator of glucocorticoid signaling, whereas GRβ can act as a dominant negative inhibitor of GRα (157-159). Since commercially available antibodies for the mouse glucocorticoid receptor do not discriminate between GRα and GRβ isoforms, we relied on isoform-specific qRT-PCR to determine whether miR-433 inhibition might cause differences in the expression of GRα versus GRβ mRNA. miR-433 decoy cells were cultured in the absence or presence of Dox for 24 hours, and then treated with or without dexamethasone for 2 hours. GRα mRNA was increased in miR-433 decoy cells cultured in Dox, and treatment with dexamethasone did not alter GRα mRNA levels (Figure 3.6B). GRβ mRNA levels were also increased in Dox treated cells, however dexamethasone

decreased GRβ mRNA levels by about 50%, whether the miR-433 decoy was expressed or not (Figure 3.6C). These data suggest that although

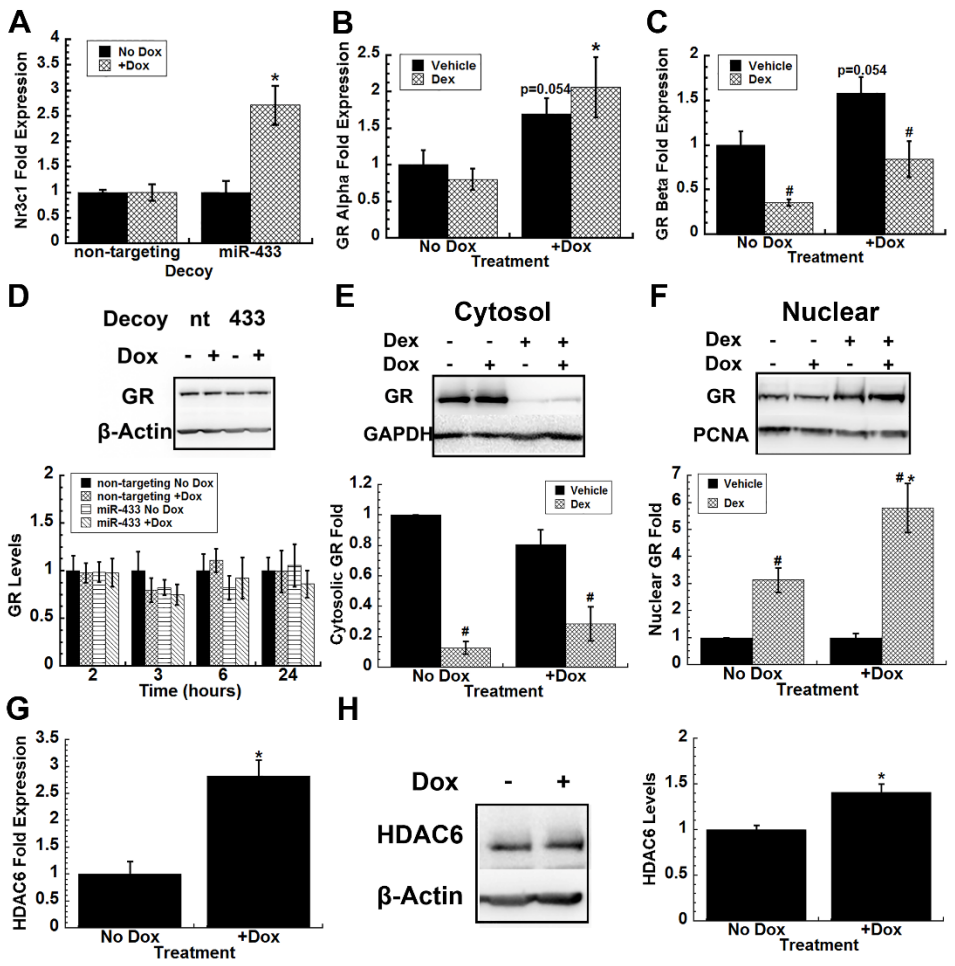

Figure 3.6. miR-433 regulates glucocorticoid receptor mRNA and subcellular localization.

Non-targeting and miR-433 decoy cells were serum-deprived for 24 hours in the presence or absence of Dox, and then treated with 100 nM dexamethasone for 2 hours. (A) Total glucocorticoid receptor mRNA, and glucocorticoid receptor mRNA isoforms, (B) GRα and (C) GRβ were quantified (n=8). (D) miR-433 decoy cells were serum-deprived in the presence or absence of Dox for 24 hours, then treated with 100 nM dexamethasone for 2, 3, 6, or 24 hours. Total glucocorticoid receptor protein levels were determined by Western blot (representative blot, 2 hour time point, above) and were quantified (below) (n=4). miR-433 decoy cells were serum-deprived for 24 hours in the presence or absence of Dox, and then treated for 2 hours with 100 nM dexamethasone. Glucocorticoid receptor subcellular localization was determined by Western blot (representative blot, above) and were quantified (below): (E) cytoplasmic

and (F) nuclear extracts (n=10). miR-433 decoy cells were serum-deprived for 24 hours in the absence or presence of Dox, and HDAC6 (G) mRNA and (H) protein were quantified (n=7). * = significantly different from corresponding no Dox control, $p < 0.05$; # = significantly different from corresponding vehicle treated control, $p < 0.05$.

dexamethasone affects the mRNA ratio of GRα to GRβ, inhibition of miR-433 activity does not impact this ratio.

Since the miR-433 decoy increased glucocorticoid signaling in the absence of significant increases in GR protein levels or changes in receptor isoform mRNA, we next examined whether miR-433 levels might affect the nuclear versus cytosolic localization of the GR. In the absence of ligand, GR is localized primarily in the cytoplasm, in a complex that includes heat shock protein 90, immunophilins and non-receptor tyrosine kinases (160). Upon ligand binding to the GR, this complex is dissociated and GR dimers translocate to the nucleus to elicit transcriptional regulation of target genes. We hypothesized that miR-433 inhibition might increase nuclear GR with glucocorticoid stimulation. To test this, miR-433 decoy cells were cultured in the presence or absence of Dox for 24 hours, then treated with or without dexamethasone for 2 hours. The levels of GR in nuclear and cytoplasmic compartments were evaluated by Western blotting. In the absence of dexamethasone, the majority of glucocorticoid receptor was found in the cytoplasm, and expression of the miR-433 decoy did not significantly alter its abundance. As expected, when cells were treated with dexamethasone, the abundance of GR in the cytoplasm was dramatically decreased; this decrease was also not significantly affected by expression of the miR-433 decoy (Figure 3.6E). Examining the nuclear compartment,

in the absence of dexamethasone stimulation, GR levels were similar in cells with or without the miR-433 decoy. However, in cells treated with dexamethasone there was an increase in nuclear GR levels, which was significantly enhanced by expression of the miR-433 decoy (Figure 3.6F). The enhanced translocation and possibly maintenance of the glucocorticoid receptor to the nucleus upon ligand binding provides a potential mechanism for the enhanced responsiveness of miR-433 decoy cells to dexamethasone.

Heat shock protein 90 (HSP90) plays an important chaperone function for GR in both the cytoplasm and nucleus. Hyperacetylation of HSP90 results in loss of its GR chaperone activity, causing defects in GR ligand binding, nuclear translocation and transcriptional activation (135,161). Histone deacetylase 6 (HDAC6) can deacetylate HSP90, and in humans, miR-433 has been shown to target HDAC6 (135). Should the miR-433 decoy increase expression of HDAC6, it could represent a potential mechanism for increasing GR nuclear localization. In miR-433 decoy cells cultured in the presence of Dox, HDAC6 mRNA expression and protein levels were significantly increased (Figure 3.6G, H), indicating that miR-433 targets HDAC6 in mice as well as humans. miR-433 effects on HDAC6 could contribute to its regulation of glucocorticoid sensitivity.

Glucocorticoids down regulate miR-433

Since microRNAs often participate in feedback loops, we determined whether glucocorticoids might regulate the expression of miR-433. In serum deprived C3H/10T1/2 cells treated with 100 nM dexamethasone for up to 24 hours, we found a modest (20-

25%) but significant reduction of miR-433 only at the 24 hour time point (Figure 3.7A). Serum deprived confluent cultures of primary BMSCs displayed a similar decrease in miR-433 expression with dexamethasone treatment (Figure 3.7B). This delay in response suggests dexamethasone indirectly regulates miR-433 expression, or it could reflect the generally long half-life of many miRNAs.

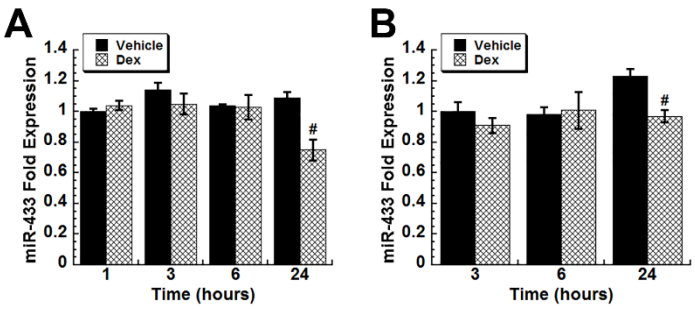

Figure 3.7. Dexamethasone decreases miR-433 expression.
miR-433 levels in serum-deprived (A) C3H/10T1/2 cells or (B) mouse bone marrow stromal cells treated with vehicle or 100 nM dexamethasone for up to 24 hours. # = significantly different from vehicle control, $p < 0.05$. n=4.

miR-433 regulates circadian clocks and osteoblastic genes *in vivo*

Our *in vitro* studies indicated that miR-433 activity dampens glucocorticoid signaling and is important for maintaining rhythmic gene expression in osteoblastic cells. To determine whether miR-433 plays a similar role in the regulation of the circadian clocks *in vivo*, we developed a transgenic mouse model in which the miR-433 decoy, contained within the 3' UTR of the red fluorescent reporter gene tdTomato, was expressed under the control of a 3.6 kb fragment of the rat Col1a1 promoter (miR-433 decoy^{Col1a1} mice) (Figure 3.8A, B). Previous studies document that transgenes under the control of this promoter are expressed most abundantly in osteoblastic cells, with lesser expression in other type I collagen containing tissues (162,163). Fluorescence microscopy of calvarial

sections from miR-433 decoy^{Col1a1} mice demonstrated that signal for tdTomato was localized to osteocytes embedded in the bone matrix, and cells on the periosteal and endosteal surfaces, where new bone is formed (Figure 3.9A).

A.

GACGGCGCTAGGATCATCAACACACCGAGGAGCCTAACCATCATGATCAAGTATTCTGG
TCACAGAATACAACACACCGAGGAGCCTAACCATCATGATCAAGATGATCCTAGCGCCG
TCCaggttgttccaatgccaatctgtaaatacgagattcttaacgggttcaattcgcaactattggacaacaacacaaatggacc
GACGGCGCTAGGATCATCAACACACCGAGGAGCCTAACCATCATGATCAAGTATTCTGG
TCACAGAATACAACACACCGAGGAGCCTAACCATCATGATCAAGATGATCCTAGCGCCG
TCGGCCGGCCGTCGACCTGCAGTtttgaagaagagatccgctccagtaatggagaatattcttgatgtGACGG
CGCTAGGATCATCAACACACCGAGGAGCCTAACCATCATGATCAAGTATTCTGGTCACA
GAATACAACACACCGAGGAGCCTAACCATCATGATCAAGATGATCCTAGCGCCGTCCGA

B.

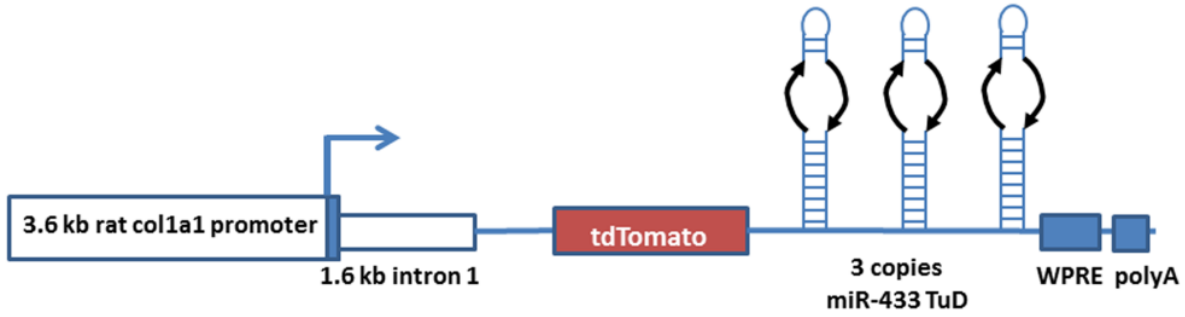

Figure 3.8. Sequence of miR-433 decoy used in vivo.
(A) Sequence of miR-433 decoy used for transgenic mouse: Three miR-433 tough decoys were assembled. DNA from the coding region of the C. elegans Cut3 gene was used as spacer between the repeats of miR-433 decoy, and is denoted by lower case letters. The miR-433 binding sites are underlined. The fragment was custom synthesized by GenScript.
(B) Schematic of Col3.6/1.6_tdTomato_miR-433 decoy transgene cassette. A 3.6 kb fragment of the rat Col1a1 gene, plus the first intron, was used to drive expression of the reporter gene tdTomato and a 3' UTR containing 3 copies of a miR-433 tough decoy (miR-433 binding sites are denoted by black arrows), a Woodchuck Hepatitis Virus Posttranscriptional Regulatory Element (WPRE), and bovine growth hormone polyadenylation signal (polyA).

To determine the impact of miR-433 on circadian rhythm, RNA was isolated from

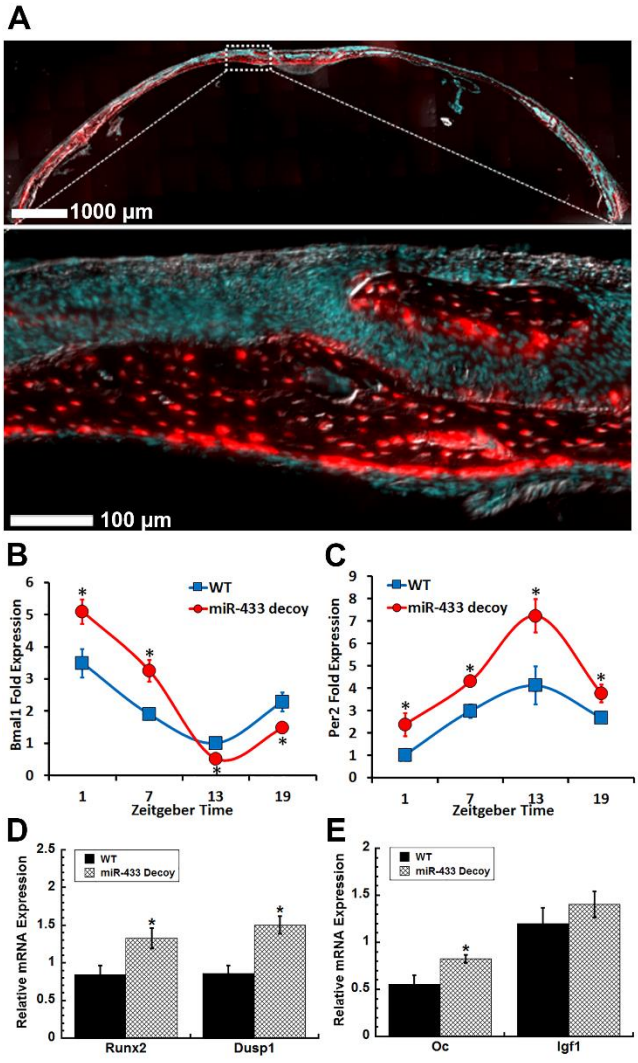

Figure 3.9. miR-433 regulation of circadian clocks and osteoblast genes *in vivo*. Calvaria were isolated from male transgenic mice expressing the miR-433 decoy under the control of a Col1a1 promoter (miR-433 decoy^{Col1a1} mice) and wild type litter mate controls. (A) Example of TD Tomato transgene and Dapi fluorescence in a calvarium from a 4 week old male miR-433 decoy^{Col1a1} mouse at ZT13. mRNA levels from calvaria of 8 week old mice for (B) Bmal1 and (C) Per2 at ZT 1, 7, 13, and 19. (D) Runx2 and Dusp1 and (E) osteocalcin (Oc) and Igf1 mRNA were quantified in calvaria at ZT13. Pooled data from 2 miR-433 decoy^{Col1a1} lines having a similar level of transgene expression. n=7 for WT; n=8 for miR-433 decoy^{Col1a1}. * = significantly different WT littermates, $p < 0.05$.

calvaria of 8 week old male miR-433 decoy^{Col1a1} mice and matched litter mate controls euthanized every 6 hours over an 18 hour period. Bmal1 and Per2 mRNA expression

showed rhythmic and anti-phasic expression in both wildtype and miR-433 decoy^{Col1a1} mice (Figure 3.9B, C). However, the amplitude of Bmal1 mRNA rhythm in miR-433 decoy^{Col1a1} mice was significantly increased compared to littermate controls (Figure 3.9B). The amplitude of Per2 mRNA rhythm was also significantly increased in miR-433 decoy^{Col1a1} mice (Figure 3.9C). Thus, miR-433 dampens the rhythm of circadian clock genes *in vivo,* supporting its role in the regulating circadian rhythm.

miR-433 can directly target Runx2 and Igf1, suggesting that it may negatively regulate osteoblastogenesis (101). Indeed, calvaria from miR-433 decoy^{Col1a1} mice had 1.5 fold higher levels of Runx2 mRNA, as well as elevated mRNA for the Runx2 target gene, osteocalcin. In contrast, Igf1 mRNA was similar in wild type and miR-433 decoy^{Col1a1} mice (Figure 3.9). Overall, inhibition of miR-433 activity increased the expression of glucocorticoid-responsive genes and increased expression of a subset of osteoblast marker genes *in vivo*, supporting *in vitro* observations.

DISCUSSION

The circadian clocks are crucial regulators of organismal physiology and behavior, operating through a series of positive and negative feedback loops, the regulation of which includes microRNAs. In this study, we demonstrate that miR-433 displays a robust rhythmic expression in the calvaria and that miR-433 is important in maintaining the rhythmic expression of the circadian clocks *in vitro* and *in vivo*. miR-433 serves to limit the responsiveness of mesenchymal cells to glucocorticoids, which could contribute to its

regulation of circadian rhythm (Figure 3.10). In addition, we identified 2 novel targets of miR-433, Igf1 and Hif1α, both of which display rhythmicity *in vivo* and play an important role in osteogenesis. Altogether, we showed that miR-433 can modify responsiveness of cells to glucocorticoids, providing a potential mechanism contributing to its ability to regulate rhythmic gene expression in bone, and possibly other tissues.

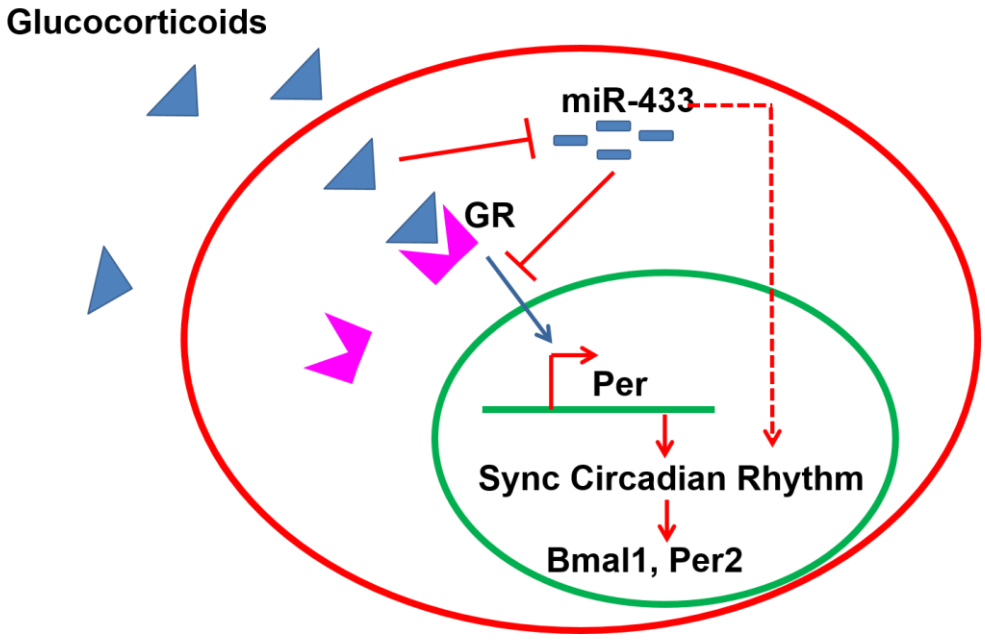

Figure 3.10. Working model of miR-433 regulation of glucocorticoid-induced synchronization of circadian rhythm.

Although microRNAs were shown to be important regulators of circadian rhythm in non-skeletal tissues (93,99,111), to our knowledge, this is the first study examining the role of miRNAs in circadian rhythm in bone. In our study, miR-433 displayed a sizeable rhythmicity in the calvaria, its rhythm had a larger amplitude compared with miR-29a and miR-30a, two microRNAs previously shown to display significant rhythmicity in the liver (92). It is likely that other miRNAs display circadian rhythm in the calvaria, and this remains to be examined.

miRNAs can regulate circadian rhythm through direct targeting of the circadian clocks, by regulation of entrainment, or by reducing target mRNAs' oscillation amplitude or frequency (102). Several miRNAs have been found to impact circadian rhythms in the liver, with miR-122 being the most studied. The miR-122 locus in under the direct regulation of REV-ERBα, an important circadian protein that functions by recruiting histone deacetylases (HDACs), repressing gene expression (115). Systemic administration of miR-122 antisense oligonucleotides caused substantial alterations in amplitude, magnitude, and phase of several rhythmic mRNAs in liver, with corresponding changes in expression of genes involved in cholesterol and lipid metabolism (115). Whereas previous studies examined the direct regulation of miRNAs on the circadian clocks, our study suggests that miR-433 regulation of glucocorticoid signaling in peripheral tissues could impact the rhythmic expression of the circadian clocks *in vivo*, i.e. synchrony.

Glucocorticoids, among other hormones, are important entrainment signals that synchronize circadian rhythms in the kidney, liver, heart, and other tissues (70). High levels of glucocorticoids can disrupt circadian rhythm (78). In humans, serum levels of glucocorticoids cycle, with their peak in the early morning, just before waking, and their lowest levels in the evening (73). The circadian clocks can be directly regulated by glucocorticoid signaling, as the glucocorticoid receptor transcriptionally activates expression of Per1 through a GRE in its promoter, and Per2 through a GRE in the first

intron (74-76). Indeed, oscillating levels of circulating glucocorticoids correspond to Per1 levels in peripheral tissues (77).

Glucocorticoid receptor-induced transcriptional activity can also be directly suppressed by Clock, which assists with acetylating the GR hinge domain (68,128). This acetylation attenuates the binding of the GR to GREs, limiting its actions. In peripheral tissues, the Bmal1/Clock-mediated counter regulation of glucocorticoid signaling provides a mechanism to prevent over exposure of target tissues to glucocorticoids at times when serum levels of glucocorticoid are at their peak (147). Similarly, we demonstrate that miR-433 activity blunts glucocorticoid signaling. In mice, miR-433 levels peak just after dark (Figure 1), and serum glucocorticoids peak just before dark (164). In calvaria of miR-433 decoy^{Col1a1} mice, we observed increased mRNA for the glucocorticoid receptor target genes Per2 and Dusp1, further supporting the concept that miR-433 serves as an additional mechanism to limit exposure of osteoblastic cells to glucocorticoids in vivo.

In humans, miR-433 has been shown to target HDAC6 (135), suggesting that miR-433 levels could regulate the acetylation status of HDAC6 targets. Indeed, HDAC6 can deacetylate Hsp90, which plays an important chaperone function for GR in both the cytoplasm and nucleus. Hyperacetylation of HSP90 results in loss of its GR chaperone activity, causing defects in ligand binding, nuclear translocation and transcriptional activation of GR target genes (135,161). Our results indicate that miR-433 can regulate the sensitivity of cells to glucocorticoids through decreasing translocation of the GR to the

nucleus. It is possible that the ability of miR-433 to target HDAC6 helps to control HSP90 acetylation and chaperone function, fine-tuning glucocorticoid responsiveness.

The role of glucocorticoid signaling in bone is complex. Normal, endogenous glucocorticoids are critical for skeletal health (reviewed by (79)). Glucocorticoids can enhance the expression of osteoblast differentiation markers such as alkaline phosphatase, osteocalcin and bone sialoprotein *in vitro* (reviewed by (80)). In contrast, excessive exposure of the skeleton to glucocorticoids leads to the development of osteoporosis, which is frequently seen in patients treated long term with glucocorticoids for autoimmune disorders, inflammatory disease or malignancy. Glucocorticoid excess causes bone loss due to decreased osteoblast activity, reduced osteoblast number, increased osteocyte apoptosis, and disruption of extracellular matrix production (reviewed by (81)). In our *in vivo* model, calvaria from mice expressing the miR-433 decoy in osteoblastic cells had increased mRNA for Runx2 and its downstream target, osteocalcin. This was not unexpected, since miR-433 was previously shown to target Runx2 (101). That Igf1 was not similarly increased suggests other mechanisms, transcriptional or post-transcriptional, predominate in the regulation of this gene *in vivo*. We are in the process of fully characterizing the skeletal phenotype of miR-433 decoy^{Col1a1} mice, to better understand the function of miR-433 in bone.

We identified 2 new miR-433 targets, Hif1α and Igf1, which have been shown to be to be important factors in bone formation and homeostasis (165-168). Igf1 enhances osteoblast differentiation and induces osteoblast proliferation (167). Hif1α is important in

coupling angiogenic and osteogenic activity, to promote bone formation (166,168). In calvaria, miR-433 levels are highest when mRNA of its targets, Runx2 and Igf1, are the lowest. In contrast, the peak of miR-433 coincides with a broad peak in Hif1α mRNA. It is possible that miR-433 serves to fine tune expression of this regulator.

Transcription of the miR-433 locus has been shown to be induced by orphan receptor estrogen related receptor γ (ERRγ), a negative regulator of osteogenesis, whereas its transcription can be repressed by small heterodimer partner (SHP) which promotes osteoblast differentiation (101,169,170). Although estrogen related receptors have been linked to energy homeostasis and can display circadian regulation, it is not known whether these mechanisms are active in calvaria (171,172). Disruption of normal circadian rhythm resulting in changes of clock amplitude, period length, or frequency lead to alterations in chromatin modification, gene regulation, cellular metabolism, and immune responses (42). Consequently, chronic desynchrony is associated with the development and progression of cardiovascular disease, cancer, mental illnesses, and severe metabolic disorders (reviewed by (45)).

Overall, we found miR-433 displays rhythmicity in calvaria, regulates cell sensitivity to glucocorticoids, and helps maintain rhythmic gene expression. Since miR-433 levels in bone peak when circulating glucocorticoid levels are high, it likely plays a role in balancing the glucocorticoid response. We speculate that miR-433 can modify responsiveness of peripheral tissues to variations in circulating glucocorticoids and alter bone metabolism. miR-433 also targets HDAC6, providing a mechanism for modulating the acetylation

status of multiple HDAC6 targets. These findings provide an added dimension to our understanding of the mechanisms regulating glucocorticoid responsiveness, circadian rhythm, and their potential impact on the skeleton, and possibly other tissues.

EXPERIMENTAL PROCEDURES

Mice

C57BL/6 male mice were kept under a 12 hour light/dark cycle, and provided with food and water ad libitum. Eight week old male mice were euthanized every 4 hours and calvaria were collected. We created mice expressing a transgene in which a 3.6 kb fragment of the rat col1A1 promoter, plus 1.6 kb of the first intron drive expression of the tdTomato reporter gene carrying a miR-433 tough decoy (TuD) in its 3' UTR (custom synthesis, GenScript, Piscataway, NJ) (156,162). Mice were generated in a C57BL/6 background by pronuclear injection of the transgene cassette at the UConn Health Gene Targeting and Transgenic Facility. The miR-433 decoy serves as a competitive inhibitor of miR-433 activity, relieving the suppression of endogenous miR-433 targets. The sequence of the miR-433 TuD and diagram of the transgene cassette is provided in Figure 3.9. Eight week old male mice were euthanized at ZT13 and calvaria were collected.

All animal protocols were reviewed and approved by the UConn Health Institutional Animal Care and Use Committee (IACUC).

Cell culture and synchronization

C3H/10T1/2, Clone 8, a multipotent mouse mesenchymal cell line, was obtained from the American Type Culture Collection (ATCC® CCL-226™) and cultured in DMEM

(Gibco Life Technologies, Carlsbad, CA) supplemented with 10% heat-inactivated Fetal Bovine Serum (FBS, Lonza, Basel, Switzerland). Primary bone marrow stromal cells (BMSCs) were flushed from the long bones of 6-8 week old male C57BL/6 mice and maintained in DMEM supplemented with 10% FBS. Cells were synchronized by 24 hours of serum deprivation, followed by treatment for 2 hours with 100 nM dexamethasone (Sigma-Aldrich, St. Louis, MO). The dexamethasone was then replaced with serum-free medium for the remainder of the experiment (140). Amplitude was determined by calculating the difference between a peak and the mean value of the wave.

Quantitative real time PCR

Total RNA from calvaria samples was extracted using the miRNeasy Mini Kit (Qiagen, Valencia, CA). Calvaria were homogenized in Qiazol. RNA was isolated from cell cultures using TRIzol Reagent (Life Technologies). RNA samples were DNased using RQ1 DNase (Promega, Madison, WI). DNased RNA was reverse-transcribed using Moloney murine leukemia virus-reverse transcriptase (Invitrogen, Carlsbad, CA). Gene expression was quantified by qPCR with iQ SYBR Green Supermix (Bio-Rad) and normalized to 18S rRNA. Primer sets are shown in Table 3.2. microRNA expression levels were analyzed using the TaqMan MicroRNA Assay (Life Technologies). RNA was reverse transcribed with gene-specific primers to generate cDNA. microRNA expression was detected by qPCR and normalized to snoRNA 202. RNA experiments were performed at least twice and each experiment contained at least 3 biological replicates. Each sample was assayed in duplicate.

Table 3.2: Primer sequences used for qPCR analysis.

Gene (mouse)	Sequence
18S (sense) *18S* (antisense)	5'-GCGTGTGCCTACCCTACGCC -3' 5'-ACGCAAGCTTATGGCCCGCA-3'
Bmal1 (sense) *Bmal1* (antisense)	5'-AACCTTCCCGCAGCTAACAG -3' 5'-AGTCCTCTTTGGGCCACCTT -3'
Per2 (sense) *Per2* (antisense)	5'-AGAACGCGGATATGTTTGCTG-3' 5'-ATCTAAGCCGCTGCACACACT-3'
Hif1α (sense) *Hif1α* (antisense)	5′-ACCTTCATCGGAAACTCCAAAG -3′ 5′-ACTGTTAGGCTCAGGTGAACT-3′
Nr3c1 (sense) *Nr3c1* (antisense)	5′-GTGAGTTCTCCTCCGTCCAG -3′ 5′-TGCAATCATTTCTTCCAGCA-3′
Runx2 (sense) *Runx2 (antisense)*	5′-CCTCTGGCCTTCCTCTCTCAGT -3′ 5′-GCCACTCTGGCTTTGGGAAGAG -3′
Igf1(sense) *Igf1 (antisense)*	5′-CACACTGACATGCCCAAGAC -3′ 5′-GGGAGGCTCCTCCTACATTC -3′
GFP (sense) *GFP (antisense)*	5′-GTGAGCAAGGGCGAGGAGCTGTTC -3′ 5′-GTAGGTCAGGGTGGTCACGAGGG -3′
GRα (sense) *GRα (antisense)*	5′-AAAGAGCTAGGAAAAGCCCATTGTC-3′ 5′-TCAGCTAACATCTCTGGGAATTCA -3′
GRβ (sense) *GRβ (antisense)*	5′-AAAGAGCTAGGAAAAGCCCATTGTC-3′ 5′-CTGTCTTTGGGCTTTTGAGATAGG -3′
Dusp1 (sense) *Dusp1 (antisense)*	5′-CAGCTGCTGCAGTTTGAGTC -3′ 5′-GGGATGGAAACAGGGAAGTT -3′

Luciferase assay

Gene-specific PCR primers were used to amplify from genomic DNA template the 3' UTR for Igf1 (mouse, base pairs 1-6217), Hif1α (human, base pairs 2612-3906), and Per2 (human, base pairs 866-2041). These fragments were subcloned downstream of a Cytomegalovirus (CMV) promoter-driven Luciferase reporter (pMIR-REPORT vector, Ambion, Carlsbad, CA). Constructs were verified by sequencing.

C3H/10T11/2 cells were plated a 25,000 cells/cm^2. BioT transfection reagent (1.5ul:1μg DNA; Bioland Scientific, Paramount, CA) was used to co-transfect luciferase constructs containing the 3' UTR of target mRNA, a constitutively active β-galactosidase

construct (control for transfection efficiency), and miRNA hairpin inhibitors (Dharmacon/Thermo Fisher Scientific, Waltham, MA). 80 nM of anti-miR-433 or a negative control (non-targeting) miRNA inhibitors were used. Cell lysates were analyzed for luciferase activity using the Luciferase Assay System (Promega) and normalized to β-Galactosidase using Galacton® (Life Technologies). Each luciferase experiment was performed at least 3 times, and each experiment contained 6 biological replicates. More than one preparation of each DNA construct was tested.

Establishment of a stable inducible miR-433 knockdown model

To achieve knockdown of miR-433 activity, C3H/10T11/2 cells were transduced using lentiviral constructs containing a miR-433 tough decoy (custom synthesis, GenScript) driven by a doxycycline (Dox)-inducible promoter. The miR-433 decoy contains complementary sites that will bind endogenous miR-433 (Table 3.1). The miR-433 decoy was subcloned into the single lentivector for inducible knockdown (pSLIK) system and confirmed by sequencing (144) (Addgene, Cambridge, MA). Doxycycline treatment stimulates the decoy. As a control, we developed a non-targeting tough decoy containing *C. elegans* miR-67 binding sites (custom synthesis, GenScript), which is not predicted to interact with mammalian miRNAs (Table 3.1). Cells stably transduced with the pSLIK-miR-433 decoy or non-targeting decoy were selected for hygromycin resistance.

Western blot

C3H/10T1/2 cells were plated at 200,000 cells/cm^2 and treated with Doxycyline for 24 hours in serum-free medium, to induce expression of the decoy. Cells were lysed with RIPA buffer containing Halt™ protease inhibitors (Thermo Fisher Scientific). A BCA assay (Thermo Fisher Scientific) was performed to quantify protein, and 20 µg protein was subjected to electrophoresis on a 10% SDS polyacrylamide gel. Proteins were transferred to a PVDF membrane (Millipore, Billerica, MA). Rabbit anti-mouse glucocorticoid receptor primary antibody (1:1000 Cell Signaling, Danvers, MA, Cat #D6H2L), rabbit anti-β-actin antibody (1:2000, Cell Signaling #13E5), and goat anti-rabbit horseradish peroxidase conjugated antibody (1:10000, Sigma Aldrich A0545) were used.

To analyze nuclear versus cytosolic localization of the glucocorticoid receptor, C3H/10T1/2 cells were serum deprived for 24 hours, in the presence or absence of doxycycline, then treated with or without 100 nM dexamethasone for 2 hours. Cells were trypsinized and pelleted. Pellets were suspended in a cytosolic extraction buffer (10 mM Hepes, 60 mM KCl, 1 mM EDTA, 0.075% Igepal 40, 1 mM DTT, and 1 mM PMSF). The lysate was pelleted and the supernatant was collected as the cytosolic fraction. Pellets were resuspended in nuclear extraction buffer (20 mM Tris-Cl, 420 mM NaCl, 1.5 mM $MgCl_2$, 0.2 mM EDTA, 1 mM PMSF, and 25% Glycerol), and then pelleted; the supernatant was collected as the nuclear fraction. Half of each lysate was subjected to electrophoresis on a 10% SDS polyacrylamide gel, transferred to PVDF membrane, and the same antibody dilutions as noted above were used for the glucocorticoid receptor and β-actin. For the nuclear fraction, rabbit anti-mouse PCNA was used to control for loading (1:2000 Cell Signaling Cat #13110P). Chemiluminescent signal was achieved using

SuperSignal West Pico Kit (Thermo Fisher Scientific) and captured using the Bio-Rad ChemiDoc XRS+ Imaging system. Densitometry of protein bands were performed using Image J analysis (173). Expression of the glucocorticoid receptor was normalized to either β-actin or PCNA.

Cryohistology and microscopy imaging

Calvaria from 4 week old male mice were fixed (4% paraformaldehyde), decalcified (14% EDTA-acid, 0.9% ammonium hydroxide), and washed in a 30% sucrose PBS solution at 4º C. Samples were embedded in O.C.T. compound (VWR, Radnor, PA). 7 µm sections were collected with a Cryofilm type II tape transfer system (Section Lab Co. Ltd. Japan). Sections were mounted for imaging (50% glycerol buffered with PBS containing 0.2 mg/ml DAPI, Thermo Scientific Fisher), imaged with a Zeiss Observer Z.1 microscope, and captured using an Axiocam MRc digital camera and Axiovision software (Zeiss).

Statistics

All data are represented as a mean ± SEM, and are either a representative of 2 experiments (n=3-4 biological replicates/experiment) or pooled data from several experiments (n>4 biological replicates). Statistical significance was determined using two tailed ANOVA with Bonferroni post-hoc test or a Student's t test as appropriate (KaleidaGraph, Synergy Software, Reading, PA).

ACKNOWLEDGEMENTS

We thank Laura D'Angelo for cloning the Hif1α luciferase construct, Catherine Kessler for expert technical assistance, and Ryan Russell for assistance with bone imaging.

CONFLICT OF INTEREST

The authors declare that they have no conflicts of interest with the contents of this article.

AUTHOR CONTRIBUTIONS

SSS and AMD designed the research. SSS, NSD, TF, HCH, and AMD performed the research and analyzed the data. SSS and AMD wrote the manuscript and take responsibility for data analysis. All authors approved manuscript submission.

FUNDING

This work was supported by the National Institute of Arthritis and Musculoskeletal and Skin Diseases of the National Institutes of Health [AR44877]; the National Institutes for Dental and Craniofacial Research [5T90DE21989]; a Grant-in-Aid award from the American Society for Bone and Mineral Research; the UConn Health Center Research Advisory Council; and the Center for Molecular Medicine at UConn Health. **The content is solely the responsibility of the authors and does not necessarily represent the official views of the National Institutes of Health.**

CHAPTER 4

microRNA-433 Dampens TGF-β Signaling and Restrains Osteoblast and Chondrocyte Differentiation

Spenser S Smith[1], Neha S Dole[1, 3], Hicham Drissi[2], Rosa Guzzo[2], Anne M Delany[1,*]

[1] Center for Molecular Medicine, UConn Health, Farmington, CT, 06030, USA

[2] Department of Orthopedic Surgery, UConn Health, Farmington, CT, 06030, USA

Present Address:

[3] Department of Orthopedic Surgery, University of California San Francisco School of Medicine, San Francisco, CA, 94143 USA

Abstract

Osteoblasts, chondrocytes, and adipocytes arise from a common progenitor, and microRNAs (miRNAs) are key post-transcriptional regulators of lineage commitment and differentiation. Transforming growth factor β (TGF-β) is critical for both osteoblastic and chondrogenic commitment; bioinformatic analyses suggest that miR-433 could target key components of the TGF-β signaling pathway. Therefore, we examined the function of miR-433 in osteoblast and chondrocyte differentiation using a mesenchymal cell line where miR-433 activity was inhibited using a tough decoy. Inhibiting miR-433 amplified TGF-β signaling, determined by SBE4 luciferase reporter. Moreover, inhibition of miR-433 increased pSMAD2 and SMAD2 in TGF-β treated mesenchymal cells. 3'UTR luciferase assays validated SMAD2 and TGFBR1 as novel miR-433 targets. Examining miR-433 during lineage commitment in primary cultures of mouse bone marrow stromal

cells (BMSCs), we found that osteogenic differentiation profoundly decreased miR-433 expression. In contrast, miR-433 levels were dramatically increased during the chondrogenic differentiation of mouse BMSCs or human induced pluripotent stem cell (iPSC) derived mesenchymal-like progenitors. In multipotent C3H/10T1/2 cells expressing the miR-433 tough decoy, inhibition of miR-433 enhanced BMP2-induced osteogenic differentiation, and promoted mineralized matrix deposition. In miR-433 decoy cells induced toward the chondrogenic lineage, miR-433 inhibition promoted expression of chondrogenic mRNAs, Sox9, Col2a1, and ColXa1. Overall, miR-433 dampens TGF-ß signaling and targets SMAD2 and TGFBR1 RNA. This effect likely contributes to the ability of miR-433 to restrain osteoblastic and chondrogenic differentiation, with potential implications for bone and cartilage repair.

Introduction

The appendicular skeleton forms through endochondral ossification, a developmental process whereby a cartilage template is gradually replaced by bone. Bone tissue itself is also continuously remodeled, in a highly regulated cycle of coupled osteoclast-mediated bone resorption followed by osteoblast-mediated bone formation. This is the only process whereby adults can renew bone tissue, and it is also critical for mineral homeostasis. Prevalent skeletal diseases, such as osteoporosis, are caused by an imbalance in bone remodeling.

miRNAs are now well appreciated post-transcriptional regulators of both bone and cartilage homeostasis. These small non-coding RNAs bind to complementary regions in target mRNAs, frequently in the 3' untranslated region (UTR), resulting in mRNA degradation and/or translational suppression. Most miRNAs function to fine tune the timing and tempo of gene expression, acting on multiple targets within the same or correlated pathways, and causing significant changes in cellular signaling.

Some miRNAs, such as the miR-29 family, have been extensively studied in the context of bone and cartilage. miR-29 promotes osteogenesis, in part by targeting negative regulators of Wnt signaling (174,175). In cartilage, Sox9, a master transcription factor essential for chondrogenic commitment, represses miR-29. The increased levels of miR-29 seen in osteoarthritic lesions could contribute to an increase in canonical Wnt signaling, thought to play a role in pathogenesis (176,177). These studies illustrate the tissue-specific effects of miRNA-29 and its targets in the skeleton.

Although the impact of some miRNAs on the skeleton has been well documented, other miRNAs, such as miR-433, are still poorly understood. We initially found that miR-433 could differentially target a single nucleotide polymorphism (SNP) in osteonectin (SPARC). This SNP was associated with bone mass in men with idiopathic osteoporosis and caused changes in bone mass in a knock-in mouse model (129-134). In human cells, inhibition of miR-433 activity enhanced expression of the osteoblast marker genes alkaline phosphatase and osteocalcin (134). Others demonstrated that miR-433 can

target Runx2 in the multi-potential C3H/10T1/2 cell line, further suggesting that miR-433 is a negative regulator of osteoblastic function (101). However, the function of miR-433 in chondrogenesis has not been established.

We sought to define the role of miR-433 in mesenchymal lineage commitment and differentiation by identifying novel miR-433 targets. We used an *in silico* approach to search for pathways that might be regulated by miR-433, and our analysis suggested that several components of the transforming growth factor-ß (TGF-ß) signaling pathway could be miR-433 targets. TGF-β is important in osteoblastogenesis, chondrogenesis and adipogenesis. TGF-β interacts at the plasma membrane with a receptor dimer consisting of one type I and one type II TGF-β receptor. Upon binding of TGF-β, the type II receptor transphosphorylates and activates the type I receptor, initiating an intracellular signaling cascade involving phosphorylation of SMAD2 and SMAD3. These activated SMADs form a complex with SMAD4, allowing translocation into the nucleus and interaction with SMAD binding elements (SBEs) and other DNA binding proteins, to activate or repress gene transcription (reviewed by (21)).

In other tissues, miRNAs have been shown to target the TGF-β receptors and downstream SMADs (178-181). However, information on miRNA regulation of TGF-β signaling in skeletal cells is limited. This pathway is of interest because, unlike canonical Wnt signaling, TGF-ß appears to play a similar role in bone and cartilage. TGF-ß signaling promotes the commitment of progenitors to the osteoblast lineage, but inhibits terminal

osteoblast maturation. Likewise, TGF-ß promotes chondrogenesis, but inhibits the terminal differentiation stage of hypertrophy. In this study, we defined the expression pattern of miR-433 during differentiation of osteoblasts, chondrocytes and adipocytes arising from murine bone marrow stromal cells (BMSCs). We demonstrated that miR-433 limits TGF-β signaling, targets SMAD2 and TGFBR1, and that miR-433 is a negative regulator of osteoblastogenesis and chondrogenesis in vitro.

Results

miR-433 inhibits TGF-β signaling

We first examined the impact of miR-433 on TGF-β signaling in mesenchymal-like cells using the SBE4-luc construct, a well characterized TGF-β-responsive luciferase reporter in which four SMAD2/3 binding elements drive expression of luciferase. C3H/10T1/2 cells, a multipotent cell line, were cotransfected with the SBE4 construct and a non-targeting or miR-433 inhibitor. Cells were treated with vehicle or TGF-β1, and luciferase activity was quantified. In cells transfected with a non-targeting inhibitor, TGF-β1 induced SBE4 promotor activity as expected (Figure 4.1A). Transfection of the miR-433 inhibitor augmented TGF-β1 activation of the SBE4 promoter, indicating that miR-433 can inhibit TGF-β signaling.

Bioinformatic analysis suggested that several components of the TGF-β pathway could be directly targeted by miR-433, including the TGF-β receptors, TGFBR1 and

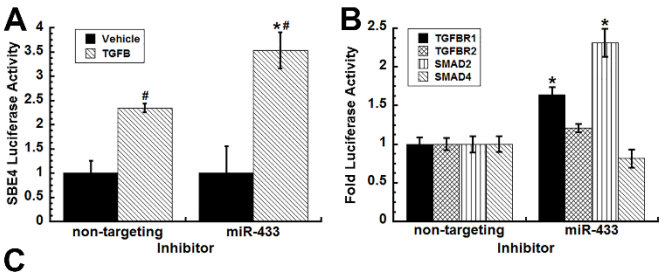

C

Target mRNA	Site Position	Seed Binding Region 3′ Untranslated Region	miR-SVR Score
TGFβR1	2493	3' uguggCUCCUCGGGUAGUACUa 5' miR-433 | ||: : |||||| 5' aaaagGUGGGAUGGAUCAUGAu 3' mRNA	-0.0786
TGFβR1	3209	3' ugUGGCUCCUCGGGUA-GUACUa 5'miR-433 |:: | ||: ||| |||| 5' cgAUUUUGUAGUACAUGCAUGAg 3' mRNA	-0.4316
TGFβR1	3733	3' ugugGCUCCUCGGGUAGUACUa 5' miR-433 :|| | :||||||| 5' uuugUGAACUGAAUAUCAUGAa 3' mRNA	-0.8299
TGFβR2	2126	3' uguggcuccUCGGGU-AGUACUa 5'miR-433 :|:||| |||||| 5' uagaauacuGGUCCAUUCAUGAg 3' mRNA	-0.4274

D

Target mRNA	Site Position	Seed Binding Region 3′ Untranslated Region	miR-SVR Score
SMAD2	302	3' uguggcUCC-UCGGGUAGUACUa 5'miR-433 ||| | : :||||||| 5' guguacAGGUAAUGUAUCAUGAu 3' mRNA	-0.0209
SMAD2	3250	3' uguggcUCCUCGGGUAGUACUa 5'miR-433 || || |: ||||| 5' cuuuaaAGAAG-CUUUCAUGAu 3' mRNA	-0.0003
SMAD2	4632	3' uguggcuccucGGGUAGUACUa 5'miR-433 ::|||||||| 5' guccuaauuucUUCAUCAUGAa 3' mRNA	-0.0150
SMAD2	5039	3' uguggcuccucggguAGUACUa 5' miR-433 |||||| 5' cuauacuagauagccUCAUGAu 3' mRNA	-0.0001
SMAD4	5884	3' uguggcUCCUCGGG--UAGUACUa 5'miR-433 ||| ::| :|||||| 5' aguuuaAGGCUUUCGAGUCAUGAc 3' mRNA	-0.0004
SMAD4	5665	3' ugUGGCUCCUCGGG--UAGUACUa5'miR-433 |:: ||| ::| :|||||| 5' uuAUUAAGGCUUUCGAGUCAUGAc 3' mRNA	-0.0007

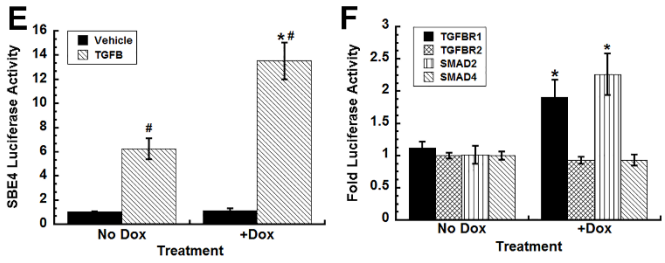

Figure 4.1. miR-433 inhibits TGF-β signaling and targets SMAD2 and TGFBR1.
(A) Activity of the TGF-β responsive SBE4 luciferase reporter in C3H/10T1/2 cells co-transfected with a non-targeting or miR-433 inhibitor. C3H/T101/2 cells were treated with vehicle or 5 ng/ml TGF-β1 for 24 hours. (B) Activity of the SMAD2, SMAD4, TGFBR1, and TGFBR2 luciferase-3-UTR reporter constructs transiently transfected into C3H/10T1/2 cells, along with a miR-433 or non-targeting inhibitor. Potential interaction of miR-433 with (C) the TGF-β receptor or (D) SMAD2 and SMAD4 3' UTRs, as predicted by miRanda (153). Activity of (E) SBE4 or (F) target 3' UTR luciferase reporters in C3H/10T1/2 stably transduced with a Doxycycline (Dox)-inducible construct carrying a miR-433 decoy. Cells were treated with 1 ug/ml Dox for 24 hours, in the presence or absence of 5 ng/ml TGF-β. Luciferase activity is

expressed relative to the vehicle treated non-targeting or no Dox controls. # = significantly different from vehicle, $p < 0.05$. * = significantly different from non-targeting or no Dox control, $p < 0.05$. (n=12)

TGFBR2, as well as the downstream signaling components SMAD2 and SMAD4 (miRanda, TargetScan, RNAhybrid; Figure 4.1C, D). Three of these candidate RNAs contained multiple potential miR-433 binding sites. Target gene 3' UTRs were cloned downstream of a constitutively expressed luciferase gene in the reporter plasmid pMIR-REPORT-Luciferase. The luciferase constructs containing the target 3' UTRs were transiently cotransfected into C3H/10T1/2 cells with a non-targeting or miR-433 inhibitor, and luciferase activity was quantified. miR-433 inhibition significantly increased the luciferase activity of SMAD2 and TGFBR1 3' UTR constructs, compared to the non-targeting control. In contrast, miR-433 inhibitor did not affect SMAD4 and TGFBR2 3' UTR activity (Figure 4.1B). The targeting SMAD2 and TGFBR1 3' UTR by miR-433 could contribute to inhibition of TGF-β signaling.

We had previously developed a stably transduced C3H/10T1/2 cell line in which the activity of miR-433 could be knocked down in a Doxycycline (Dox) inducible manner (144). These cells express a miR-433 tough decoy (competitive inhibitor), in which a green fluorescent protein (GFP) reporter carries 2 miR-433 binding sites in its 3' UTR (156). The activity of this miR-433 decoy phenocopies that of the transiently transfected miR-433 inhibitor, with regard to relieving repression of miR-433 targets (182). To confirm that the miR-433 decoy mimics the miR-433 inhibitor with respect to TGF-β signaling, the SBE4 luciferase reporter and target 3' UTR constructs were transfected into miR-433 decoy cells, and cultured in the absence or presence of Dox. Expression of the miR-433

decoy in the Dox treated cells caused a 2 fold increase in TGF β-induced SBE-4-luciferase activity, compared with TGF β treated cells cultured in the absence of Dox (Figure 4.1E). When examining the activity of the 3' UTR reporter constructs, increased luciferase activity was observed in Dox treated cells that were transfected with SMAD2 or TGFBR1 3' UTR reporter constructs (Figure 4.1F). However, expression of the miR-433 decoy did not alter activity of the SMAD4 or TGFBR2 3' UTR constructs. These results demonstrate that the miR-433 decoy inhibits miR-433 activity, and confirm miR-433 regulation of TGF-β signaling.

Since inhibition of miR-433 activity increased expression of the SBE4-luciferase reporter, and miR-433 can target the SMAD2 3' UTR, we examined the impact of miR-433 on SMAD2 levels and SMAD2 phosphorylation. miR-433 decoy cells were serum deprived in the absence or presence of Dox for 24 hours, then treated with vehicle or 1 ng/ml TGF-β1 for 1 hour. As expected, TGF-β1 increased pSMAD2 in the absence of Dox. However, expression of the miR-433 decoy further enhanced TGF-β-induced pSMAD2 levels by 1.9 fold (Figure 4.2A, B). Although expression of the miR-433 decoy did not alter total SMAD2 levels in vehicle treated cells, treatment with TGF-β increased SMAD2 levels in cells expressing the decoy (Figure 4.2C). The presence of the miR-433 decoy did not alter the ratio of pSMAD2/SMAD2, indicating that the increased pSMAD2 is due to increased total SMAD2 available for signaling (Figure 4.2D). Overall, these data show that miR-433 attenuates TGF-β signaling.

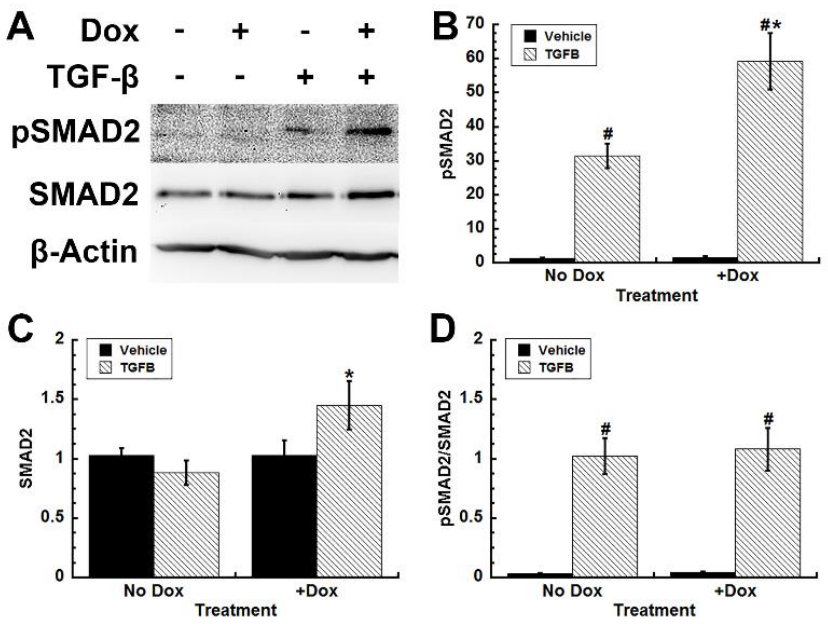

Figure 4.2. miR-433 inhibits pSMAD2 and SMAD2 protein levels.
miR-433 decoy cells were cultured in the absence or presence of 1 ug/ml Dox, in the absence of serum for 24 hours. Cells were then treated with 1 ng/ml TGF-β1 for 1 hour in the absence or presence of Dox. (A) Representative Western blot. Levels of (B) pSMAD2 and (C) SMAD2 normalized to β-actin. (D) Ratio of pSMAD2/SMAD2. # = significantly different from vehicle control. * = significantly different from no Dox control, $p < 0.05$. (n=9)

TGF-β downregulates miR-433

microRNAs often participate in positive or negative feedback loops; because miR-433 inhibits TGF-β signaling, we determined whether TGF-β could regulate the expression of miR-433. C3H/10T1/2 cells were serum deprived for 24 hours and treated with 5 ng/ml TGF-β1 for up to 48 hours. In cells treated with TGF-β1, miR-433 expression decreased 40% at 24 and 48 hours (Figure 4.3A). In serum-deprived confluent cultures of primary mouse BMSCs, treatment with TGF-β1 caused a similar repression of miR-433 (Figure 4.3B), suggesting a miR-433-TGF-β negative regulatory loop (Figure 4.3C).

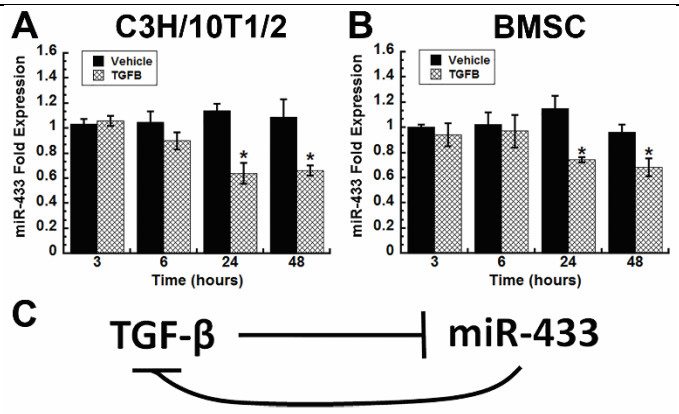

Figure 4.3. TGF-β represses miR-433 expression
miR-433 was quantified in (A) C3H/10T1/2 cells and (B) bone marrow stromal cells treated with 5 ng/ml TGF-β1 for up to 48 hours. (C) Model for miR-433 and TGF-β1 interaction. * = significantly different from time matched control, $p < 0.05$. (n=6)

miR-433 expression decreased during osteogenic differentiation of bone marrow stromal cells

In C3H/10T1/2 cells, miR-433 was suggested to be a negative regulator of osteoblast differentiation (101). However, the expression of miR-433 during osteogenesis in primary cells has not been examined. Therefore, primary bone marrow stromal cells (BMSCs) were induced to differentiate along the osteoblast lineage by culture in the presence of ascorbic acid and β-glycerophosphate for up to 4 weeks. During this process, RNA for osteogenic marker genes alkaline phosphatase, Runt-related transcriptional factor 2 (Runx2), and osteocalcin, were increased substantially, as was alkaline phosphatase activity and deposition of mineralized matrix (Alizarin Red S staining) (Figure 4.4A, B). In contrast, miR-433 expression significantly decreased during osteogenic differentiation, with a 70% reduction at week 3 (Figure 4.4C). To induce the differentiation of C3H/10T1/2 cells towards the osteoblastic lineage, the cells were cultured for up to 3 weeks in the presence of 50 ng/ml bone morphogenetic protein

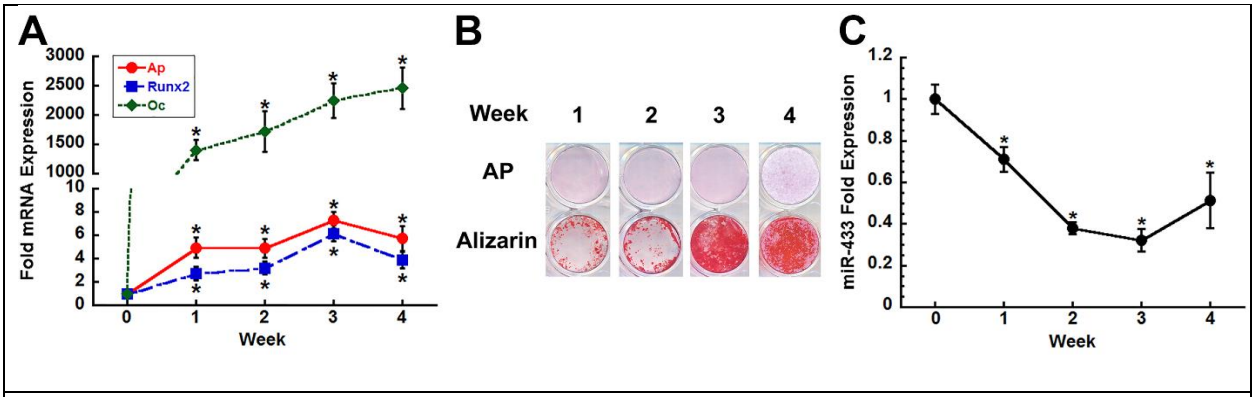

Figure 4.4 miR-433 decreases during osteogenic differentiation of bone marrow stromal cells

Bone marrow stromal cells were differentiated with 5 mM β-glycerophosphate and 50 µg/ml ascorbic acid for up to 4 weeks. (A) Alkaline phosphatase (Ap), Runx2, and osteocalcin (Oc) mRNA expression. (B) Alkaline phosphatase and Alizarin Red S staining. (C) miR-433 expression. * = significantly different from day 0, $p < 0.05$. (n=8)

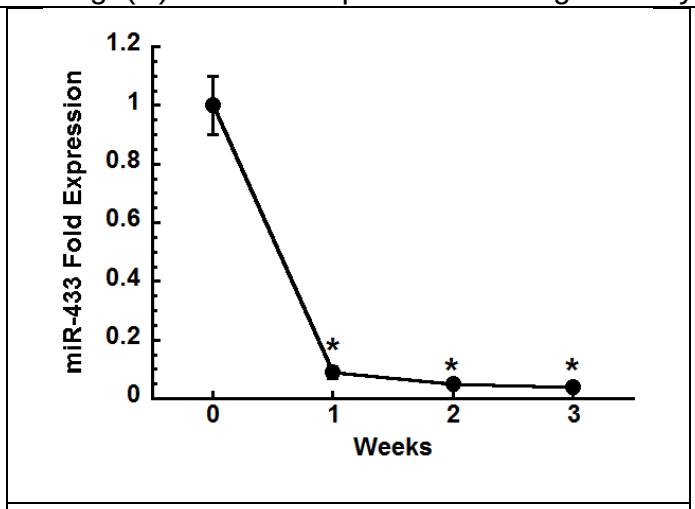

Figure 4.5 miR-433 decreases during osteogenic differentiation of C3H/10T1/2 cells

C3H/10T1/2 miR-433 decoy cells treated with no doxycycline were differentiated with 50 ng/ml BMP-2, 8 mM β-glycerophosphate and 50 µg/ml ascorbic acid for up to 3 weeks and measured for miR-433 expression. * = significantly different from day 0, $p < 0.05$. (n=4)

(BMP-2). In these cells, expression of miR-433 was also dramatically reduced (Figure 4.5; 90.0% decline after 1 week of culture), which corroborates a previous report showing the BMP- 2 induced reduction of miR-433 24 hours after treatment (101).

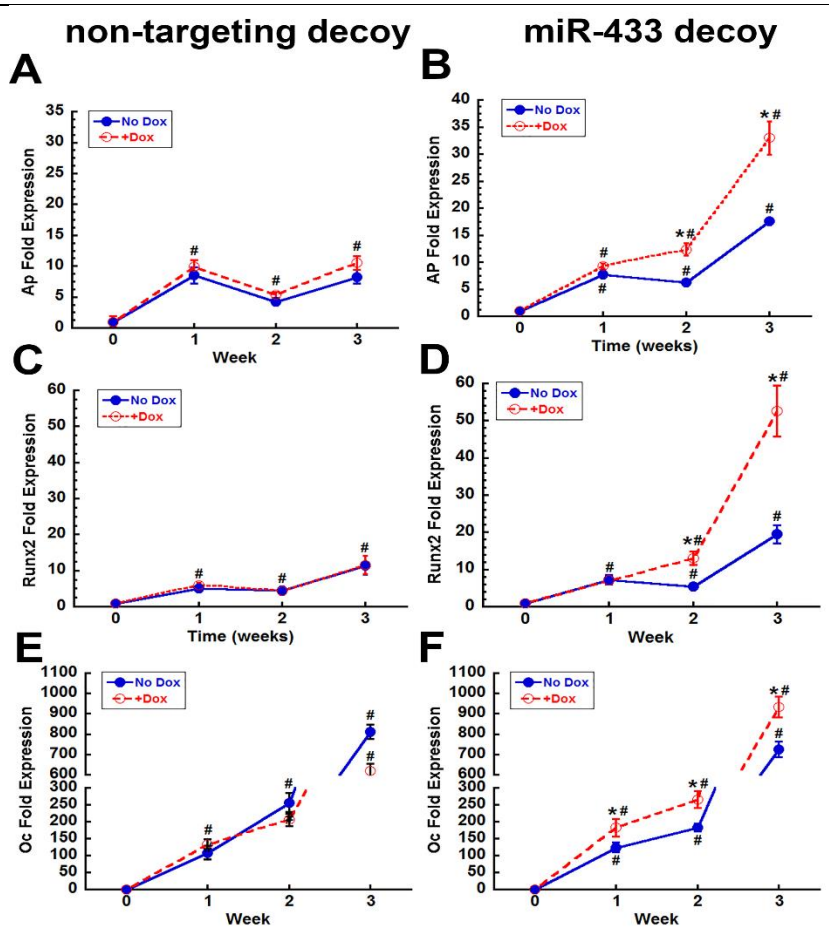

Figure 4.6. miR-433 decoy enhances osteogenic differentiation *in vitro*
Non-targeting and miR-433 decoy cells were differentiated with 100 µg/ml ascorbic acid, 8 mM β-glycerophosphate, and 50 ng/ml BMP-2 for up to 3 weeks in the absence or presence of 1 ug/ml Dox. Alkaline phosphatase (Ap) mRNA expression in (A) non-targeting and (B) miR-433 decoy cells. Runx2 mRNA expression in (C) non-targeting and (D) miR-433 decoy cells. Osteocalcin mRNA expression in (E) non-targeting and (F) miR-433 decoy cells. # = significantly different from day 0, $p < 0.05$. * = significantly different from corresponding no Dox control, $p < 0.05$. (n=4)

miR-433 negatively regulates osteogenesis

Although it has been previously reported that miR-433 is a negative regulator of osteogenesis in C3H10T1/2 cells, osteoblastic gene expression had only been examined after an acute (up to 3 days) treatment with BMP-2 (101,134). To better define the impact of miR-433 on the regulation of osteogenic differentiation, we cultured

C3H/10T1/2 cells stably transduced with the Dox-inducible non-targeting miRNA decoy or miR-433 decoy with a BMP-2-containing osteogenic cocktail for up to 3 weeks. In non-targeting decoy cells, osteogenic marker genes alkaline phosphatase, Runx2, and osteocalcin increased at all time points compared to day 0, and gene expression was not altered by the absence or presence of Dox (Figure 4.6A, C, E). In contrast, expression of the miR-433 decoy significantly enhanced expression of the early osteoblastic marker genes alkaline phosphatase and Runx2, with a maximal effect observed at week 3 (Figure 4.6B, D). Although the miR-433 decoy significantly enhanced mRNA levels for the terminal osteoblast differentiation marker osteocalcin at all time points, the effect was not as robust as that observed with the earlier markers (Figure 4.6F). Moreover, miR-433 inhibition also increased mineralized matrix production (1.5 ± 0.1 fold at week 3; $p<0.05$). Growth curves for the non-targeting and miR-433 decoy cells cultured in the presence or absence of Dox were superimposable, suggesting that enhanced cell number did not play a role in the observed effects (Figure 4.7). Overall, miR-433 appears to be a negative regulator of osteoblastic differentiation *in vitro,* with a particularly strong impact on early osteogenesis.

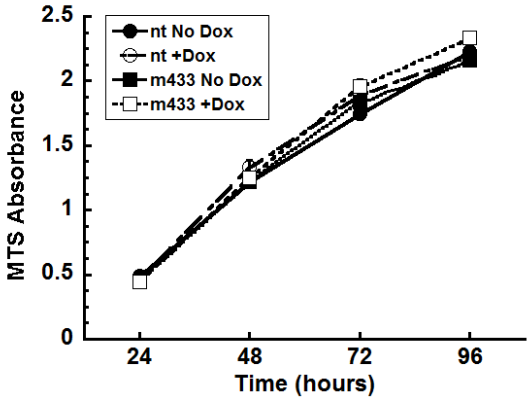

Figure 4.7. The non-targeting and miR-433 decoy does not alter cell proliferation.
C3H/10T1/2 cells transduced with a non-targeting or miR-433 decoy were cultured in the absence or presence of 1000 ng/ml Dox for up to 96 hours and were assessed by MTS assay read at 490 nm. (n=12)

miR-433 is unchanged during adipogenesis

Osteoblasts and adipocytes arise from a common progenitor in the bone marrow, and marrow adipogenesis is often inversely correlated with bone mass (183). Indeed, TGF-β is a negative regulator of adipogenesis, inhibiting the transactivation of

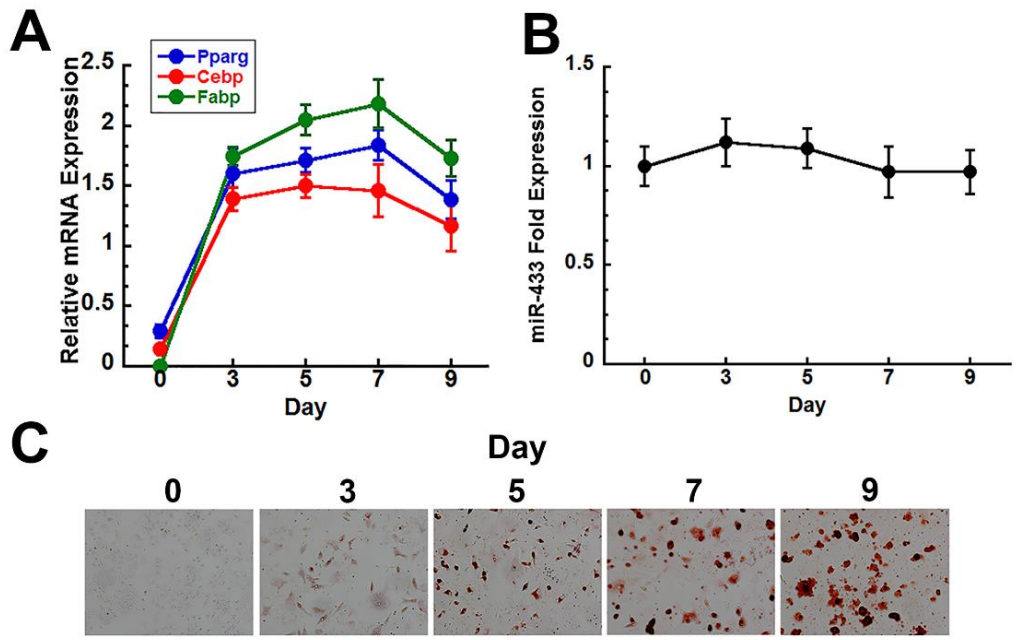

Figure 4.8. miR-433 expression is not altered during adipogenic differentiation of bone marrow stromal cells
Bone marrow stromal cells were differentiated with 500 nM rosiglitazone and 1 µM insulin for up to 9 days. (A) CCAAT enhanced binding protein α (Cebpα), peroxisome proliferator activated receptor gamma (Pparγ), and fatty acid binding protein 4 (Fabp4) mRNA expression. (B) miR-433 expression. (C) Oil Red O staining. * = significantly different from day 0, $p < 0.05$. (n=8)

CCAAT/enhancer binding protein α (Cebpα), a critical pro-adipogenic transcription factor (184). Therefore, we next examined miR-433 expression during the adipogenic differentiation of BMSCs, stimulated by culture in a cocktail containing rosiglitazone and insulin for up to 9 days. mRNA levels for Cebpα, peroxisome proliferator activated receptor gamma (Pparγ), and fatty acid binding protein 4 (Fabp4) were examined as

markers of adipogenesis. The adipocyte differentiation protocol significantly induced adipogenic marker genes at all time points compared to day 0 (Figure 4.8A). Oil red O staining showed increasing lipid droplet accumulation throughout the 9 day differentiation (Figure 4.8C). However, miR-433 expression was not significantly changed over the course of adipogenic differentiation of BMSCs or C3H/10/1/2 cells (Figure 4.8B, Figure 4.9).

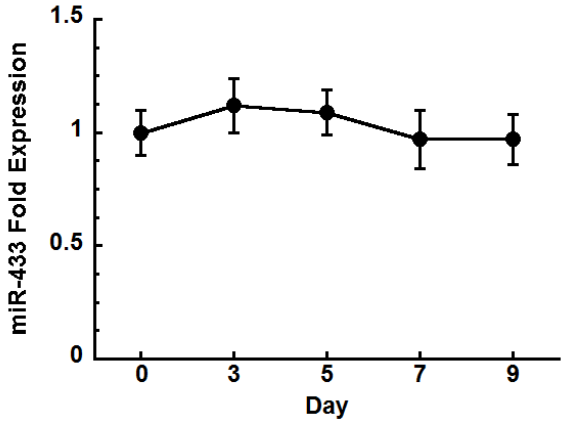

Figure 4.9. miR-433 expression is not altered during adipogenic differentiation of C3H/10T1/2 cells. C3H/10T1/2 cells were differentiated with 500 nM rosiglitazone and 1 µM insulin for up to 9 days and examined for miR-433 expression. (n=8)

miR-433 does not alter adipogenic differentiation

Although miR-433 expression was unchanged during adipogenesis, it could still potentially play a role in regulating adipogenic differentiation. To examine this, non-targeting and miR-433 decoy cells were differentiated toward the adipogenic lineage with rosiglitazone and insulin, in the absence or presence of Dox. In non-targeting decoy cells, Cebpα, Pparγ, and Fabp4 mRNA expression were induced, and they were not altered by treatment with Dox (Figure 4.10A, C, E). In miR-433 decoy cells, the expression of adipogenic marker genes were the same in the presence or absence of Dox (Figure 4.10B, D, F), indicating that miR-433 does not regulate adipogenic differentiation.

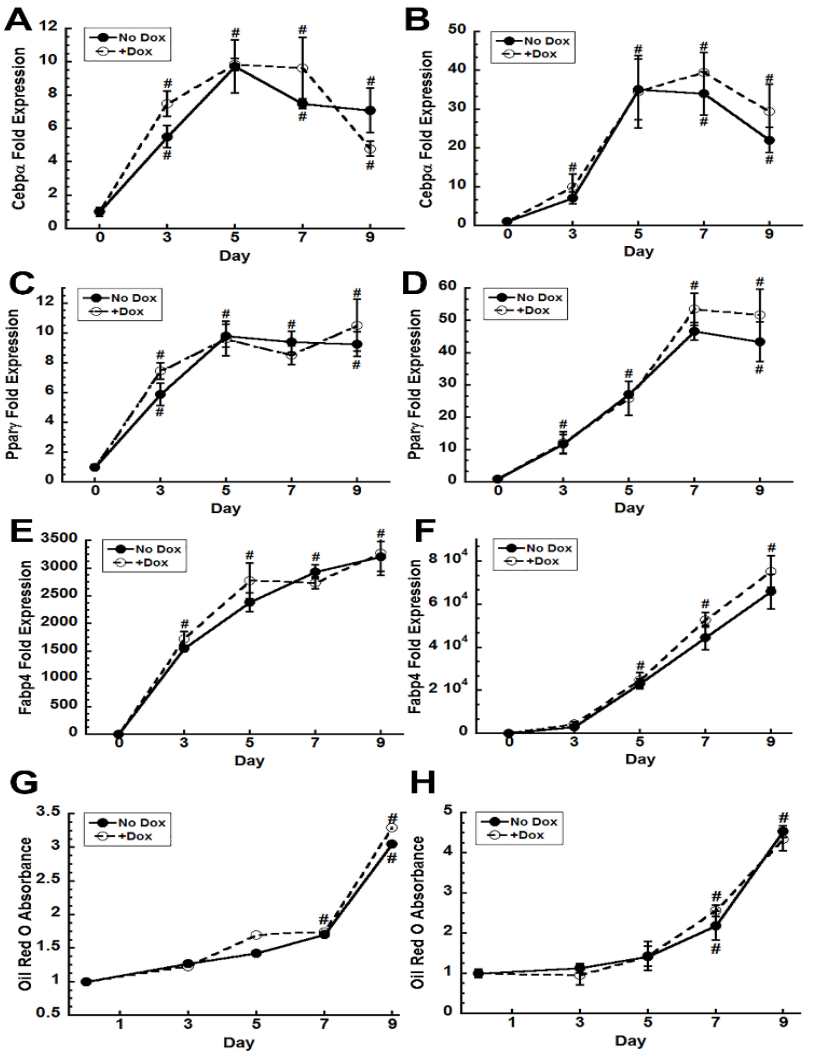

Figure 4.10. miR-433 inhibition does not alter adipogenesis
Non-targeting and miR-433 decoy cells were differentiated with 500 nM rosiglitazone and 1 µM insulin for up to 9 days in the absence of presence of 1 ug/ml Dox. Cebpα mRNA expression in (A) non-targeting and (B) miR-433 decoy cells. Pparγ mRNA expression in (C) non-targeting and (D) miR-433 decoy cells. Fabp4 mRNA expression in (E) non-targeting and (F) miR-433 decoy cells. Quantification of lipid droplet formation by Oil Red O staining in (G) non-targeting and (H) miR-433 decoy cells. # = significantly different from day 0, $p < 0.05$. (n=4).

miR-433 expression increases during chondrogenic differentiation

TGF-β is a crucial mediator of chondrogenic differentiation. Since miR-433 is a negative regulator of TGF-β signaling, we next examined miR-433 expression in BMSCs

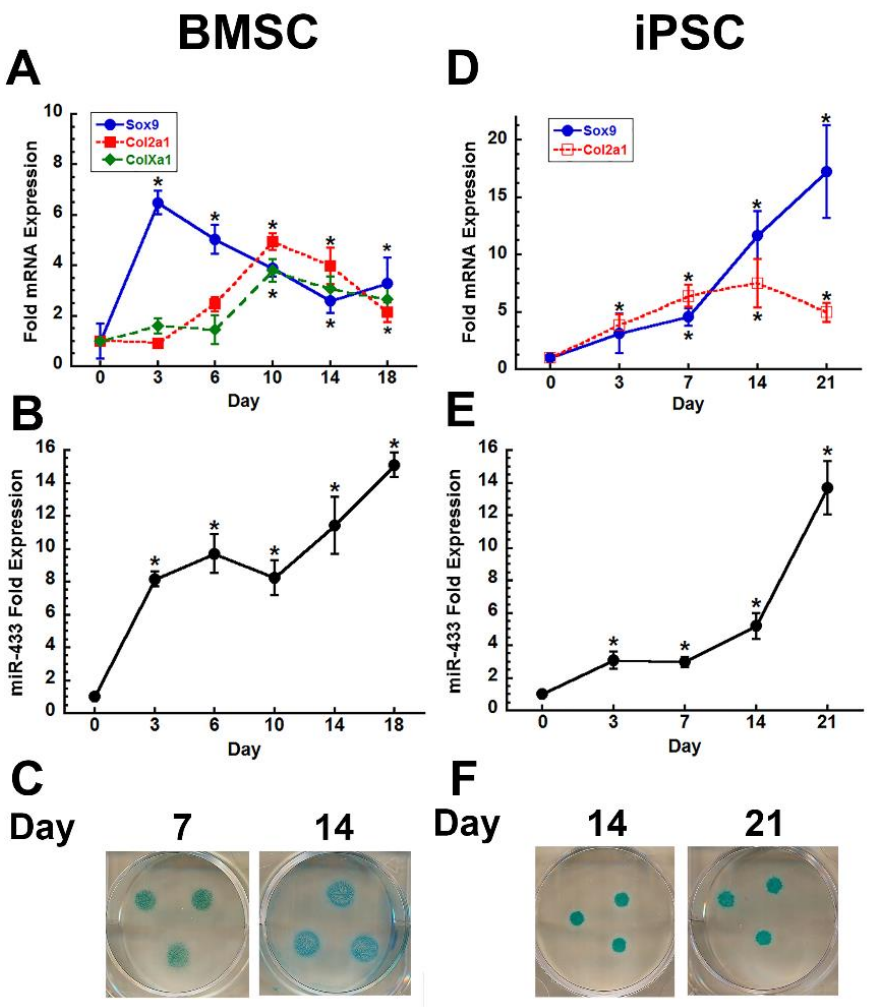

Figure 4.11. miR-433 expression increases during chondrogenic differentiation of bone marrow stromal cells and iPSC derived mesenchymal cells
(A) Sox9, Col2a1, and ColXa1 mRNA, (B) miR-433 expression, and (C) Alcian Blue staining in bone marrow stromal cells differentiated with a chondrogenic cocktail containing 10 ng/ml TGF-β1 for up to 18 days. (D) Sox9 and Col2a1 mRNA, (E) miR-433 expression, and Alcian Blue staining in mesenchymal cells derived from human iPSCs differentiated with a chondrogenic cocktail containing 100 ng/ml BMP-2 for up to 21 days. * = significantly different from day 0, $p < 0.05$. (n=4)

cultured in high density micromasses and differentiated with a chondrogenic cocktail

containing TGF-β1 and BMP-2. Expression of the early chondrogenic marker gene Sox9 increased first, followed by induction of the later chondrogenic genes type 2 collagen a1 (Col2a1) and type 10 collagen a1 (ColXa1), and the production of proteoglycans measured by Alcian Blue staining (Figure 4.11A, E). miR-433 expression increased substantially during chondrogenic differentiation, with a 14 fold induction by 18 days of differentiation in comparison to day 0 (Figure 4.11C). miR-433 expression was similarly, although less dramatically induced during the chondrogenic differentiation of C3H/10T1/2 cells (Figure 4.12).

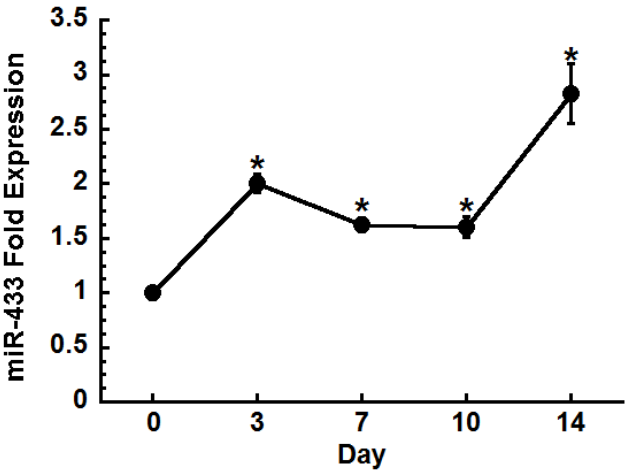

Figure 4.12. miR-433 expression increases during chondrogenic differentiation of C3H/10T1/2 cells
miR-433 decoy cells were differentiated a chondrogenic cocktail containing 10 ng/ml TGF-β1 and 100 ng/ml BMP-2 for up to 14 days in the absence Dox and measured for miR-433 expression. * = significantly different from day 0, $p < 0.05$ (n=4)

Induced pluripotent stem cells (iPSCs) show promise for clinical applications in the repair of cartilage defects. Indeed, iPSC derived-MSCs can be potently differentiated towards the chondrogenic lineage (185). To determine whether miR-433 expression showed a similar response in human cells, we examined a previously characterized skin dermal fibroblast-derived iPSC line (185). The MSC-like progenitors derived from iPSCs were cultured in high density micromasses with a chondrogenic cocktail containing BMP-2, and expression of chondrocyte markers and miR-433 was examined. Sox9 and Col2a1

mRNA expression, and proteoglycan synthesis, were significantly increased with chondrogenic differentiation (Figure 4.12D, F), and miR-433 was significantly increased at all time points compared to day 0, reaching a 14 fold induction by day 21 of differentiation, as seen in the mouse BMSCs (Figure 4.12E). This demonstrates that miR-433 levels increase during chondrogenesis in both murine and human cells.

miR-433 restrains chondrogenesis

To examine the role of miR-433 in chondrocytes, non-targeting and miR-433 decoy cells were grown as micromasses, cultured under chondrogenic conditions, and examined for chondrocyte marker genes and proteoglycan deposition. Sox9, Col2a1, and ColXa1 mRNA expression in non-targeting decoy cells increased significantly at all time points, and culture in the presence of Dox did not affect chondrogenic marker gene expression (Figure 4.13A, C, E). In the absence of Dox, miR-433 decoy cells showed a similar response in chondrocyte marker mRNA expression. However, miR-433 inhibition potently enhanced expression of the early marker Sox9 mRNA at days 7 and 10 (Figure 4.13B). The miR-433 decoy appreciably increased Col2a1 mRNA by day 7, an effect sustained through day 14 (Figure 4.13D). miR-433 inhibition also increased mRNA for the hypertrophic marker ColXa1 at days 7 and 14 (Figure 4.13F). As seen with osteoblasts, miR-433 also suppressed chondrogenic differentiation.

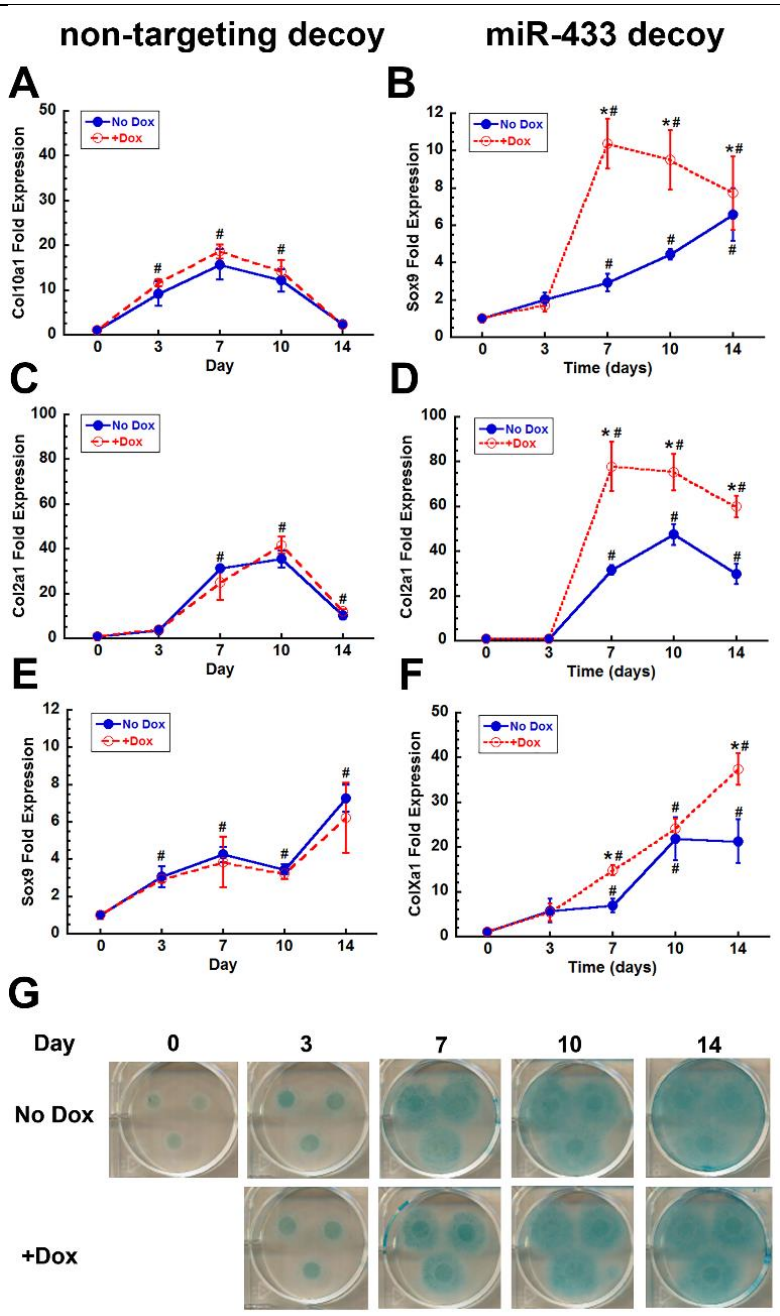

Figure 4.13. miR-433 inhibition induces chondrogenic differentiation
Non-targeting and miR-433 decoy cells were differentiated a chondrogenic cocktail containing 10 ng/ml TGF-β1 and 100 ng/ml BMP-2 for up to 14 days in the absence of presence of 1 ug/ml Dox. Sox9 mRNA expression in (A) non-targeting and (B) miR-433 decoy cells. Col2a1 mRNA expression in (C) non-targeting and (D) miR-433 decoy cells. ColXa1 mRNA expression in (E) non-targeting and (F) miR-433 decoy cells. (G) miR-433 decoy cells stained with Alcian Blue in the absence or presence of Dox. # = significantly different from day 0, $p < 0.05$. * = significantly different from corresponding no Dox control, $p < 0.05$. (n=4)

miR-433 promotes trabecular bone volume and suppresses SMAD2 and TGFBR1 mRNA in vivo

Since miR-433 inhibition enhanced osteoblast gene marker expression *in vitro*, we next developed an in vivo model to determine if miR-433 plays a similar role in regulating the skeleton. We created transgenic mice in which the miR-433 decoy, contained within the 3' UTR of the red fluorescent reporter gene tdTomato, was expressed under the control of a 3.6 kb fragment of the rat Col1a1 promoter (miR-433 decoy mice). We obtained 3 germline founders (A, B, and C). Expression of the tdTomato-miR-433 decoy in 8 week old male calvaria was determined by qRT-PCR. TdTomato mRNA from miR-433 decoy^{Col1a1} mice demonstrated similar transgene expression in lines B and C, whereas transgene expression in line A is ~5 fold lower (Figure 4.14). As expected, frozen sections show the decoy (tdTomato signal) is expressed in periosteum, endosteum, trabecular osteoblasts, and early osteocytes in both male and female mice at 8 weeks (Figure 4.15).

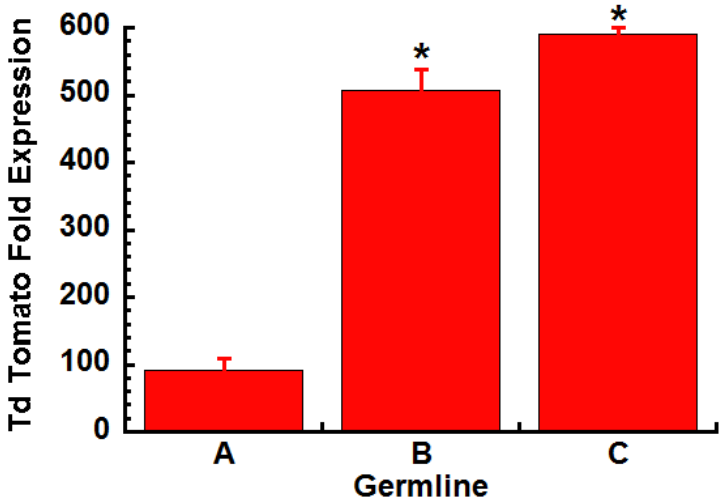

Figure 4.14. Transgene expression in 3 germlines. Calvaria were isolated from 8 week old male transgenic mice expressing the miR-433 decoy under the control of a Col1a1 promoter (miR-433 decoy^{Col1a1} mice) and wild type litter mate controls between 3 germlines. TdTomato mRNA were quantified in calvaria at ZT13 and compared to WT littermates. n=7. * = significantly different germline A, $p < 0.05$.

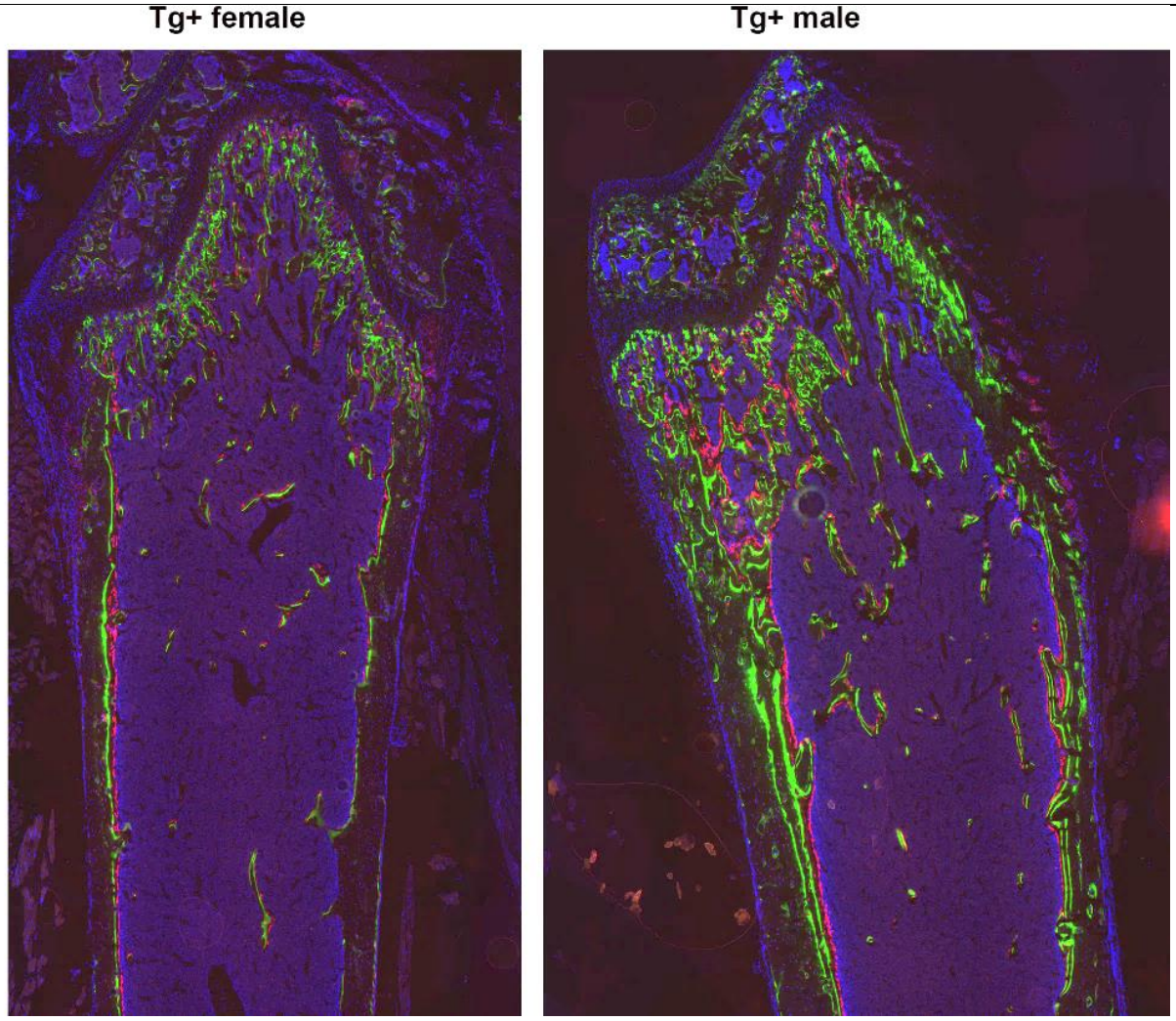

Figure 4.15. Frozen section from miR-433 decoy^{Col1a1} mice. 8 week old mouse femur from female and male. Red=tdTomato from decoy; green=calcien; blue/teal=DAPI

Our *in vitro* studies indicated that miR-433 targets SMAD2 and TGFBR1 and inhibits TGF-β signaling. To determine whether miR-433 plays a similar role in the regulation of the TGF-β signaling *in vivo*, we examined SMAD2 and TGFBR1 mRNA expression in miR-433 decoy^{Col1a1} mice. In 8 week old male mice, the presence of the miR-433 decoy enhanced SMAD2 and TGFBR1 mRNA expression by 2 and 1.65 fold,

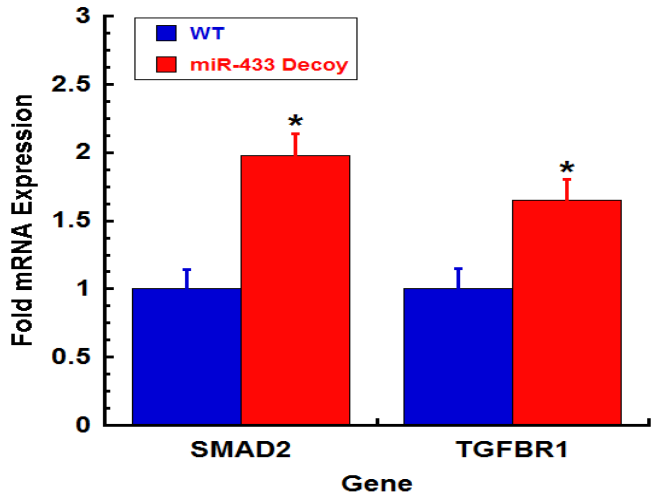

Figure 4.16. miR-433 inhibits SMAD2 and TGFBR1 mRNA expression in vivo.
Calvaria were isolated from 8 week old male transgenic mice expressing the miR-433 decoy under the control of a Col1a1 promoter (miR-433 decoy^{Col1a1} mice) and wild type litter mate controls. SMAD2 and TGFBR1 mRNA were quantified in calvaria at ZT13. n=7. * = significantly different WT littermates, $p < 0.05$.

respectively (Figure 4.16). Inhibition of miR-433 activity increased the expression of TGF-β signaling components *in vivo*, corroborating our *in vitro* results.

Using micro CT, we analyzed the trabecular and cortical phenotype in femurs of male and female miR-433 decoy^{Col1a1} mice at 4 and 8 weeks of age and compared them to matched littermate controls. The first thing we noted was that each transgenic line displayed a similar bone phenotype, suggesting that the level of transgene expression in Line A is sufficient. Therefore, we combined the data from the 3 lines in our subsequent analyses.

At 4 weeks of age, female miR-433 decoy^{Col1a1} and WT littermates displayed similar trabecular bone parameters (Table 4.2). In contrast, 4 week old miR-433 decoy^{Col1a1} male mice had a marked reduction in trabecular bone, with a 20% reduction in BV/TV (Table 4.1). Trabecular thickness and number were also significantly decreased in miR-433 decoy^{Col1a1} mice, with increased trabecular spacing (Table 4.1). In miR-433 decoy^{Col1a1} mice, multiple bone parameters were also markedly decreased, including connective density, apparent density, tissue density, total volume, and bone volume (Table 4.1). SMI (structural model index) evaluation suggested that trabecular bone in miR-433 decoy^{Col1a1} mice also has an increased cylindrical structure compared to WT mice (Table 4.1). Cortical measurements in 4 week old male mice revealed no significant differences between miR-433 decoy^{Col1a1} and WT mice. Overall, miR-433 increases trabecular bone in 4 week old male mice, but does not affect female mice. At 8 weeks of age, no significant differences were observed in male or female mice in trabecular or cortical bone in miR-433 decoy^{Col1a1} and WT mice (Table 4.3, 4.4).

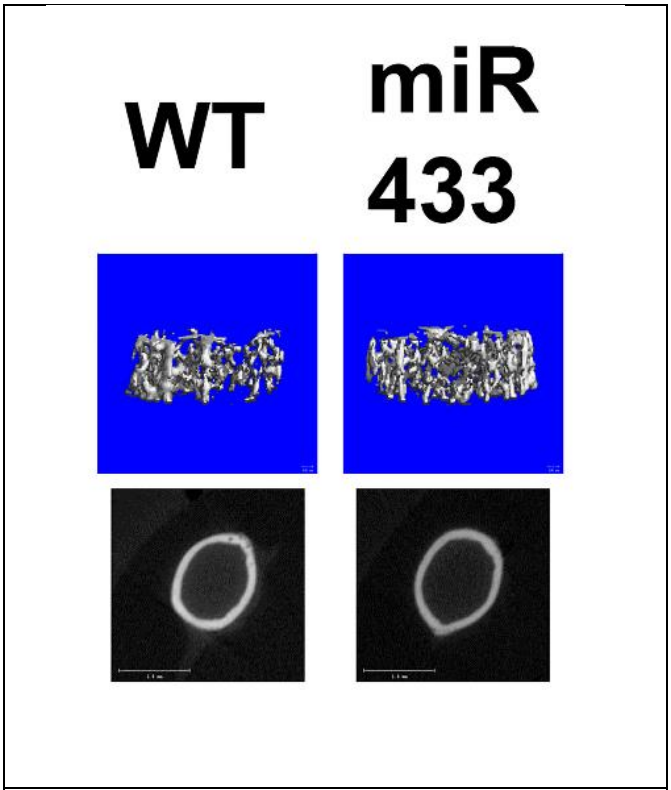

Figure 4.17. Representative microCT image of trabecular and cortical bone in 4 week old male miR-433 decoy^{Col1a1} mice.

Table 4.1. Male Trabecular Bone Measurements. * = p < 0.05. ** = p < 0.01. *** = p < 0.001.

Age	**4 week**			**8 week**	
Genotype	**WT**	**miR-433 Decoy^{Col1a1}**		**WT**	**miR-433 Decoy^{Col1a1}**
	n=16	n=18		n=8	n=10
Bone Parameters					
BVF (Bone Volume/Total Volume) (%)	12.8 ± 2.80	10.0 ± 1.70***		15.9 ± 3.6	16.4 ± 5.90
Trab. Thickness (µM)	51.0 ± 5.00	46.4 ± 2.40***		57.0 ± 4.4	53.9 ± 7.90
Trab. Number (1/mm)	4.81 ± 0.29	4.39 ± 0.35***		4.92 ± 0.63	5.11 ± 0.58
Trab. Spacing (µM)	210 ± 13.0	232 ± 20.0***		204 ± 31.0	195 ± 26.0
Connect. Density (1/mm^3)	93.0 ± 22.0	75.1 ± 22.5**		109 ± 35.7	111 ± 38.2
Apparent Density (mg/ccm HA)	131 ± 15.0	112 ± 11.4***		190 ± 32.9	183 ± 43.2
Tissue Density (mg/ccm HA)	627 ± 19.0	613 ± 26.0*		814 ± 15.0	786 ± 35.0
Total Volume (TV, mm^3)	1.17 ± 0.09	1.13 ± 0.09		1.82 ± 0.23	1.78 ± 0.25
Bone Volume (BV, mm^3)	0.15 ± 0.03	0.11 ± 0.02***		0.29 ± 0.09	0.30 ± 0.13
Structural Model Index	2.80 ± 0.20	3.00 ± 0.18*		2.48 ± 0.32	2.41 ± 0.51
Bone Surface (BS, mm^2)	6.60 ± 1.10	5.40 ± 0.97***		12.1 ± 3.48	12.3 ± 4.13
BS/BV (mm^2)	53.0 ± 6.30	58.8 ± 3.73**		46.5 ± 4.72	49.7 ± 11.0
BS/TV (1/mm)	5.60 ± 0.80	4.75 ± 0.70***		6.56 ± 1.34	6.76 ± 1.71
BS/MV (1/mm)	6.50 ± 1.20	5.29 ± 0.89***		7.87 ± 1.85	8.25 ± 0.14

Table 4.2. Female Trabecular Bone Measurements					
Age	**4 week**			**8 week**	
Genotype	**WT**	**miR-433 Decoy^{Col1a1}**		**WT**	**miR-433 Decoy ^{Col1a1}**
	n=10	n=6		n=9	n=11
Bone Parameters					
BVF (Bone Volume/Total Volume) (%)	7.3 ± 1.50	8.2 ± 1.00		5.50 ± 0.80	5.50 ± 1.30
Trab. Thickness (µM)	45.0 ± 1.50	45.7 ± 2.10		40.6 ± 1.20	40.5 ± 3.30
Trab. Number (1/mm)	3.87 ± 0.51	4.10 ± 0.56		3.67 ± 0.29	3.64 ± 0.24
Trab. Spacing (µM)	265 ± 33.0	252 ± 33.0		278 ± 23.0	277 ± 18.0
Connect. Density (1/mm^3)	47.4 ± 14.8	52.9 ± 11.1		24.4 ± 7.92	26.1 ± 14.6
Apparent Density (mg/ccm HA)	95.2 ± 11.3	101 ± 7.30		88.9 ± 10.5	82.1 ± 10.7
Tissue Density (mg/ccm HA)	615 ± 22.0	610 ± 27.0		792 ± 24	790 ± 29.0
Total Volume (TV, mm^3)	1.09 ± 0.09	1.08 ± 0.08		1.50 ± 0.12	1.48 ± 0.12
Bone Volume (BV, mm^3)	0.08 ± 0.02	0.09 ± 0.01		0.08 ± 0.01	0.08 ± 0.02
Structural Model Index	3.19 ± 0.18	3.07 ± 0.17		3.38 ± 0.14	3.35 ± 0.23
Bone Surface (BS, mm^2)	3.85 ± 1.05	4.26 ± 0.61		4.11 ± 0.57	4.08 ± 0.99
BS/BV (mm^2)	60.9 ± 2.10	59.5 ± 4.25		66.7 ± 2.21	67.4 ± 5.38
BS/TV (1/mm)	3.48 ± 0.75	3.94 ± 0.47		2.74 ± 0.42	2.76 ± 0.62
BS/MV (1/mm)	3.76 ± 0.86	4.29 ± 0.55		2.91 ± 0.47	2.92 ± 0.71

Table 4.3. Male Cortical Bone Measurements					
Age	**4 week**			**8 week**	
Genotype	**WT**	**miR-433 Decoy^{Col1a1}**		**WT**	**miR-433 Decoy ^{Col1a1}**
	n=16	n=18		n=8	n=10
Bone Parameters					
Length (mm)	11.5 ± 0.40	11.6 ± 0.300		14.1 ± 0.50	14.1 ± 0.40
Sub-periosteal area (mm^2)	1.35 ± 0.13	1.31 ± 0.05		1.80 ± 0.17	1.80 ± 0.20
Sub-endosteal area (mm^2)	0.95 ± 0.08	0.93 ± 0.03		1.07 ± 0.10	1.07 ± 0.12
Cortical Mask (mm^2)	0.40 ± 0.06	0.37 ± 0.03		0.72 ± 0.07	0.73 ± 0.10
Segmented Bone (mm^2)	0.34 ± 0.05	0.32 ± 0.03		0.72 ± 0.07	0.73 ± 0.10
Periosteal Perimeter (mm)	3.06 ± 0.25	3.01 ± 0.18		4.48 ± 0.39	4.47 ± 0.42
Endosteal Perimeter (mm)	3.45 ± 0.14	3.42 ± 0.06		3.67 ± 0.18	3.65 ± 0.19
Cortical Porosity (mm^2)	0.05 ± 0.00	0.05 ± 0.00		0.00 ± 0.00	0.00 ± 0.00
Cortical Thickness (mm)	0.08 ± 0.01	0.08 ± 0.01		0.16 ± 0.01	0.16 ± 0.02
Polar Moment of Inertia (MOI) (mm^4)	0.13 ± 0.03	0.12 ± 0.01		0.35 ± 0.06	0.36 ± 0.08
Max MOI (mm^4)	0.08 ± 0.02	0.07 ± 0.01		0.23 ± 0.04	0.24 ± 0.05
Min MOI (mm^4)	0.05 ± 0.01	0.05 ± 0.00		0.12 ± 0.02	0.12 ± 0.03

Table 4.4. Female Cortical Bone Measurements		
Age	**8 week**	
Genotype	**WT**	**miR-433 Decoy ^{Col1a1}**
	n=9	n=11
Bone Parameters		
Length (mm)	14.1 ± 0.53	14.1 ± 0.43
Sub-periosteal area (mm^2)	1.80 ± 0.17	1.80 ± 0.20
Sub-endosteal area (mm^2)	1.08 ± 0.10	1.06 ± 0.11
Cortical Mask (mm^2)	0.72 ± 0.08	0.74 ± 0.10
Segmented Bone (mm^2)	0.70 ± 0.08	0.73 ± 0.10
Periosteal Perimeter (mm)	4.48 ± 0.39	4.47 ± 0.42
Endosteal Perimeter (mm)	3.67 ± 0.18	3.66 ± 0.19
Cortical Porosity (mm^2)	0.00 ± 0.00	0.00 ± 0.00
Cortical Thickness (mm)	0.16 ± 0.01	0.16 ± 0.02
Polar MOI (mm^4)	0.35 ± 0.06	0.36 ± 0.08
Max MOI (mm^4)	0.23 ± 0.04	0.24 ± 0.05
Min MOI (mm^4)	0.12 ± 0.02	0.12 ± 0.03

Discussion

TGF-β is an essential growth factor directing lineage commitment of mesenchymal cells. In this study, we identified miR-433 as a negative regulator of TGF-β signaling, and demonstrated novel miR-433 targets *in vitro* and *in vivo*, SMAD2 and TGFBR1. In addition, we identified 3 distinct patterns of miR-433 expression with cell lineage progression: decreased expression during osteogenesis, unchanged expression during adipogenesis, and increased expression during chondrogenesis. Moreover, we confirmed that miR-433 serves to limit differentiation of osteoblasts, but does not affect adipogenesis. However, the function of miR-433 in vivo is important for trabecular bone volume in growing male mice, whereas it does not appear to impact bone in young female mice. Most promising, we identified miR-433 as a potent inhibitor of chondrogenesis. Strategies aimed at inhibiting miR-433 activity could represent a novel avenue for the stimulation of cartilage formation.

Information on the mechanisms regulating miR-433 expression is limited. Transcription of the miR-433 locus is induced by orphan receptor estrogen related receptor γ (ERRγ), a repressor of osteogenesis, and negative regulator of chondrocyte proliferation (186). In contrast, miR-433 transcription can be repressed by small heterodimer partner (SHP, NR0B2), which promotes osteoblast differentiation (101,169,170). The miR-433 promoter also contains CpG islands, and changes in promoter methylation status have been shown to contribute to its regulation in cancer cells (187). Although miR-433 expression is increased in osterix-null mouse calvaria,

direct regulation of the miR-433 promoter by osterix was not demonstrated (188). The molecular mechanisms regulating miR-433, particularly during chondrogenesis, remain to be determined.

TGF-ß plays an important but complex role at every stage of bone formation. TGF-ß promotes osteoblast proliferation and acts as a chemoattractant during early stages of differentiation, but inhibits terminal differentiation by suppressing alkaline phosphatase and osteocalcin, as well as suppressing matrix mineralization (22,189-191). Thus, the timing and intensity of TGF-ß signaling needs to be tightly controlled for optimal osteoblast function. miRNAs often function to fine tune the expression of their targets, and in the case of miR-433, it could play a role in moderating the TGF-ß response during osteogenic differentiation, to ensure an optimal level of signaling. However, the regulation of osteogenesis by miR-433 is not limited to TGF-ß mediated mechanisms. miR-433 was previously shown to target Runx2, Igf-1, osteonectin, and glucocorticoid receptor mRNA, all of which play important roles during osteogenic differentiation (101,134,182). miR-433 likely restrains osteogenic differentiation *in vitro* by inhibiting multiple pathways important for differentiation.

Given the cell autonomous actions of miR-433 identified *in vitro*, it was somewhat surprising to find that inhibition of miR-433 activity *in vivo* resulted in decreased trabecular bone volume in males. In miR-433 decoy^{Col1a1} male mice at 4 weeks of age, the trabecular bone compartment had reduced BV/TV, trabecular number and thickness, with increased

trabecular spacing. By 8 weeks of age, the trabecular bone phenotype in miR-433 decoy^{Col1a1} mice was normalized. It is also possible that enhanced TGFβ signaling in cells expressing the miR-433 decoy could lead to the accumulation of osteoid that is later mineralized. We recently demonstrated that miR-433 can attenuate glucocorticoid signaling. The miR-433 decoy^{Col1a1} mice may have upregulated glucocorticoid signaling, and it is well documented that glucocorticoid excess decreases bone formation (reviewed by (81); (192)). It is also possible that miR-433 could be targeting pathways that are more important in growing mice than in adults. For example, knockdown of parathyroid receptor signaling in mice at 4 weeks of age reduced osteoblast number to a greater extent than when the receptor was knocked down at 8 weeks (193). However, since the activity of the Col1a1 promoter-driven transgene is higher in growing mice than in adults, it is very likely reduced transgene expression in the 8 week old mice contributes to the normalization of the trabecular bone phenotype (162,194).

In contrast to the male mice, our microCT analysis did not demonstrate a bone phenotype in female miR-433 decoy^{Col1a1} mice. This could be due to multiple reasons. One reason may be due to a lower sample number of female miR-433 decoy^{Col1a1} mice analyzed at 4 weeks of age. We may potentially see more modest differences by increasing the sample size. Alternatively, since female C57BL/6 mice lose trabecular bone volume with age, analysis of older female mice may be revealing. Additionally, there could be a differential role of miR-433, or differential expression, between male and female mice. Another potential reason for differences between the sexes could be the result of higher glucocorticoid levels in female mice, suggesting that males might be more

sensitive to smaller variations in glucocorticoid signaling (195,196).

Calvarial bone from miR-433 decoy^{Col1a1} mice had increased SMAD2 and TGFBR1 mRNA expression, and we previously demonstrated that they have increased Runx2 and osteocalcin mRNA, suggesting that miR-433 may, indeed, be a negative regulator of bone formation. Yet, trabecular bone volume was decreased in growing miR-433 decoy^{Col1a1} male mice This suggests there may be potential alterations in miR-433 regulation of the skeleton depending on the age of mice, or that there may be differential regulation between the calvaria and femur bones. Further analysis of bone formation rate and osteoclastic parameters is needed to fully understand the role of miR-433 in the skeleton.

TGF-β is also a potent inducer of chondrogenesis (reviewed by (25)). TGF-β promotes type II collagen synthesis through the interaction of SMAD2/3 with Sox9 on type II collagen enhancer elements (31). However, TGF-β can inhibit chondrocytes from terminally differentiating into hypertrophic chondrocytes, reducing extracellular matrix mineralization (reviewed by (25)). miR-433 expression is profoundly induced during chondrogenic differentiation of both murine and human cells. Moreover, this increase in miR-433 was observed using chondrogenic differentiation cocktails that contained TGF-ß and those that lacked TGF-ß, suggesting a fundamental, well conserved mechanism.

During early stages of chondrogenesis, low levels of miR-433 could help augment the TGF-ß response, while at later stages, where miR-433 expression is highest, this miRNA

could weaken the TGF-ß response to allow progression towards hypertrophy. That TGFBR1 is decreased with chondrocyte hypertrophy of BMSCs reinforces the concept that TGF-ß signaling should be limited during this phase (197). As with osteoblasts, miR-433 likely targets other pathways important for chondrogenesis, contributing to its role as a repressor of differentiation.

In humans, miR-433 has been linked to a form of dominant X-linked chondrodysplasia, in which a histone deacetylase 6 (HDAC6) 3' UTR variant causes a change in miR-433 seed region targeting (135). Affected patients have increased HDAC6 protein levels due to altered miR-433 binding, suggesting that miR-433 levels could regulate acetylation of HDAC6 targets (135). In mice, overexpression of HDAC4, a class II HDAC related to HDAC6, prevents mineralization of hypertrophic chondrocytes and causes shortened limbs, due the altered acetylation of the Runx2 promoter, which decreases its activity (198). HDAC6 and Runx2 have been found to interact together in osteoblasts (199). It is possible that targeting of HDAC6 by miR-433 could contribute to its actions in chondrogenic differentiation by affecting acetylation and thus transcriptional regulation of downstream targets.

In extra-skeletal tissues, miR-433 was shown to promote renal fibrosis, and that miR-433 expression is increased in response to TGF-ß in kidney tubular epithelial cells (200,201). In these studies, SMAD3 promoted the expression of miR-433, whereas SMAD2 repressed miR-433 levels (200). Functional SMAD binding sites were identified

in the miR-433 proximal promoter, suggesting direct regulation, although the induction of miR-433 by TGF-ß in these studies was not observed until 12 hours post treatment. In contrast, we showed that TGF-ß decreased the expression of miR-433 in mesenchymal lineage cells after 24 hours of treatment. The differential regulation of miR-433 by TGF-ß is likely cell type specific, possibly related to differences in SMAD2 vs SMAD3 signaling in mesenchymal and epithelial cells. The delay in the response of miR-433 to TGF-ß in mesenchymal cells could suggest a requirement for prolonged TGF-ß signaling, or an indirect effect of TGF-ß on miR-433 transcription, or could reflect the time needed for the turnover of existing miR-433, since miRNAs are, in general, fairly stable (202,203). Within the skeleton, a TGF-ß-miR-433 negative regulatory loop could allow for the renewal of cell sensitivity to TGF-ß.

There are multiple skeletal pathologies in which defects in TGF-ß regulation are implicated. For example, over activation of TGF-ß signaling is important in the pathogenesis of connective tissue disorders such as Loeys-Dietz syndrome, Marfan syndrome, and Camurati-Engelmann disease (204-206). Moreover, TGF-ß released from the bone matrix plays a supportive role in the survival of bone metastatic breast cancer cells and multiple myeloma cells (207). In fracture repair, osteoprogenitors migrate and respond to TGF-ß released from bone and platelets (208,209). Identifying miR-433 targets in the TGF-ß signaling pathway enhances to our understanding of the possible function of miR-433 in these diseases, as well as comprehending its function in other tissues expressing miR-433, such as liver, cartilage, brain, and immune cells (126,135,210-212).

Overall, we show that miR-433 targets SMAD2 and TGFBR1, and downregulates TGF-ß signaling. This likely contributes to the inhibitory effect of miR-433 on osteoblastic and chondrogenic differentiation. These findings add to our understanding of how miRNAs regulate differentiation and their impact on skeletal development and remodeling.

Materials and Methods.

Mice

C57BL/6 male mice were provided with food and water ad libitum. All animal protocols were reviewed and approved by the UConn Health Institutional Animal Care and Use Committee (IACUC).

We created mice expressing a transgene in which a 3.6 kb fragment of the rat col1A1 promoter, plus 1.6 kb of the first intron drive expression of the tdTomato reporter gene carrying a miR-433 tough decoy (TuD) in its 3' UTR (custom synthesis, GenScript, Piscataway, NJ) (156,162). Mice were generated in a C57BL/6 background by pronuclear injection of the transgene cassette at the UConn Health Gene Targeting and Transgenic Facility. The miR-433 decoy serves as a competitive inhibitor of miR-433 activity, relieving the suppression of endogenous miR-433 targets.

Cell culture and cell proliferation

C3H/10T1/2, Clone 8, a multipotent mouse mesenchymal cell line, was obtained from the American Type Culture Collection (ATCC® CCL-226™) and cultured in DMEM (Gibco Life Technologies, Carlsbad, CA) supplemented with 10% heat-inactivated Fetal Bovine Serum (FBS, Lonza, Basel, Switzerland) and 1% penicillin-streptomycin. Primary bone marrow stromal cells (BMSCs) were flushed from the long bones of 8 week old male C57BL/6 mice by centrifugation and maintained in αMEM supplemented with 10% FBS and 1% penicillin-streptomycin (213).

Mesenchymal stem cell (MSC)-like cells were derived from human dermal fibroblast iPSC line (HDFa-YK26), as previously described (21). iPSC-derived MSCs were maintained in growth media consisting of DMEM-HG (Gibco Life Technologies, Carlsbad, CA), 10% defined FBS (Hyclone), 1% nonessential amino acids, 5 ng/mL human recombinant bFGF (Invitrogen), and 1% penicillin-streptomycin.

Cell proliferation was assessed on days 1 through 4 post-plating, using MTS CellTiter 96 Aqueous One solution cell proliferation assay kit (Promega, Madison, WI), according to manufacturer's instructions. Cells were plated at 5,000 cells/well and were treated in the absence or presence of 1 μg/ml Dox in DMEM with 10% FBS and 1% Penicillin/Streptomycin.

Osteogenic, chondrogenic, and adipogenic differentiation

For osteogenic differentiation of BMSCs, αMEM was supplemented with 10% FBS, 5 mM β-glycerophosphate (Sigma-Aldrich) and 50 µg/ml ascorbic acid (Sigma-Aldrich), once cells had reached confluence. For osteogenic differentiation of C3H/10T1/2 cells, DMEM was supplemented with 10% FBS, 8 mM β-glycerophosphate, 100 µg/ml ascorbic acid, 2 µM purmorphamine (Sigma-Aldrich), and 50 ng/ml BMP (gift from Medtronic). Calcium deposition was measured by staining cells with 1% alizarin red S pH 6.45 (Sigma-Aldrich). Alizarin red stain was extracted and quantified at absorbance 405 nm (134). Cells were stained for alkaline phosphatase activity using an Alkaline Phosphatase kit (#86R, Sigma-Aldrich).

Adipogenic differentiation was achieved by culturing cells in αMEM supplemented with 10% FBS, 500 nM rosiglitazone (Sigma-Aldrich) and 1 µM insulin (Sigma-Aldrich). Cells were stained with 0.5% Oil Red O solution, extracted with 100% isopropanol, and absorbance was measured at 492 nm.

For chondrogenic differentiation of BMSCs and C3H/10/T1/2 cells, cells were cultured in high density micromasses ($2x10^5$ cells/10uL drop) in wells coated with 0.1% gelatin. Twenty-four hours after micromass formation, culture media was replaced with chondrogenic media consisting of αMEM supplemented with 1% insulin-transferrin-selenium, 40 µg/ml L-proline, 50 µg/ml ascorbic acid, 100 nM dexamethasone (Sigma-Aldrich), 1 mM sodium pyruvate (ThermoScientific), 1% non-essential amino acids, 10

ng/ml TGF-β1 (R&D Systems), and 100 ng/ml BMP (Medtronic). iPSC-MSCs were differentiated in the same chondrogenic cocktail, but excluding TGF-β1 (185). Micromass cultures were fixed in 10% formalin, then stained with 1% Alcian Blue (Sigma-Aldrich) in acetic acid to visualize proteoglycan synthesis after 14 days of differentiation.

Establishment of a stable inducible miR-433 knockdown model

To knockdown activity of miR-433, C3H/10T1/2 cells were transduced using lentiviral constructs in which a doxycycline (Dox)-inducible promoter drives expression of a miR-433 tough decoy (custom synthesis, GenScript). The miR-433 decoy acts as a competitive inhibitor for endogenous miR-433 activity because it contains complementary miR-433 binding sites. Briefly, the miR-433 decoy was subcloned into the single lentivector for inducible knockdown (pSLIK) system and confirmed by sequencing (144) (Addgene, Cambridge, MA). This vector contains a ubiquitin C promoter driving constitutive expression of reverse Tet transactivator (rtTA3). Doxycycline treatment stimulates the rtTA to drive transcription of TRE, allowing for inducible expression of the decoy. A non-targeting tough decoy was developed as a control. The non-targeting decoy contains *C. elegans* miR-67 binding sites (custom synthesis, GenScript), which are not predicted to interact with mammalian miRNAs. Cells stably transduced with the pSLIK-miR-433 decoy or non-targeting decoy were selected for hygromycin resistance.

Luciferase assay

The TGF-ß-responsive Luciferase reporter SBE4-luc construct contains 4 SMAD2/3/4 binding sites (SBE, SMAD binding element) regulating the expression of Luciferase (Addgene) (214).

Gene-specific PCR primers were used to amplify from human genomic DNA the 3' UTR for SMAD2 (base pairs 2619-5306), SMAD4 (base pairs 3804-6011), TGFBR1 (base pairs 2147-3947), and TGFBR2 (base pairs 537-2524). Using the appropriate restriction enzymes, these fragments were subcloned downstream of a Cytomegalovirus (CMV) promoter-driven Luciferase reporter (pMIR-REPORT vector, Ambion, Carlsbad, CA). Constructs were verified by sequencing.

C3H/10T1/2 cells were plated at 25,000 cells/cm^2. BioT transfection reagent (1.5ul:1µg DNA; Bioland Scientific, Paramount, CA) was used to co-transfect luciferase constructs containing the 3' UTR of target mRNA, a constitutively active β-galactosidase construct (control for transfection efficiency), and miRNA hairpin inhibitors (Dharmacon/Thermo Fisher Scientific, Waltham, MA). 80 nM of anti-miR-433 or a negative control (non-targeting) miRNA inhibitors were used. Cells were serum deprived for 24 hours and cell lysates were analyzed for luciferase activity using the Luciferase Assay System (Promega) and normalized to β-Galactosidase using Galacton® (Life Technologies). Each luciferase experiment was performed at least 3 times, and each

experiment contained 6 biological replicates. More than one preparation of each DNA construct was tested.

Western blot

C3H/10T1/2 cells were plated at 300,000 cells/cm^2 and treated with Doxycyline for 24 hours in serum-free medium, to induce expression of the decoy. Cells were lysed with RIPA buffer containing Halt™ protease and phosphatase inhibitors (Thermo Fisher Scientific). A BCA assay (Thermo Fisher Scientific) was performed to quantify protein, and 20 µg protein was subjected to electrophoresis on a 10% SDS polyacrylamide gel. Proteins were transferred to a PVDF membrane (Millipore, Billerica, MA). Membranes were blocked with 5% BSA in TBS, 0.1% Tween. Rabbit anti-mouse phopho-SMAD2 primary antibody (1:1000 Cell Signaling, Danvers, MA, Cat #138D4), rabbit anti-mouse SMAD2 primary antibody (1:1000 Cell Signaling, Cat #D43B4), rabbit anti-β-actin antibody (1:2000, Cell Signaling #13E5), and goat anti-rabbit horseradish peroxidase conjugated antibody (1:10000, Sigma Aldrich A0545) were used.

Quantitative real time PCR

RNA was isolated from cell cultures using TRIzol Reagent (Life Technologies), with added GlycoBlue Blue Coprecipitate (Life Technologies). RNA quality was determined using gel electrophoresis or an Experion High Resolution RNA Chip, assessing ribosomal bands 28S and 18S (Bio-Rad, Hercules, CA). RNA samples were additionally DNased using RQ1 DNase (Promega, Madison, WI). DNased RNA was

reverse-transcribed using Moloney murine leukemia virus-reverse transcriptase (Invitrogen, Carlsbad, CA). Gene expression was quantified by qPCR with iQ SYBR Green Supermix (Bio-Rad) and normalized to 18S rRNA levels. A cDNA standard curve was utilized to determine the relative quantity of gene expression. The primer sets used are shown in Table 4.5.

Table 4.5: Primer sequences used for qPCR analysis.

Gene (mouse)	**Sequence**
18S (sense) *18S* (antisense)	5'-GCGTGTGCCTACCCTACGCC -3' 5'-ACGCAAGCTTATGGCCCGCA-3'
Ap (sense) *Ap* (antisense)	5'-CCACTCGGGTGAACCACGCC -3' 5'-CCGCCACCCATGATCACGTCG -3'
Runx2 (sense) *Runx2* (antisense)	5'- CCTCTGGCCTTCCTCTCTCAGT -3' 5'- GCCACTCTGGCTTTGGGAAGAG -3'
Oc (sense) *Oc* (antisense)	5′-TGGTGCACACCTAGCAGACAC -3′ 5′-CCGCTGGGCTTGGCATCTGT-3′
Sox9 (sense) *Sox9*(antisense)	5′-ACGAAGCTGGCAGACCAGTA -3′ 5′-CGTTCTTCACCGACTTCCTC-3′
Col2a1 (sense) *Col2a1 (antisense)*	5′-ACTGGTAAGTGGGGCAAGAC -3′ 5′-CCACACCAAATTCCTGTTCA -3′
ColXa1(sense) *ColXa1 (antisense)*	5′-CTTTGTGTGCCTTTCAATCG -3′ 5′-GTGAGGTACAGCCTACCAGTTTT -3′
Cebpα (sense) *Cebpα (antisense)*	5′-CAAGCCAGGACTAGGAGATT -3′ 5′-CCAAGGCACAAGGTTACTTC -3′
Pparγ (sense) *Pparγ (antisense)*	5′-GAAATTACCATGGTTGAGACAGAG -3′ 5′-GTGAATGGAATGTCTTCATAGTG -3′
Fabp4 (sense) *Fabp4 (antisense)*	5′-GGAACCTGGAAGCTTGTCTC -3′ 5′-TTCCTGTCGTCCTGCGGTGAT -3′
Gene (human)	**Sequence**
18S (sense) 18S (antisense)	5′-CCGATAACGAACGAGACTCTGG -3′ 5′-TAGGGTAGGCACACGCTGAGCC -3′
Sox9 (sense) Sox9 (antisense)	5′-GGAACCTGGAAGCTTGTCTC -3′ 5′-TTCCTGTCGTCCTGCGGTGAT -3′
Col2a1(sense) Col2a1 (antisense)	5′-CGTCCAGATGACCTTCCTACG -3′ 5′-TGAGCAGGGCCTTCTTGAG -3′

microRNA expression levels were analyzed using the TaqMan MicroRNA Assay (Life Technologies). RNA was reverse transcribed with gene-specific primers to generate cDNA. microRNA expression was detected by qPCR and normalized to snoRNA 202 levels. RNA experiments were performed at least twice and each experiment contained at least 4 biological replicates. Each sample was assayed in duplicate.

Micro CT

Trabecular and cortical bone was measured by conebeam micro-focus x-ray computed tomography in male and female mice within the mid-diaphysis and distal metaphysis regions (µCT 40, Scanco Medical AG, Bassersdorf, Switzerland). Serial tomographic volumes were acquired at 55kV and 145µA, collecting 1000 projections per rotation at 300 µsec integration time. Three-dimensional 16-bit grayscale images were reconstructed using standard convolution back-projection algorithms with Shepp and Logan filtering, and rendered within a 12.3 mm field of view at a discrete density of 578,704 voxels/mm3 (isometric 16-µm voxels). Segmentation of bone from marrow and soft tissue was performed in conjunction with a constrained Gaussian filter to reduce noise, applying hydroxyapatite-equivalent density thresholds of 300 mg/cm3 for cortical bone at 4 weeks, 200 mg/cm3 for trabecular compartments at 4 weeks, and 400 mg/cm3 for cortical and trabecular compartments at 8 weeks. Volumetric regions for trabecular analysis were selected within the endosteal borders to include the secondary spongiosa of femoral metaphyses located 960 µm from the growth plate and extending 1 mm proximally. Trabecular morphometry was characterized be measuring the bone volume fraction (BV/TV), trabecular thickness, trabecular number, trabecular spacing, apparent density, tissue density, total volume, bone volume, and SMI. Cortical morphometry was characterized by length, sub-periosteal and sub-endosteal area, cortical mask, segmented bone, periosteal and endosteal perimeter, cortical porosity, and cortical thickness (215).

Statistics

All data are shown as mean ± SEM, and are either a representative of 2 experiments containing 3 to 4 biological replicates per experiment; or pooled data from several experiments, representing 4 or more biological replicates. Details on biological replicates for each set of experiments are provided in the Figure Legends. Statistical significance was determined using two tailed ANOVA with Bonferroni post-hoc test or a Student's t test as appropriate (KaleidaGraph, Synergy Software, Reading, PA).

Acknowledgements.

This work was supported by the National Institute of Arthritis and Musculoskeletal and Skin Diseases of the National Institutes of Health [AR44877, AMD]; the National Institutes for Dental and Craniofacial Research [5T90DE21989]; a Grant-in-Aid award from the American Society for Bone and Mineral Research; the UConn Health Center Research Advisory Council; and the Center for Molecular Medicine at UConn Health. **The content is solely the responsibility of the authors and does not necessarily represent the official views of the National Institutes of Health.** The authors thank Medtronic for the gift of BMP2, and thank the UConn Health microCT Core for performing microCT analysis of long bones.

Conflict of interest.

The authors declare that they have no conflicts of interest with the contents of this article.

Author contributions.

SSS, RG, DH, and AMD designed the research. SSS, NSD, RG, and AMD performed the research and analyzed the data. SSS and AMD wrote the manuscript and take responsibility for data analysis.

CHAPTER 5

Summary, Significance, and Conclusions

Summary

The overall goal of this work was to determine how miR-433 regulates cell signaling to impact lineage commitment and osteoblast function, thereby affecting the development, growth and maintenance of the skeleton.

In our first study, we determined that miR-433 regulates the rhythm of the circadian clocks *in vitro* and *in vivo*. miR-433 displays a robust rhythmicity in murine calvaria, with peak expression just after light removal. 3'UTR luciferase reporter assays revealed that miR-433 directly targets 2 rhythmically expressed osteoblast genes, Igf1 and Hif1α, the regulation of which was confirmed by qRT-PCR analysis. miR-433 regulated the phase of Bmal1 and Per2 mRNA expression synchronized cells *in vitro*, and as well as Igf1 and Hif1α rhythmicity. To determine potential mechanisms underlying miR-433 regulation of the circadian clocks, we examined the ability of miR-433 to regulate glucocorticoid signaling, an important pathway for entrainment of the circadian clocks *in vivo*. Indeed, inhibition of miR-433 enhanced glucocorticoid signaling, measured by induction of direct glucocorticoid receptor transcriptional targets Dusp1 and Per2. Although miR-433 inhibits mRNA expression of the glucocorticoid receptor (both GRα and GRβ isoforms), it did not alter total glucocorticoid receptor protein levels.

Therefore, to further investigate the mechanism of miR-433 regulation of circadian clocks, we examined glucocorticoid receptor localization. Inhibition of miR-433 increased nuclear localization of glucocorticoid receptor when ligand was present, suggesting that it attenuates glucocorticoid sensitivity by limiting the residence of the glucocorticoid receptor in the nucleus.

To confirm and extend our results to the *in vivo* setting, we developed a transgenic mouse model in which the miR-433 decoy, contained within the 3' UTR of the red fluorescent reporter gene tdTomato, was expressed under the control of a 3.6 kb fragment of the rat Col1a1 promoter. In these mice, the miR-433 is expressed primarily in osteoblastic cells. In murine calvaria, expression of the miR-433 decoy increased the amplitude of Bmal1 and Per2 mRNA rhythm, and decreased Runx2 and osteocalcin mRNA. Overall, miR-433 regulates the expression of circadian clock genes in osteoblasts and dampens glucocorticoid signaling, likely contributing to the maintenance of circadian rhythm.

In our second study, we examined the role of miR-433 in regulating TGF-β signaling and the impact on lineage commitment of mesenchymal progenitor cells. miR-433 inhibits TGF-β signaling at least in part by targeting the 3'UTR of SMAD2 and TGFBR1. Inhibition of miR-433 activity in the presence of TGF-β induced SMAD2 protein levels and SMAD2 phosphorylation.

Since TGF-β is an important growth factor for initiation of osteogenic and chondrogenic differentiation, we examined miR-433 expression during lineage commitment of mesenchymal bone marrow stromal cells, to ascertain its possible role. During osteogenic differentiation, miR-433 expression decreased substantially, and miR-433 inhibitor experiments showed that miR-433 is a negative regulator of osteogenic marker gene expression and calcium deposition. During adipogenic differentiation, miR-433 expression did not change, nor did it play a role in regulating adipogenesis. miR-433 expression robustly increased during chondrogenic differentiation of murine mesenchymal bone marrow stromal cells and a human fibroblast-derived mesenchymal-like induced pluripotent stem cell line. miR-433 inhibitor experiments showed that miR-433 restrained chondrogenic differentiation, as indicated by chondrocyte gene marker expression. *In vivo*, inhibition of miR-433 activity in osteoblasts decreased trabecular volume in growing male mice, suggesting that in the complex microenvironment of a whole animal, miR-433 plays an important role in regulating signaling pathways that promote bone formation and/or indirectly limit bone resorption.

Significance

Overall, this is the first study examining miRNA mediation of osteoblast circadian rhythm and provides further evidence of miRNA regulation of the entrainment of circadian clocks in other tissues. Since miR-433 levels in bone peak when circulating glucocorticoid levels are high, it likely plays a role in balancing the glucocorticoid response. We speculate that miR-433 can modify responsiveness of peripheral tissues to variations in circulating glucocorticoids and alter bone metabolism. These findings provide an added

dimension to our understanding of the mechanisms regulating glucocorticoid responsiveness, circadian rhythm, and their potential impact on the skeleton, and could have wide ranging impacts in other tissues.

Although it is well appreciated that microRNAs regulate bone development and homeostasis, the molecular mechanisms by which many microRNAs regulate these processes are still not well understood. We identified miR-433 as a negative regulator of TGF-β signaling, an important pathway that promotes osteogenesis through recruitment of osteoprogenitors, as well as an important inducer of chondrogenesis. In this study, we provided new insights into miR-433 regulation of osteoblast differentiation and function *in vitro* and *in vivo*. In addition, we have determined that miR-433 shows differential expression patterns across 3 different lineages, although the molecular mechanisms regulating of miR-433 transcription in these tissues remains largely undetermined. We also identified 4 novel targets of miR-433: Igf1, Hif1α, SMAD2, and TGFBR1. These findings add to our understanding of how miRNAs regulate differentiation and their impact on skeletal development and remodeling.

Systemic glucocorticoids are commonly used to treat inflammatory disease, but they can have detrimental side effects. Indeed, systemic administration of glucocorticoids is the most common cause of secondary osteoporosis (216). Prolonged glucocorticoid excess can also lead to the development of glucose intolerance, diabetes, and other metabolic disorders. This study provides important information on how miR-433 regulates GR signaling, which could provide new strategies for ameliorating some of the negative

effects of glucocorticoid therapies. In addition, since miR-433 also limits TGF-β signaling, this miRNA may play a role in skeletal diseases where TGF-β signaling is altered, as in the case of Loeys-Dietz or Marfan syndromes. A thorough understanding of miR-433 function and its biological impact on the bone and cartilage in vivo could contribute to the development of therapeutics aimed at augmenting bone formation and/or cartilage repair.

Increasing evidence suggests that miRNA-based therapeutics have strong potential, because their chemistry and stability can be altered to improve their function (217,218). For example, Miravirsen is a locked nucleic acid (LNA) anti-sense oligonucleotide targeting miR-122 (Santaris Pharma). It is currently in Phase 2 clinical trials for the treatment of hepatitis. Miravirsen is designed to suppress miR-122-mediated protection of the nucleolytic degradation of hepatitis C virus (HCV), providing a mechanism for repressing HCV infection and blocking replication (219).

An additional microRNA based therapeutic, MRX34, is currently in Phase 1 trials for the treatment of selected solid malignancies (miRNA Therapeutics, Inc). MRX34 contains double stranded RNA mimics for miR-34a, a microRNA that is downregulated in cervical, ovarian, colon, and lung cancers (220). miR-34a has been found to directly target several oncogenes which play a role in cell cycle and apoptosis, including cyclin dependent kinase 4 (CDK4), B cell lymphoma 2 (BCL2), and Wnt 1/3, (220). MRX34 compound consists of the double stranded miR-34 mimic encapsulated in a liposome nanoparticle carrier, which is designed to enhance uptake by cancer cells (220,221).

Perhaps the greatest barrier to miRNA-based therapeutic is the ability to target them to the appropriate tissues. Recently, a system for targeting small RNAs to bone formation surfaces was reported. It consists of 8 aspartate repeats conjugated with a liposome containing miRNA inhibitors. The aspartate repeats enhance the binding of the liposome to crystalized hydroxyapatite surfaces found at sites of bone formation (222). These clinical trials and continued advances in the targeting miRNA-based therapeutics to the bone compartment provide a strong basis for future work on the use of miRNA based therapeutics to treat skeletal disorders.

Conclusion

Overall, miR-433 is a potent inhibitor of glucocorticoid and TGF-β signaling, and restrains osteogenic and chondrogenic differentiation in vitro. Although miR-433 decoy^{Col1a1} mice have decreased trabecular bone volume, they display increased mRNA for Runx2 and osteocalcin, as well as SMAD2. The interaction of pathways targeted by miR-433 in the context of the complex in vivo environment give rise the skeletal phenotype we observe, and the underlying mechanisms need to be identified.

miRNAs target multiple mRNAs and can lead to substantial changes in signaling, therefore their effects can be wide ranging and diverse within an organism. The utilization of *in vitro* models to study molecular mechanisms of regulation, combined with *in vivo* models to understand phenotypic alterations, are critical for a three-dimensional understanding of bone physiology and the role of miRNAs. These findings add to our understanding of how miRNAs regulate differentiation and their impact on skeletal development and remodelling.

Currently, our lab is investigating the phenotype of the miR-433 decoy^{Col1a1} mice, to understand how miR-433 affects bone formation. It remains to be investigated whether glucocorticoid or TGF-β signaling is altered in bone from miR-433 decoy^{Col1a1} mice. The implications of miR-433 regulation of circadian rhythm could have wide ranging impacts on skeletal cells, including effects on metabolism. The circadian clocks primarily function to maintain energy metabolism, to match peak metabolic action with physical activity. In

addition, the circadian clocks coordinate tissue repair, and could potentially play a role in fracture healing, although that has yet to be investigated.

To investigate the role of miR-433 of cartilage *in vivo*, we developed a mouse transgenic mouse model in which the miR-433 decoy, contained within the 3' UTR of the red fluorescent reporter gene tdTomato, was expressed under the control a Col2a1 promoter. We currently have 4 founders, and plan to investigate the phenotype of these transgenic mice. We predict mice will have elongated growth plates, induced cartilage formation, and enhanced mineralization, as well as enhanced TGF-β signaling. Since Runx2 promotes chondrocyte hypertrophy, and miR-433 targets Runx2, we may see earlier progression towards hypertrophy in transgenic mice. miR-433 has been linked to a form of dominant X-linked chondrodysplasia in which a HDAC6 3' UTR variant causes a change in miR-433 seed region targeting (135). It is possible that targeting of HDAC6 by miR-433 could contribute to its actions in chondrogenic differentiation, by affecting acetylation levels of HDAC6 clients.

In conclusion, much remains to be elucidated about the role of miR-433 in cartilage and bone, yet our research has made significant strides towards adding to our current understanding. We have identified mechanisms and targets, pointing the way to pathways to be investigated using *in vivo* models.

References

1. Sambrook, P., and Cooper, C. (2006) Osteoporosis. *Lancet* **367**, 2010-2118
2. Center, J. (2013) *Chapter 35: Outcomes following osteoporotic fractures.*, Academic Press (Elsevier
3. Burge, R., Dawson-Hughes, B., Solomon, D. H., Wong, J. B., King, A., and Tosteson, A. (2007) Incidence and economic burden of osteoporosis-related fractures in the United States, 2005-2025. *Journal of bone and mineral research : the official journal of the American Society for Bone and Mineral Research* **22**, 465-475
4. Boskey, A. L. (1992) Mineral-matrix interactions in bone and cartilage. *Clinical orthopaedics and related research*, 244-274
5. Komori, T., Yagi, H., Nomura, S., Yamaguchi, A., Sasaki, K., Deguchi, K., Shimizu, Y., Bronson, R. T., Gao, Y. H., Inada, M., Sato, M., Okamoto, R., Kitamura, Y., Yoshiki, S., and Kishimoto, T. (1997) Targeted disruption of Cbfa1 results in a complete lack of bone formation owing to maturational arrest of osteoblasts. *Cell* **89**, 755-764
6. Adhami, M. D., Rashid, H., Chen, H., Clarke, J. C., Yang, Y., and Javed, A. (2015) Loss of Runx2 in committed osteoblasts impairs postnatal skeletogenesis. *Journal of bone and mineral research : the official journal of the American Society for Bone and Mineral Research* **30**, 71-82
7. Nakashima, K., Zhou, X., Kunkel, G., Zhang, Z., Deng, J. M., Behringer, R. R., and de Crombrugghe, B. (2002) The novel zinc finger-containing transcription factor osterix is required for osteoblast differentiation and bone formation. *Cell* **108**, 17-29
8. Martin, R. B. (2000) Toward a unifying theory of bone remodeling. *Bone* **26**, 1-6
9. Bonewald, L. F., and Johnson, M. L. (2008) Osteocytes, mechanosensing and Wnt signaling. *Bone* **42**, 606-615
10. Cawthorn, W. P., Bree, A. J., Yao, Y., Du, B., Hemati, N., Martinez-Santibanez, G., and MacDougald, O. A. (2012) Wnt6, Wnt10a and Wnt10b inhibit adipogenesis and stimulate osteoblastogenesis through a beta-catenin-dependent mechanism. *Bone* **50**, 477-489
11. Rosen, E. D., Walkey, C. J., Puigserver, P., and Spiegelman, B. M. (2000) Transcriptional regulation of adipogenesis. *Genes & development* **14**, 1293-1307
12. Akiyama, H., Chaboissier, M. C., Martin, J. F., Schedl, A., and de Crombrugghe, B. (2002) The transcription factor Sox9 has essential roles in successive steps of the chondrocyte differentiation pathway and is required for expression of Sox5 and Sox6. *Genes & development* **16**, 2813-2828
13. Hattori, T., Muller, C., Gebhard, S., Bauer, E., Pausch, F., Schlund, B., Bosl, M. R., Hess, A., Surmann-Schmitt, C., von der Mark, H., de Crombrugghe, B., and von der Mark, K. (2010) SOX9 is a major negative regulator of cartilage vascularization, bone marrow formation and endochondral ossification. *Development (Cambridge, England)* **137**, 901-911
14. Karsenty, G., Kronenberg, H. M., and Settembre, C. (2009) Genetic control of bone formation. *Annu Rev Cell Dev Biol* **25**, 629-648

15. Stouffer, G. A., and Owens, G. K. (1994) TGF-beta promotes proliferation of cultured SMC via both PDGF-AA-dependent and PDGF-AA-independent mechanisms. *The Journal of clinical investigation* **93**, 2048-2055
16. Vinals, F., and Pouyssegur, J. (2001) Transforming growth factor beta1 (TGF-beta1) promotes endothelial cell survival during in vitro angiogenesis via an autocrine mechanism implicating TGF-alpha signaling. *Mol Cell Biol* **21**, 7218-7230
17. Fang, Y., Yu, S., and Braley-Mullen, H. (2012) TGF-beta promotes proliferation of thyroid epithelial cells in IFN-gamma(-/-) mice by down-regulation of p21 and p27 via AKT pathway. *The American journal of pathology* **180**, 650-660
18. Moses, H. L., and Serra, R. (1996) Regulation of differentiation by TGF-beta. *Current opinion in genetics & development* **6**, 581-586
19. Massague, J., Blain, S. W., and Lo, R. S. (2000) TGFbeta signaling in growth control, cancer, and heritable disorders. *Cell* **103**, 295-309
20. Verrecchia, F., and Mauviel, A. (2002) Transforming growth factor-beta signaling through the Smad pathway: role in extracellular matrix gene expression and regulation. *The Journal of investigative dermatology* **118**, 211-215
21. Janssens, K., ten Dijke, P., Janssens, S., and Van Hul, W. (2005) Transforming growth factor-beta1 to the bone. *Endocrine reviews* **26**, 743-774
22. Bonewald, L. F., and Dallas, S. L. (1994) Role of active and latent transforming growth factor beta in bone formation. *J Cell Biochem* **55**, 350-357
23. Centrella, M., Horowitz, M. C., Wozney, J. M., and McCarthy, T. L. (1994) Transforming growth factor-beta gene family members and bone. *Endocrine reviews* **15**, 27-39
24. Spinella-Jaegle, S., Roman-Roman, S., Faucheu, C., Dunn, F. W., Kawai, S., Gallea, S., Stiot, V., Blanchet, A. M., Courtois, B., Baron, R., and Rawadi, G. (2001) Opposite effects of bone morphogenetic protein-2 and transforming growth factor-beta1 on osteoblast differentiation. *Bone* **29**, 323-330
25. van der Kraan, P. M., Blaney Davidson, E. N., Blom, A., and van den Berg, W. B. (2009) TGF-beta signaling in chondrocyte terminal differentiation and osteoarthritis: modulation and integration of signaling pathways through receptor-Smads. *Osteoarthritis and cartilage / OARS, Osteoarthritis Research Society* **17**, 1539-1545
26. Song, J. J., Aswad, R., Kanaan, R. A., Rico, M. C., Owen, T. A., Barbe, M. F., Safadi, F. F., and Popoff, S. N. (2007) Connective tissue growth factor (CTGF) acts as a downstream mediator of TGF-beta1 to induce mesenchymal cell condensation. *Journal of cellular physiology* **210**, 398-410
27. Tuli, R., Tuli, S., Nandi, S., Huang, X., Manner, P. A., Hozack, W. J., Danielson, K. G., Hall, D. J., and Tuan, R. S. (2003) Transforming growth factor-beta-mediated chondrogenesis of human mesenchymal progenitor cells involves N-cadherin and mitogen-activated protein kinase and Wnt signaling cross-talk. *The Journal of biological chemistry* **278**, 41227-41236
28. Leonard, C. M., Fuld, H. M., Frenz, D. A., Downie, S. A., Massague, J., and Newman, S. A. (1991) Role of transforming growth factor-beta in chondrogenic pattern formation in the embryonic limb: stimulation of mesenchymal condensation and fibronectin gene expression by exogenenous TGF-beta and

evidence for endogenous TGF-beta-like activity. *Developmental biology* **145**, 99-109
29. Johnstone, B., Hering, T. M., Caplan, A. I., Goldberg, V. M., and Yoo, J. U. (1998) In vitro chondrogenesis of bone marrow-derived mesenchymal progenitor cells. *Experimental cell research* **238**, 265-272
30. Vinatier, C., Bouffi, C., Merceron, C., Gordeladze, J., Brondello, J. M., Jorgensen, C., Weiss, P., Guicheux, J., and Noel, D. (2009) Cartilage tissue engineering: towards a biomaterial-assisted mesenchymal stem cell therapy. *Current stem cell research & therapy* **4**, 318-329
31. Darling, E. M., and Athanasiou, K. A. (2005) Growth factor impact on articular cartilage subpopulations. *Cell and tissue research* **322**, 463-473
32. Zhen, G., Wen, C., Jia, X., Li, Y., Crane, J. L., Mears, S. C., Askin, F. B., Frassica, F. J., Chang, W., Yao, J., Carrino, J. A., Cosgarea, A., Artemov, D., Chen, Q., Zhao, Z., Zhou, X., Riley, L., Sponseller, P., Wan, M., Lu, W. W., and Cao, X. (2013) Inhibition of TGF-beta signaling in mesenchymal stem cells of subchondral bone attenuates osteoarthritis. *Nature medicine* **19**, 704-712
33. Gimble, J. M., Floyd, Z. E., and Bunnell, B. A. (2009) The 4th dimension and adult stem cells: Can timing be everything? *J Cell Biochem* **107**, 569-578
34. Zhang, R., Lahens, N. F., Ballance, H. I., Hughes, M. E., and Hogenesch, J. B. (2014) A circadian gene expression atlas in mammals: implications for biology and medicine. *Proc Natl Acad Sci U S A* **111**, 16219-16224
35. Witt-Enderby, P. A., Slater, J. P., Johnson, N. A., Bondi, C. D., Dodda, B. R., Kotlarczyk, M. P., Clafshenkel, W. P., Sethi, S., Higginbotham, S., Rutkowski, J. L., Gallagher, K. M., and Davis, V. L. (2012) Effects on bone by the light/dark cycle and chronic treatment with melatonin and/or hormone replacement therapy in intact female mice. *Journal of pineal research* **53**, 374-384
36. Kawai, M., Delany, A. M., Green, C. B., Adamo, M. L., and Rosen, C. J. (2010) Nocturnin suppresses igf1 expression in bone by targeting the 3' untranslated region of igf1 mRNA. *Endocrinology* **151**, 4861-4870
37. Hassager, C., Risteli, J., Risteli, L., Jensen, S. B., and Christiansen, C. (1992) Diurnal variation in serum markers of type I collagen synthesis and degradation in healthy premenopausal women. *J Bone Miner Res* **7**, 1307-1311
38. Pietschmann, P., Resch, H., Woloszczuk, W., and Willvonseder, R. (1990) A circadian rhythm of serum osteocalcin levels in postmenopausal osteoporosis. *Eur J Clin Invest* **20**, 310-312
39. McElderry, J. D., Zhao, G., Khmaladze, A., Wilson, C. G., Franceschi, R. T., and Morris, M. D. Tracking circadian rhythms of bone mineral deposition in murine calvarial organ cultures. *Journal of bone and mineral research : the official journal of the American Society for Bone and Mineral Research*
40. Fu, L., Patel, M. S., Bradley, A., Wagner, E. F., and Karsenty, G. (2005) The molecular clock mediates leptin-regulated bone formation. *Cell* **122**, 803-815
41. Maronde, E., Schilling, A. F., Seitz, S., Schinke, T., Schmutz, I., van der Horst, G., Amling, M., and Albrecht, U. (2010) The clock genes Period 2 and Cryptochrome 2 differentially balance bone formation. *PLoS One* **5**, e11527
42. Moller-Levet, C. S., Archer, S. N., Bucca, G., Laing, E. E., Slak, A., Kabiljo, R., Lo, J. C., Santhi, N., von Schantz, M., Smith, C. P., and Dijk, D. J. (2013) Effects

of insufficient sleep on circadian rhythmicity and expression amplitude of the human blood transcriptome. *Proceedings of the National Academy of Sciences of the United States of America* **110**, E1132-1141
43. Cedernaes, J., Osler, M. E., Voisin, S., Broman, J. E., Vogel, H., Dickson, S. L., Zierath, J. R., Schioth, H. B., and Benedict, C. (2015) Acute sleep loss induces tissue-specific epigenetic and transcriptional alterations to circadian clock genes in men. *The Journal of clinical endocrinology and metabolism*, Jc20152284
44. Liu, Z., and Chu, G. (2012) Chronobiology in mammalian health. *Molecular Biology Reports*
45. Golombek, D. A., Casiraghi, L. P., Agostino, P. V., Paladino, N., Duhart, J. M., Plano, S. A., and Chiesa, J. J. (2013) The times they're a-changing: effects of circadian desynchronization on physiology and disease. *Journal of physiology, Paris* **107**, 310-322
46. Luyster, F. S., Strollo, P. J., Jr., Zee, P. C., and Walsh, J. K. (2012) Sleep: a health imperative. *Sleep* **35**, 727-734
47. Foley, D., Ancoli-Israelb, S., Britzc, P., and Walshd, J. (2004) Sleep disturbances and chronic disease in older adults: Results of the 2003 National Sleep Foundation Sleep in America Survey. *Journal of Psychosomatic Research* **56**, 497-502
48. Chen, Y. L., Weng, S. F., Shen, Y. C., Chou, C. W., Yang, C. Y., Wang, J. J., and Tien, K. J. (2014) Obstructive sleep apnea and risk of osteoporosis: a population-based cohort study in Taiwan. *The Journal of clinical endocrinology and metabolism* **99**, 2441-2447
49. Yen, C. M., Kuo, C. L., Lin, M. C., Lee, C. F., Lin, K. Y., Lin, C. L., Chang, S. N., Sung, F. C., and Kao, C. H. (2014) Sleep disorders increase the risk of osteoporosis: a nationwide population-based cohort study. *Sleep medicine* **15**, 1339-1344
50. Swanson, C. M., Shea, S. A., Stone, K. L., Cauley, J. A., Rosen, C. J., Redline, S., Karsenty, G., and Orwoll, E. S. (2015) Obstructive sleep apnea and metabolic bone disease: insights into the relationship between bone and sleep. *J Bone Miner Res* **30**, 199-211
51. Sivertsen, B., Lallukka, T., Salo, P., Pallesen, S., Hysing, M., Krokstad, S., and Simon, O. (2014) Insomnia as a risk factor for ill health: results from the large population-based prospective HUNT Study in Norway. *Journal of sleep research* **23**, 124-132
52. Feskanich, D., Hankinson, S. E., and Schernhammer, E. S. (2009) Nightshift work and fracture risk: the Nurses' Health Study. *Osteoporosis international : a journal established as result of cooperation between the European Foundation for Osteoporosis and the National Osteoporosis Foundation of the USA* **20**, 537-542
53. White, H. D., Ahmad, A. M., Durham, B. H., Peter, R., Prabhakar, V. K., Corlett, P., Vora, J. P., and Fraser, W. D. (2007) PTH circadian rhythm and PTH target-organ sensitivity is altered in patients with adult growth hormone deficiency with low BMD. *Journal of bone and mineral research : the official journal of the American Society for Bone and Mineral Research* **22**, 1798-1807

54. Everson, C. A., Folley, A. E., and Toth, J. M. (2012) Chronically inadequate sleep results in abnormal bone formation and abnormal bone marrow in rats. *Experimental Biology and Medicine* **237**, 1101-1109
55. Stevenson, S., Hunziker, E. B., Herrmann, W., and Schenk, R. K. (1990) Is longitudinal bone growth influenced by diurnal variation in the mitotic activity of chondrocytes of the growth plate? *Journal of orthopaedic research : official publication of the Orthopaedic Research Society* **8**, 132-135
56. Gossan, N., Zeef, L., Hensman, J., Hughes, A., Bateman, J. F., Rowley, L., Little, C. B., Piggins, H. D., Rattray, M., Boot-Handford, R. P., and Meng, Q. J. (2013) The circadian clock in murine chondrocytes regulates genes controlling key aspects of cartilage homeostasis. *Arthritis and rheumatism* **65**, 2334-2345
57. Takarada, T., Kodama, A., Hotta, S., Mieda, M., Shimba, S., Hinoi, E., and Yoneda, Y. (2012) Clock genes influence gene expression in growth plate and endochondral ossification in mice. *Journal of Biological Chemistry* **287**, 36081-36095
58. Dudek, M., Gossan, N., Yang, N., Im, H. J., Ruckshanthi, J. P., Yoshitane, H., Li, X., Jin, D., Wang, P., Boudiffa, M., Bellantuono, I., Fukada, Y., Boot-Handford, R. P., and Meng, Q. J. (2016) The chondrocyte clock gene Bmal1 controls cartilage homeostasis and integrity. *The Journal of clinical investigation* **126**, 365-376
59. Yang, W., Kang, X., Liu, J., Li, H., Ma, Z., Jin, X., Qian, Z., Xie, T., Qin, N., Feng, D., Pan, W., Chen, Q., Sun, H., and Wu, S. (2016) Clock gene Bmal1 modulates human cartilage gene expression by crosstalk with Sirt1. *Endocrinology*, en20152042
60. Eastell, R., Calvo, M. S., Burritt, M. F., Offord, K. P., Russell, R. G., and Riggs, B. L. (1992) Abnormalities in circadian patterns of bone resorption and renal calcium conservation in type I osteoporosis. *The Journal of clinical endocrinology and metabolism* **74**, 487-494
61. Xu, C., Ochi, H., Fukuda, T., Sato, S., Sunamura, S., Takarada, T., Hinoi, E., Okawa, A., and Takeda, S. (2016) Circadian Clock Regulates Bone Resorption in Mice. *Journal of bone and mineral research : the official journal of the American Society for Bone and Mineral Research* **31**, 1344-1355
62. Fujihara, Y., Kondo, H., Noguchi, T., and Togari, A. (2014) Glucocorticoids mediate circadian timing in peripheral osteoclasts resulting in the circadian expression rhythm of osteoclast-related genes. *Bone* **61**, 1-9
63. Vandevyver, S., Dejager, L., and Libert, C. (2014) Comprehensive overview of the structure and regulation of the glucocorticoid receptor. *Endocrine reviews* **35**, 671-693
64. Kadmiel, M., and Cidlowski, J. A. (2013) Glucocorticoid receptor signaling in health and disease. *Trends in pharmacological sciences* **34**, 518-530
65. Izumo, M., Sato, T. R., Straume, M., and Johnson, C. H. (2006) Quantitative analyses of circadian gene expression in mammalian cell cultures. *PLoS computational biology* **2**, e136
66. Bhavsar, P., Hew, M., Khorasani, N., Torrego, A., Barnes, P. J., Adcock, I., and Chung, K. F. (2008) Relative corticosteroid insensitivity of alveolar macrophages in severe asthma compared with non-severe asthma. *Thorax* **63**, 784-790

67. Mercado, N., Hakim, A., Kobayashi, Y., Meah, S., Usmani, O. S., Chung, K. F., Barnes, P. J., and Ito, K. (2012) Restoration of corticosteroid sensitivity by p38 mitogen activated protein kinase inhibition in peripheral blood mononuclear cells from severe asthma. *PLoS One* **7**, e41582
68. Nader, N., Chrousos, G. P., and Kino, T. (2009) Circadian rhythm transcription factor CLOCK regulates the transcriptional activity of the glucocorticoid receptor by acetylating its hinge region lysine cluster: potential physiological implications. *FASEB journal : official publication of the Federation of American Societies for Experimental Biology* **23**, 1572-1583
69. Oakley, R. H., and Cidlowski, J. A. (2011) Cellular processing of the glucocorticoid receptor gene and protein: new mechanisms for generating tissue-specific actions of glucocorticoids. *The Journal of biological chemistry* **286**, 3177-3184
70. Balsalobre, A., Brown, S. A., Marcacci, L., Tronche, F., Kellendonk, C., Reichardt, H. M., Schutz, G., and Schibler, U. (2000) Resetting of circadian time in peripheral tissues by glucocorticoid signaling. *Science (New York, N.Y.)* **289**, 2344-2347
71. Hirota, T., and Fukada, Y. (2004) Resetting mechanism of central and peripheral circadian clocks in mammals. *Zoological Society* **21**, 359-368
72. Nicolaides, N. C., Charmandari, E., Chrousos, G. P., and Kino, T. (2014) Circadian endocrine rhythms: the hypothalamic-pituitary-adrenal axis and its actions. *Annals of the New York Academy of Sciences* **1318**, 71-80
73. Nader, N., Chrousos, G. P., and Kino, T. (2010) Interactions of the circadian CLOCK system and the HPA axis. *Trends in endocrinology and metabolism: TEM* **21**, 277-286
74. So, A. Y., Bernal, T. U., Pillsbury, M. L., Yamamoto, K. R., and Feldman, B. J. (2009) Glucocorticoid regulation of the circadian clock modulates glucose homeostasis. *Proceedings of the National Academy of Sciences of the United States of America* **106**, 17582-17587
75. Segall, L. A., and Amir, S. (2010) Glucocorticoid regulation of clock gene expression in the mammalian limbic forebrain. *Journal of molecular neuroscience : MN* **42**, 168-175
76. Reddy, T. E., Gertz, J., Crawford, G. E., Garabedian, M. J., and Myers, R. M. (2012) The hypersensitive glucocorticoid response specifically regulates period 1 and expression of circadian genes. *Molecular and Cellular Biology* **32**, 3756-3767
77. Son, G. H., Chung, S., Choe, H. K., Kim, H. D., Baik, S. M., Lee, H., Lee, H. W., Choi, S., Sun, W., Kim, H., Cho, S., Lee, K. H., and Kim, K. (2008) Adrenal peripheral clock controls the autonomous circadian rhythm of glucocorticoid by causing rhythmic steroid production. *Proceedings of the National Academy of Sciences of the United States of America* **105**, 20970-20975
78. Chung, S., Son, G. H., and Kim, K. (2011) Circadian rhythm of adrenal glucocorticoid: its regulation and clinical implications. *Biochimica et biophysica acta* **1812**, 581-591
79. Delany, A. M., Dong, Y., and Canalis, E. (1994) Mechanisms of glucocorticoid action in bone cells. *J Cell Biochem* **56**, 295-302

80. Moutsatsou, P., Kassi, E., and Papavassiliou, A. G. Glucocorticoid receptor signaling in bone cells. *Trends Mol Med* **18**, 348-359
81. Canalis, E., Mazziotti, G., Giustina, A., and Bilezikian, J. P. (2007) Glucocorticoid-induced osteoporosis: pathophysiology and therapy. *Osteoporosis international : a journal established as result of cooperation between the European Foundation for Osteoporosis and the National Osteoporosis Foundation of the USA* **18**, 1319-1328
82. Booth, S. L., Centi, A., Smith, S. R., and Gundberg, C. (2013) The role of osteocalcin in human glucose metabolism: marker or mediator? *Nat Rev Endocrinol* **9**, 43-55
83. Karsenty, G., and Ferron, M. (2012) The contribution of bone to whole-organism physiology. *Nature* **481**, 314-320
84. Brennan-Speranza, T. C., Henneicke, H., Gasparini, S. J., Blankenstein, K. I., Heinevetter, U., Cogger, V. C., Svistounov, D., Zhang, Y., Cooney, G. J., Buttgereit, F., Dunstan, C. R., Gundberg, C., Zhou, H., and Seibel, M. J. (2012) Osteoblasts mediate the adverse effects of glucocorticoids on fuel metabolism. *J Clin Invest* **122**, 4172-4189
85. Kapinas, K., and Delany, A. M. (2011) MicroRNA biogenesis and regulation of bone remodeling. *Arthritis research & therapy* **13**, 220
86. Gaur, T., Hussain, S., Mudhasani, R., Parulkar, I., Colby, J. L., Frederick, D., Kream, B. E., van Wijnen, A. J., Stein, J. L., Stein, G. S., Jones, S. N., and Lian, J. B. (2010) Dicer inactivation in osteoprogenitor cells compromises fetal survival and bone formation, while excision in differentiated osteoblasts increases bone mass in the adult mouse. *Developmental Biology* **340**, 10-21
87. Lee, K. S., Kim, H. J., Li, Q. L., Chi, X. Z., Ueta, C., Komori, T., Wozney, J. M., Kim, E. G., Choi, J. Y., Ryoo, H. M., and Bae, S. C. (2000) Runx2 is a common target of transforming growth factor beta1 and bone morphogenetic protein 2, and cooperation between Runx2 and Smad5 induces osteoblast-specific gene expression in the pluripotent mesenchymal precursor cell line C2C12. *Molecular Cell Biology* **23**, 8783-8792
88. Li, Z., Hassan, M. Q., Volinia, S., van Wijnen, A. J., Stein, J. L., Croce, C. M., Lian, J. B., and Stein, G. S. (2008) A microRNA signature for a BMP2-induced osteoblast lineage commitment program. *Proc Natl Acad Sci U S A* **105**, 13906-13911
89. Kapinas, K., Kessler, C. B., and Delany, A. M. (2009) miR-29 supression of osteonectin in osteoblasts: regulation during differentiation and by canonical Wnt signaling. *Journal of Cellular Biochemistry* **108**, 216-224
90. Kapinas, K., and Delany, A. M. (2011) MicroRNA biogenesis and regulation of bone remodeling. *Arthritis Research and Therapy* **13**, 220-231
91. Smith, S. S., Kessler, C. B., Shenoy, V., Rosen, C. J., and Delany, A. M. (2013) Igf-I 3' untranslated region: strain-specific polymorphisms and motifs regulating igf-I in osteoblasts. *Endocrinology* **154**, 253-262
92. Vollmers, C., Schmitz, R. J., Nathanson, J., Yeo, G., Ecker, J. R., and Panda, S. (2012) Circadian oscillations of protein-coding and regulatory RNAs in a highly dynamic mammalian liver epigenome. *Cell Metab* **16**, 833-845

93. Xu, S., Witmer, P. D., Lumayag, S., Kovacs, B., and Valle, D. (2007) MicroRNA (miRNA) transcriptome of mouse retina and identification of a sensory organ-specific miRNA cluster. *The Journal of biological chemistry* **282**, 25053-25066
94. Floris, I., Billard, H., Boquien, C. Y., Joram-Gauvard, E., Simon, L., Legrand, A., Boscher, C., Roze, J. C., Bolanos-Jimenez, F., and Kaeffer, B. (2015) MiRNA Analysis by Quantitative PCR in Preterm Human Breast Milk Reveals Daily Fluctuations of hsa-miR-16-5p. *PLoS One* **10**, e0140488
95. Yan, Y., Salazar, T. E., Dominguez, J. M., 2nd, Nguyen, D. V., Li Calzi, S., Bhatwadekar, A. D., Qi, X., Busik, J. V., Boulton, M. E., and Grant, M. B. (2013) Dicer expression exhibits a tissue-specific diurnal pattern that is lost during aging and in diabetes. *PLoS One* **8**, e80029
96. Chen, R., D'Alessandro, M., and Lee, C. (2013) miRNAs are required for generating a time delay critical for the circadian oscillator. *Current biology : CB* **23**, 1959-1968
97. Du, N. H., Arpat, A. B., De Matos, M., and Gatfield, D. (2014) MicroRNAs shape circadian hepatic gene expression on a transcriptome-wide scale. *eLife* **3**, e02510
98. Alvarez-Saavedra, M., Antoun, G., Yanagiya, A., Oliva-Hernandez, R., Cornejo-Palma, D., Perez-Iratxeta, C., Sonenberg, N., and Cheng, H. Y. (2010) miRNA-132 orchestrates chromatin remodeling and translational control of the circadian clock. *Hum Mol Genet* **20**, 731-751
99. Na, Y. J., Sung, J. H., Lee, S. C., Lee, Y. J., Choi, Y. J., Park, W. Y., Shin, H. S., and Kim, J. H. (2009) Comprehensive analysis of microRNA-mRNA co-expression in circadian rhythm. *Experimental & molecular medicine* **41**, 638-647
100. Tan, X., Zhang, P., Zhou, L., Yin, B., Pan, H., and Peng, X. (2012) Clock-controlled mir-142-3p can target its activator, Bmal1. *BMC Mol Biol* **13**, 27
101. Kim, E. J., Kang, I. H., Lee, J. W., Jang, W. G., and Koh, J. T. (2013) MiR-433 mediates ERRgamma-suppressed osteoblast differentiation via direct targeting to Runx2 mRNA in C3H10T1/2 cells. *Life sciences* **92**, 562-568
102. Nandi, A., Vaz, C., Bhattacharya, A., and Ramaswamy, R. (2009) miRNA-regulated dynamics in circadian oscillator models. *BMC systems biology* **3**, 45
103. Kiriakidou, M., Nelson, P. T., Kouranov, A., Fitziev, P., Bouyioukos, C., Mourelatos, Z., and Hatzigeorgiou, A. (2004) A combined computational-experimental approach predicts human microRNA targets. *Genes & development* **18**, 1165-1178
104. Meng, F., Henson, R., Lang, M., Wehbe, H., Maheshwari, S., Mendell, J. T., Jiang, J., Schmittgen, T. D., and Patel, T. (2006) Involvement of human micro-RNA in growth and response to chemotherapy in human cholangiocarcinoma cell lines. *Gastroenterology* **130**, 2113-2129
105. Nagel, R., Clijsters, L., and Agami, R. (2009) The miRNA-192/194 cluster regulates the Period gene family and the circadian clock. *The FEBS journal* **276**, 5447-5455
106. Gast, H., Gordic, S., Petrzilka, S., Lopez, M., Muller, A., Gietl, A., Hock, C., Birchler, T., and Fontana, A. (2012) Transforming growth factor-beta inhibits the expression of clock genes. *Ann N Y Acad Sci*

107. Lee, K. H., Kim, S. H., Lee, H. R., Kim, W., Kim, D. Y., Shin, J. C., Yoo, S. H., and Kim, K. T. (2013) MicroRNA-185 oscillation controls circadian amplitude of mouse Cryptochrome 1 via translational regulation. *Molecular biology of the cell* **24**, 2248-2255
108. Shende, V. R., Neuendorff, N., and Earnest, D. J. (2013) Role of miR-142-3p in the post-transcriptional regulation of the clock gene Bmal1 in the mouse SCN. *PLoS One* **8**, e65300
109. Daimiel-Ruiz, L., Klett-Mingo, M., Konstantinidou, V., Mico, V., Aranda, J. F., Garcia, B., Martinez-Botas, J., Davalos, A., Fernandez-Hernando, C., and Ordovas, J. M. (2015) Dietary lipids modulate the expression of miR-107, an miRNA that regulates the circadian system. *Molecular nutrition & food research* **59**, 552-565
110. Liu, K., and Wang, R. (2012) MicroRNA-mediated regulation in the mammalian circadian rhythm. *Journal of theoretical biology* **304**, 103-110
111. Cheng, H. Y., Papp, J. W., Varlamova, O., Dziema, H., Russell, B., Curfman, J. P., Nakazawa, T., Shimizu, K., Okamura, H., Impey, S., and Obrietan, K. (2007) microRNA modulation of circadian-clock period and entrainment. *Neuron* **54**, 813-829
112. Ferrell, J. M., and Chiang, J. Y. (2015) Circadian rhythms in liver metabolism and disease. *Acta pharmaceutica Sinica. B* **5**, 113-122
113. Krutzfeldt, J., Rajewsky, N., Braich, R., Rajeev, K. G., Tuschl, T., Manoharan, M., and Stoffel, M. (2005) Silencing of microRNAs in vivo with 'antagomirs'. *Nature* **438**, 685-689
114. Esau, C., Davis, S., Murray, S. F., Yu, X. X., Pandey, S. K., Pear, M., Watts, L., Booten, S. L., Graham, M., McKay, R., Subramaniam, A., Propp, S., Lollo, B. A., Freier, S., Bennett, C. F., Bhanot, S., and Monia, B. P. (2006) miR-122 regulation of lipid metabolism revealed by in vivo antisense targeting. *Cell metabolism* **3**, 87-98
115. Gatfield, D., Le Martelot, G., Vejnar, C. E., Gerlach, D., Schaad, O., Fleury-Olela, F., Ruskeepaa, A. L., Oresic, M., Esau, C. C., Zdobnov, E. M., and Schibler, U. (2009) Integration of microRNA miR-122 in hepatic circadian gene expression. *Genes Dev* **23**, 1313-1326
116. Green, C. B., Douris, N., Kojima, S., Strayer, C. A., Fogerty, J., Lourim, D., Keller, S. R., and Besharse, J. C. (2007) Loss of Nocturnin, a circadian deadenylase, confers resistance to hepatic steatosis and diet-induced obesity. *Proceedings of the National Academy of Sciences of the United States of America* **104**, 9888-9893
117. Kojima, S., Gatfield, D., Esau, C. C., and Green, C. B. (2012) MicroRNA-122 modulates the rhythmic expression profile of the circadian deadenylase Nocturnin in mouse liver. *PloS one* **5**, e11264
118. Curtis, A. M., Bellet, M. M., Sassone-Corsi, P., and O'Neill, L. A. (2014) Circadian clock proteins and immunity. *Immunity* **40**, 178-186
119. Curtis, A. M., Fagundes, C. T., Yang, G., Palsson-McDermott, E. M., Wochal, P., McGettrick, A. F., Foley, N. H., Early, J. O., Chen, L., Zhang, H., Xue, C., Geiger, S. S., Hokamp, K., Reilly, M. P., Coogan, A. N., Vigorito, E., FitzGerald, G. A., and O'Neill, L. A. (2015) Circadian control of innate immunity in macrophages by

miR-155 targeting Bmal1. *Proceedings of the National Academy of Sciences of the United States of America* **112**, 7231-7236
120. Quinn, S. R., Mangan, N. E., Caffrey, B. E., Gantier, M. P., Williams, B. R., Hertzog, P. J., McCoy, C. E., and O'Neill, L. A. (2014) The role of Ets2 transcription factor in the induction of microRNA-155 (miR-155) by lipopolysaccharide and its targeting by interleukin-10. *The Journal of biological chemistry* **289**, 4316-4325
121. Wang, Q., Bozack, S. N., Yan, Y., Boulton, M. E., Grant, M. B., and Busik, J. V. (2014) Regulation of retinal inflammation by rhythmic expression of MiR-146a in diabetic retina. *Investigative ophthalmology & visual science* **55**, 3986-3994
122. Han, W., Zou, J., Wang, K., Su, Y., Zhu, Y., Song, C., Li, G., Qu, L., Zhang, H., and Liu, H. (2015) High-Throughput Sequencing Reveals Hypothalamic MicroRNAs as Novel Partners Involved in Timing the Rapid Development of Chicken (Gallus gallus) Gonads. *PLoS One* **10**, e0129738
123. Rekker, K., Saare, M., Roost, A. M., Kaart, T., Soritsa, D., Karro, H., Soritsa, A., Simon, C., Salumets, A., and Peters, M. (2015) Circulating miR-200-family micro-RNAs have altered plasma levels in patients with endometriosis and vary with blood collection time. *Fertility and sterility* **104**, 938-946.e932
124. Ding, X., Sun, B., Huang, J., Xu, L., Pan, J., Fang, C., Tao, Y., Hu, S., Li, R., Han, X., Miao, P., Wang, Y., Yu, J., and Feng, X. (2015) The role of miR-182 in regulating pineal CLOCK expression after hypoxia-ischemia brain injury in neonatal rats. *Neuroscience letters* **591**, 75-80
125. Kinoshita, C., Aoyama, K., Matsumura, N., Kikuchi-Utsumi, K., Watabe, M., and Nakaki, T. (2014) Rhythmic oscillations of the microRNA miR-96-5p play a neuroprotective role by indirectly regulating glutathione levels. *Nature communications* **5**, 3823
126. Riester, A., Issler, O., Spyroglou, A., Rodrig, S. H., Chen, A., and Beuschlein, F. (2012) ACTH-dependent regulation of microRNA as endogenous modulators of glucocorticoid receptor expression in the adrenal gland. *Endocrinology* **153**, 212-222
127. Reddy, T. E., Gertz, J., Crawford, G. E., Garabedian, M. J., and Myers, R. M. The hypersensitive glucocorticoid response specifically regulates period 1 and expression of circadian genes. *Mol Cell Biol* **32**, 3756-3767
128. Nicolaides, N. C., Charmandari, E., Chrousos, G. P., and Kino, T. (2014) Recent advances in the molecular mechanisms determining tissue sensitivity to glucocorticoids: novel mutations, circadian rhythm and ligand-induced repression of the human glucocorticoid receptor. *BMC endocrine disorders* **14**, 71
129. Delany, A. M., Amling, M., Priemel, M., Howe, C., Baron, R., and Canalis, E. (2000) Osteopenia and decreased bone formation in osteonectin-deficient mice. *J Clin Invest* **105**, 915-923
130. Boskey, A. L., Moore, D. J., Amling, M., Canalis, E., and Delany, A. M. (2003) Infrared analysis of the mineral and matrix in bones of osteonectin-null mice and their wildtype controls. *J Bone Miner Res* **18**, 1005-1011
131. Delany, A. M., Kalajzic, I., Bradshaw, A. D., Sage, E. H., and Canalis, E. (2003) Osteonectin-null mutation compromises osteoblast formation, maturation, and survival. *Endocrinology* **144**, 2588-2596

132. Kessler, C. B., and Delany, A. M. (2007) Increased Notch 1 expression and attenuated stimulatory G protein coupling to adenylyl cyclase in osteonectin-null osteoblasts. *Endocrinology* **148**, 1666-1674
133. Delany, A. M., McMahon, D. J., Powell, J. S., Greenberg, D. A., and Kurland, E. S. (2008) Osteonectin/SPARC polymorphisms in Caucasian men with idiopathic osteoporosis. *Osteoporos Int* **19**, 969-978
134. Dole, N. S., Kapinas, K., Kessler, C. B., Yee, S. P., Adams, D. J., Pereira, R. C., and Delany, A. M. (2015) A single nucleotide polymorphism in osteonectin 3' untranslated region regulates bone volume and is targeted by miR-433. *Journal of bone and mineral research : the official journal of the American Society for Bone and Mineral Research* **30**, 723-732
135. Simon, D., Laloo, B., Barillot, M., Barnetche, T., Blanchard, C., Rooryck, C., Marche, M., Burgelin, I., Coupry, I., Chassaing, N., Gilbert-Dussardier, B., Lacombe, D., Grosset, C., and Arveiler, B. (2010) A mutation in the 3'-UTR of the HDAC6 gene abolishing the post-transcriptional regulation mediated by hsa-miR-433 is linked to a new form of dominant X-linked chondrodysplasia. *Human molecular genetics* **19**, 2015-2027
136. Zvonic, S., Ptitsyn, A. A., Kilroy, G., Wu, X., Conrad, S. A., Scott, L. K., Guilak, F., Pelled, G., Gazit, D., and Gimble, J. M. (2007) Circadian oscillation of gene expression in murine calvarial bone. *Journal of Bone and Mineral Research* **22**, 357-365
137. Barnea, M., Sherman, H., Genzer, Y., and Froy, O. (2013) Association Between Phase Shifts, Expression Levels, and Amplitudes in Peripheral Circadian Clocks. *Chronobiol Int*
138. Reznikoff, C. A., Bertram, J. S., Brankow, D. W., and Heidelberger, C. (1973) Quantitative and qualitative studies of chemical transformation of cloned C3H mouse embryo cells sensitive to postconfluence inhibition of cell division. *Cancer research* **33**, 3239-3249
139. Pinney, D. F., and Emerson, C. P., Jr. (1989) 10T1/2 cells: an in vitro model for molecular genetic analysis of mesodermal determination and differentiation. *Environmental health perspectives* **80**, 221-227
140. Merrill, G. F. (1998) Cell synchronization. *Methods in cell biology* **57**, 229-249
141. Wu, X., Yu, G., Parks, H., Hebert, T., Goh, B. C., Dietrich, M. A., Pelled, G., Izadpanah, R., Gazit, D., Bunnell, B. A., and Gimble, J. M. (2008) Circadian mechanisms in murine and human bone marrow mesenchymal stem cells following dexamethasone exposure. *Bone* **42**, 861-870
142. Takarada, T., Kodama, A., Hotta, S., Mieda, M., Shimba, S., Hinoi, E., and Yoneda, Y. (2012) Clock genes influence gene expression in growth plate and endochondral ossification in mice. *The Journal of biological chemistry* **287**, 36081-36095
143. Woo, K. C., Kim, T. D., Lee, K. H., Kim, D. Y., Kim, W., Lee, K. Y., and Kim, K. T. (2009) Mouse period 2 mRNA circadian oscillation is modulated by PTB-mediated rhythmic mRNA degradation. *Nucleic acids research* **37**, 26-37
144. Shin, K. J., Wall, E. A., Zavzavadjian, J. R., Santat, L. A., Liu, J., Hwang, J. I., Rebres, R., Roach, T., Seaman, W., Simon, M. I., and Fraser, I. D. (2006) A single lentiviral vector platform for microRNA-based conditional RNA interference

and coordinated transgene expression. *Proc Natl Acad Sci U S A* **103**, 13759-13764
145. Scherr, M., Venturini, L., Battmer, K., Schaller-Schoenitz, M., Schaefer, D., Dallmann, I., Ganser, A., and Eder, M. (2007) Lentivirus-mediated antagomir expression for specific inhibition of miRNA function. *Nucleic acids research* **35**, e149
146. Shipp, L. E., Lee, J. V., Yu, C. Y., Pufall, M., Zhang, P., Scott, D. K., and Wang, J. C. (2010) Transcriptional regulation of human dual specificity protein phosphatase 1 (DUSP1) gene by glucocorticoids. *PloS one* **5**, e13754
147. Gimble, J. M., Floyd, Z. E., and Bunnell, B. A. (2009) The 4th dimension and adult stem cells: Can timing be everything? *Journal of Cellular Biochemistry* **107**, 569-578
148. Reppert, S. M., and Weaver, D. R. (2002) Coordination of circadian timing in mammals. *Nature* **418**, 935-941
149. Eckel-Mahan, K., and Sassone-Corsi, P. (2013) Metabolism and the circadian clock converge. *Physiological reviews* **93**, 107-135
150. Witt-Enderby, P., A., Slater, J. P., Johnson, N. A., Bondi, C. D., Dodda, B. R., Kotlarczyk, M. P., Clafshenkel, W. P., Sethi, S., Higginbotham, S., Rutkowski, J. L., Gallagher, K. M., and Davis, V. L. (2012) Effects on bone by the light/dark cycle and chronic treatment with melatonin and/or hormone replacement therapy in intact female mice. *Journal of Pineal Research* **53**, 374-384
151. Zvonic, S., Ptitsyn, A. A., Kilroy, G., Wu, X., Conrad, S. A., Scott, K., Guilak, F., Pelled, G., Gazit, D., and Gimble, J. M. (2007) Circadian oscillation of gene expression in murine calvarial bone. *Journal of Bone and Mineral Research* **22**, 357-365
152. Heshmati, H. M., Riggs, B. L., Burritt, M. F., McAlister, C. A., Wollan, P. C., and Khosla, S. (1998) Effects of the circadian variation in serum cortisol on markers of bone turnover and calcium homeostasis in normal postmenopausal women. *J Clin Endocrinol Metab* **83**, 751-756
153. Betel, D., Koppal, A., Agius, P., Sander, C., and Leslie, C. (2010) Comprehensive modeling of microRNA targets predicts functional non-conserved and non-canonical sites. *Genome biology* **11**, R90
154. Lewis, B. P., Burge, C. B., and Bartel, D. P. (2005) Conserved seed pairing, often flanked by adenosines, indicates that thousands of human genes are microRNA targets. *Cell* **120**, 15-20
155. Rehmsmeier, M., Steffen, P., Hochsmann, M., and Giegerich, R. (2004) Fast and effective prediction of microRNA/target duplexes. *RNA (New York, N.Y.)* **10**, 1507-1517
156. Haraguchi, T., Ozaki, Y., and Iba, H. (2009) Vectors expressing efficient RNA decoys achieve the long-term suppression of specific microRNA activity in mammalian cells. *Nucleic acids research* **37**, e43
157. Hinds, T. D., Jr., Ramakrishnan, S., Cash, H. A., Stechschulte, L. A., Heinrich, G., Najjar, S. M., and Sanchez, E. R. (2010) Discovery of glucocorticoid receptor-beta in mice with a role in metabolism. *Molecular endocrinology (Baltimore, Md.)* **24**, 1715-1727

158. Bamberger, C. M., Bamberger, A. M., de Castro, M., and Chrousos, G. P. (1995) Glucocorticoid receptor beta, a potential endogenous inhibitor of glucocorticoid action in humans. *The Journal of clinical investigation* **95**, 2435-2441
159. Bamberger, C. M., Schulte, H. M., and Chrousos, G. P. (1996) Molecular determinants of glucocorticoid receptor function and tissue sensitivity to glucocorticoids. *Endocrine reviews* **17**, 245-261
160. Cain, D. W., and Cidlowski, J. A. (2015) Specificity and sensitivity of glucocorticoid signaling in health and disease. *Best practice & research. Clinical endocrinology & metabolism* **29**, 545-556
161. Kovacs, J. J., Murphy, P. J., Gaillard, S., Zhao, X., Wu, J. T., Nicchitta, C. V., Yoshida, M., Toft, D. O., Pratt, W. B., and Yao, T. P. (2005) HDAC6 regulates Hsp90 acetylation and chaperone-dependent activation of glucocorticoid receptor. *Molecular cell* **18**, 601-607
162. Kalajzic, I., Kalajzic, Z., Kaliterna, M., Gronowicz, G., Clark, S. H., Lichtler, A. C., and Rowe, D. (2002) Use of type I collagen green fluorescent protein transgenes to identify subpopulations of cells at different stages of the osteoblast lineage. *J Bone Miner Res* **17**, 15-25
163. Kalajzic, Z., Liu, P., Kalajzic, I., Du, Z., Braut, A., Mina, M., Canalis, E., and Rowe, D. W. (2002) Directing the expression of a green fluorescent protein transgene in differentiated osteoblasts: comparison between rat type I collagen and rat osteocalcin promoters. *Bone* **31**, 654-660
164. Oishi, K., Ohkura, N., Kadota, K., Kasamatsu, M., Shibusawa, K., Matsuda, J., Machida, K., Horie, S., and Ishida, N. (2006) Clock mutation affects circadian regulation of circulating blood cells. *Journal of circadian rhythms* **4**, 13
165. Zhang, M., Xuan, S., Bouxsein, M. L., von Stechow, D., Akeno, N., Faugere, M. C., Malluche, H., Zhao, G., Rosen, C. J., Efstratiadis, A., and Clemens, T. L. (2002) Osteoblast-specific knockout of the insulin-like growth factor (IGF) receptor gene reveals an essential role of IGF signaling in bone matrix mineralization. *The Journal of biological chemistry* **277**, 44005-44012
166. Regan, J. N., Lim, J., Shi, Y., Joeng, K. S., Arbeit, J. M., Shohet, R. V., and Long, F. (2014) Up-regulation of glycolytic metabolism is required for HIF1alpha-driven bone formation. *Proceedings of the National Academy of Sciences of the United States of America* **111**, 8673-8678
167. Ohlsson, C., Mohan, S., Sjogren, K., Tivesten, A., Isgaard, J., Isaksson, O., Jansson, J. O., and Svensson, J. (2009) The role of liver-derived insulin-like growth factor-I. *Endocr Rev* **30**, 494-535
168. Shomento, S. H., Wan, C., Cao, X., Faugere, M. C., Bouxsein, M. L., Clemens, T. L., and Riddle, R. C. (2010) Hypoxia-inducible factors 1alpha and 2alpha exert both distinct and overlapping functions in long bone development. *J Cell Biochem* **109**, 196-204
169. Song, G., and Wang, L. (2008) Transcriptional mechanism for the paired miR-433 and miR-127 genes by nuclear receptors SHP and ERRgamma. *Nucleic Acids Res* **36**, 5727-5735
170. Jeong, B. C., Lee, Y. S., Bae, I. H., Lee, C. H., Shin, H. I., Ha, H. J., Franceschi, R. T., Choi, H. S., and Koh, J. T. (2010) The orphan nuclear receptor SHP is a positive regulator of osteoblastic bone formation. *J Bone Miner Res* **25**, 262-274

171. Dufour, C. R., Levasseur, M. P., Pham, N. H., Eichner, L. J., Wilson, B. J., Charest-Marcotte, A., Duguay, D., Poirier-Heon, J. F., Cermakian, N., and Giguere, V. (2011) Genomic convergence among ERRalpha, PROX1, and BMAL1 in the control of metabolic clock outputs. *PLoS genetics* **7**, e1002143
172. Villena, J. A., and Kralli, A. (2008) ERRalpha: a metabolic function for the oldest orphan. *Trends in endocrinology and metabolism: TEM* **19**, 269-276
173. Schneider, C. A., Rasband, W. S., and Eliceiri, K. W. (2012) NIH Image to ImageJ: 25 years of image analysis. *Nature methods* **9**, 671-675
174. Li, Z., Hassan, M. Q., Jafferji, M., Aqeilan, R. I., Garzon, R., Croce, C. M., van Wijnen, A. J., Stein, J. L., Stein, G. S., and Lian, J. B. (2009) Biological functions of miR-29b contribute to positive regulation of osteoblast differentiation. *J Biol Chem* **284**, 15676-15684
175. Kapinas, K., Kessler, C., Ricks, T., Gronowicz, G., and Delany, A. M. (2010) miR-29 modulates Wnt signaling in human osteoblasts through a positive feedback loop. *J Biol Chem* **285**, 25221-25231
176. Le, L. T., Swingler, T. E., Crowe, N., Vincent, T. L., Barter, M. J., Donell, S. T., Delany, A. M., Dalmay, T., Young, D. A., and Clark, I. M. (2016) The microRNA-29 family in cartilage homeostasis and osteoarthritis. *Journal of molecular medicine (Berlin, Germany)* **94**, 583-596
177. Blom, A. B., van Lent, P. L., van der Kraan, P. M., and van den Berg, W. B. (2010) To seek shelter from the WNT in osteoarthritis? WNT-signaling as a target for osteoarthritis therapy. *Current drug targets* **11**, 620-629
178. Martin, J., Jenkins, R. H., Bennagi, R., Krupa, A., Phillips, A. O., Bowen, T., and Fraser, D. J. (2011) Post-transcriptional regulation of Transforming Growth Factor Beta-1 by microRNA-744. *PLoS One* **6**, e25044
179. Kim, Y. J., Hwang, S. J., Bae, Y. C., and Jung, J. S. (2009) MiR-21 regulates adipogenic differentiation through the modulation of TGF-beta signaling in mesenchymal stem cells derived from human adipose tissue. *Stem cells (Dayton, Ohio)* **27**, 3093-3102
180. Braun, J., Hoang-Vu, C., Dralle, H., and Huttelmaier, S. (2010) Downregulation of microRNAs directs the EMT and invasive potential of anaplastic thyroid carcinomas. *Oncogene* **29**, 4237-4244
181. Geraldo, M. V., Yamashita, A. S., and Kimura, E. T. (2012) MicroRNA miR-146b-5p regulates signal transduction of TGF-beta by repressing SMAD4 in thyroid cancer. *Oncogene* **31**, 1910-1922
182. Smith SS, D. N., Franceschetti T, Delany AM. (2015) microRNA Regulation of Circadian Rhythm in the Osteoblastic Lineage. *ASBMR* **www.asbmr.org/education/2015-abstracts**
183. Rosen, C. J., Ackert-Bicknell, C., Rodriguez, J. P., and Pino, A. M. (2009) Marrow fat and the bone microenvironment: developmental, functional, and pathological implications. *Critical reviews in eukaryotic gene expression* **19**, 109-124
184. Choy, L., and Derynck, R. (2003) Transforming growth factor-beta inhibits adipocyte differentiation by Smad3 interacting with CCAAT/enhancer-binding protein (C/EBP) and repressing C/EBP transactivation function. *The Journal of biological chemistry* **278**, 9609-9619

185. Guzzo, R. M., Gibson, J., Xu, R. H., Lee, F. Y., and Drissi, H. (2013) Efficient differentiation of human iPSC-derived mesenchymal stem cells to chondroprogenitor cells. *J Cell Biochem* **114**, 480-490
186. Cardelli, M., Zirngibl, R. A., Boetto, J. F., McKenzie, K. P., Troy, T. C., Turksen, K., and Aubin, J. E. (2013) Cartilage-specific overexpression of ERRgamma results in Chondrodysplasia and reduced chondrocyte proliferation. *PLoS One* **8**, e81511
187. Yang, Z., Tsuchiya, H., Zhang, Y., Hartnett, M. E., and Wang, L. (2013) MicroRNA-433 Inhibits Liver Cancer Cell Migration by Repressing the Protein Expression and Function of cAMP Response Element-binding Protein. *J Biol Chem* **288**, 28893-28899
188. Chen, Q., Liu, W., Sinha, K. M., Yasuda, H., and de Crombrugghe, B. (2013) Identification and characterization of microRNAs controlled by the osteoblast-specific transcription factor Osterix. *PLoS One* **8**, e58104
189. Tang, S. Y., and Alliston, T. (2013) Regulation of postnatal bone homeostasis by TGFbeta. *BoneKEy reports* **2**, 255
190. Chen, T. L., and Bates, R. L. (1993) Recombinant human transforming growth factor beta 1 modulates bone remodeling in a mineralizing bone organ culture. *Journal of bone and mineral research : the official journal of the American Society for Bone and Mineral Research* **8**, 423-434
191. Wrana, J. L., Maeno, M., Hawrylyshyn, B., Yao, K. L., Domenicucci, C., and Sodek, J. (1988) Differential effects of transforming growth factor-beta on the synthesis of extracellular matrix proteins by normal fetal rat calvarial bone cell populations. *The Journal of cell biology* **106**, 915-924
192. Smith, S. S., Dole, N. S., Franceschetti, T., Hrdlicka, H. C., and Delany, A. M. (2016) microRNA-433 Dampens Glucocorticoid Receptor Signaling, Impacting Circadian Rhythm and Osteoblastic Gene Expression. *The Journal of biological chemistry*
193. Qiu, T., Xian, L., Crane, J., Wen, C., Hilton, M., Lu, W., Newman, P., and Cao, X. (2015) PTH receptor signaling in osteoblasts regulates endochondral vascularization in maintenance of postnatal growth plate. *Journal of bone and mineral research : the official journal of the American Society for Bone and Mineral Research* **30**, 309-317
194. Kalajzic, I., Staal, A., Yang, W. P., Wu, Y., Johnson, S. E., Feyen, J. H., Krueger, W., Maye, P., Yu, F., Zhao, Y., Kuo, L., Gupta, R. R., Achenie, L. E., Wang, H. W., Shin, D. G., and Rowe, D. W. (2005) Expression profile of osteoblast lineage at defined stages of differentiation. *J Biol Chem* **280**, 24618-24626
195. Lightman, S. L., and Conway-Campbell, B. L. (2010) The crucial role of pulsatile activity of the HPA axis for continuous dynamic equilibration. *Nature reviews. Neuroscience* **11**, 710-718
196. Harizi, H., Homo-Delarche, F., Amrani, A., Coulaud, J., and Mormede, P. (2007) Marked genetic differences in the regulation of blood glucose under immune and restraint stress in mice reveals a wide range of corticosensitivity. *Journal of neuroimmunology* **189**, 59-68
197. de Kroon, L. M., Narcisi, R., Blaney Davidson, E. N., Cleary, M. A., van Beuningen, H. M., Koevoet, W. J., van Osch, G. J., and van der Kraan, P. M.

(2015) Activin Receptor-Like Kinase Receptors ALK5 and ALK1 Are Both Required for TGFbeta-Induced Chondrogenic Differentiation of Human Bone Marrow-Derived Mesenchymal Stem Cells. *PLoS One* **10**, e0146124
198. Vega, R. B., Matsuda, K., Oh, J., Barbosa, A. C., Yang, X., Meadows, E., McAnally, J., Pomajzl, C., Shelton, J. M., Richardson, J. A., Karsenty, G., and Olson, E. N. (2004) Histone deacetylase 4 controls chondrocyte hypertrophy during skeletogenesis. *Cell* **119**, 555-566
199. Westendorf, J. J., Zaidi, S. K., Cascino, J. E., Kahler, R., van Wijnen, A. J., Lian, J. B., Yoshida, M., Stein, G. S., and Li, X. (2002) Runx2 (Cbfa1, AML-3) interacts with histone deacetylase 6 and represses the p21(CIP1/WAF1) promoter. *Mol Cell Biol* **22**, 7982-7992
200. Li, R., Chung, A. C., Dong, Y., Yang, W., Zhong, X., and Lan, H. Y. (2013) The microRNA miR-433 promotes renal fibrosis by amplifying the TGF-beta/Smad3-Azin1 pathway. *Kidney Int* **17**, 272
201. Espinosa-Diez, C., Fierro-Fernandez, M., Sanchez-Gomez, F., Rodriguez-Pascual, F., Alique, M., Ruiz-Ortega, M., Beraza, N., Martinez-Chantar, M. L., Fernandez-Hernando, C., and Lamas, S. (2015) Targeting of Gamma-Glutamyl-Cysteine Ligase by miR-433 Reduces Glutathione Biosynthesis and Promotes TGF-beta-Dependent Fibrogenesis. *Antioxidants & redox signaling* **23**, 1092-1105
202. Zhang, Z., Zou, J., Wang, G. K., Zhang, J. T., Huang, S., Qin, Y. W., and Jing, Q. (2011) Uracils at nucleotide position 9-11 are required for the rapid turnover of miR-29 family. *Nucleic Acids Res* **39**, 4387-4395
203. Zhang, Z., Qin, Y. W., Brewer, G., and Jing, Q. (2012) MicroRNA degradation and turnover: regulating the regulators. *Wiley Interdiscip Rev RNA* **3**, 593-600
204. Loeys, B. L., Mortier, G., and Dietz, H. C. (2013) Bone lessons from Marfan syndrome and related disorders: fibrillin, TGF-B and BMP at the balance of too long and too short. *Pediatr Endocrinol Rev* **2**, 417-423
205. Rhodes, S. D., Wu, X., He, Y., Chen, S., Yang, H., Staser, K. W., Wang, J., Zhang, P., Jiang, C., Yokota, H., Dong, R., Peng, X., Yang, X., Murthy, S., Azhar, M., Mohammad, K. S., Xu, M., Guise, T. A., and Yang, F. C. (2013) Hyperactive transforming growth factor-beta1 signaling potentiates skeletal defects in a neurofibromatosis type 1 mouse model. *J Bone Miner Res* **23**
206. Bolar, N., Van Laer, L., and Loeys, B. L. (2012) Marfan syndrome: from gene to therapy. *Curr Opin Pediatr* **24**, 498-504
207. Buijs, J. T., Stayrook, K. R., and Guise, T. A. (2012) The role of TGF-beta in bone metastasis: novel therapeutic perspectives. *Bonekey Rep* **1**, 96
208. Rosier, R. N., O'Keefe, R. J., and Hicks, D. G. (1998) The potential role of transforming growth factor beta in fracture healing. *Clin Orthop Relat Res* **355**, S294-300
209. Tang SY, A. T. (2013) Regulation of postnatal bone homeostasis by TGFB. *BoneKey Reports* **2**, 255
210. de Mena, L., Cardo, L. F., Coto, E., Miar, A., Diaz, M., Corao, A. I., Alonso, B., Ribacoba, R., Salvador, C., Menendez, M., Moris, G., and Alvarez, V. (2010) FGF20 rs12720208 SNP and microRNA-433 variation: no association with Parkinson's disease in Spanish patients. *Neurosci Lett* **479**, 22-25

211. Estep, M., Armistead, D., Hossain, N., Elarainy, H., Goodman, Z., Baranova, A., Chandhoke, V., and Younossi, Z. M. (2010) Differential expression of miRNAs in the visceral adipose tissue of patients with non-alcoholic fatty liver disease. *Aliment Pharmacol Ther* **32**, 487-497
212. Lin, X., Rice, K. L., Buzzai, M., Hexner, E., Costa, F. F., Kilpivaara, O., Mullally, A., Soares, M. B., Ebert, B. L., Levine, R., and Licht, J. D. (2013) miR-433 is aberrantly expressed in myeloproliferative neoplasms and suppresses hematopoietic cell growth and differentiation. *Leukemia* **27**, 344-352
213. Dobson, K. R., Reading, L., Haberey, M., Marine, X., and Scutt, A. (1999) Centrifugal isolation of bone marrow from bone: an improved method for the recovery and quantitation of bone marrow osteoprogenitor cells from rat tibiae and femurae. *Calcified tissue international* **65**, 411-413
214. Zawel, L., Dai, J. L., Buckhaults, P., Zhou, S., Kinzler, K. W., Vogelstein, B., and Kern, S. E. (1998) Human Smad3 and Smad4 are sequence-specific transcription activators. *Mol Cell* **1**, 611-617
215. Bouxsein, M. L., Boyd, S. K., Christiansen, B. A., Guldberg, R. E., Jepsen, K. J., and Muller, R. (2010) Guidelines for assessment of bone microstructure in rodents using micro-computed tomography. *Journal of bone and mineral research : the official journal of the American Society for Bone and Mineral Research* **25**, 1468-1486
216. Hartmann, K., Koenen, M., Schauer, S., Wittig-Blaich, S., Ahmad, M., Baschant, U., and Tuckermann, J. P. (2016) Molecular Actions of Glucocorticoids in Cartilage and Bone During Health, Disease, and Steroid Therapy. *Physiological reviews* **96**, 409-447
217. Jackson, A. L., and Levin, A. A. (2012) Developing microRNA therapeutics: approaching the unique complexities. *Nucleic acid therapeutics* **22**, 213-225
218. Czech, M. P., Aouadi, M., and Tesz, G. J. (2011) RNAi-based therapeutic strategies for metabolic disease. *Nature reviews. Endocrinology* **7**, 473-484
219. van Rooij, E., and Kauppinen, S. (2014) Development of microRNA therapeutics is coming of age. *EMBO molecular medicine* **6**, 851-864
220. Misso, G., Di Martino, M. T., De Rosa, G., Farooqi, A. A., Lombardi, A., Campani, V., Zarone, M. R., Gulla, A., Tagliaferri, P., Tassone, P., and Caraglia, M. (2014) Mir-34: a new weapon against cancer? *Molecular therapy. Nucleic acids* **3**, e194
221. Di Martino, M. T., Leone, E., Amodio, N., Foresta, U., Lionetti, M., Pitari, M. R., Cantafio, M. E., Gulla, A., Conforti, F., Morelli, E., Tomaino, V., Rossi, M., Negrini, M., Ferrarini, M., Caraglia, M., Shammas, M. A., Munshi, N. C., Anderson, K. C., Neri, A., Tagliaferri, P., and Tassone, P. (2012) Synthetic miR-34a mimics as a novel therapeutic agent for multiple myeloma: in vitro and in vivo evidence. *Clinical cancer research : an official journal of the American Association for Cancer Research* **18**, 6260-6270
222. Zhang, G., Guo, B., Wu, H., Tang, T., Zhang, B. T., Zheng, L., He, Y., Yang, Z., Pan, X., Chow, H., To, K., Li, Y., Li, D., Wang, X., Wang, Y., Lee, K., Hou, Z., Dong, N., Li, G., Leung, K., Hung, L., He, F., Zhang, L., and Qin, L. (2012) A delivery system targeting bone formation surfaces to facilitate RNAi-based anabolic therapy. *Nat Med* **18**, 307-314